2009-01-01

Holographic liquid crystal devices

Kotakonda Pavani
Technological University Dublin

HOLOGRAPHIC LIQUID CRYSTAL DEVICES

Kotakonda Pavani, M.Sc.

A thesis submitted for the degree of Doctor of Philosophy to the Dublin Institute of Technology

Supervisors

Dr. Vincent Toal, Dr. Izabela Naydenova
Dr. Robert Howard

Centre for Industrial and Engineering Optics
School of Physics
Dublin Institute of Technology
September 2008

Abstract

Liquid crystals have become natural candidates for use in electro-optic devices for their ability to change the orientation of the director with the application of an electric field, and exhibiting large range of refractive index. The aim of the work presented in this thesis is to fabricate liquid crystal optoelectronic devices such as electrically switchable liquid crystal diffraction gratings and polarization rotators by exploiting the holographic surface relief effect in photopolymer and by developing novel polymer dispersed liquid crystals (PDLCs).

Alignment of liquid crystals is commercially achieved by creating grooves on a conducting layer such as polyimide or indium tin oxide (ITO) by rubbing. This process has disadvantages such as creation of static electricity and dust which are undesirable. An attractive alternative technique to rubbing is investigated. A photopolymer layer coated on a conducting ITO layer on a glass plate has the grooves inscribed holographically in it. An acrylamide based dry photopolymer developed in the Centre for Industrial and Engineering Optics, Dublin Institute of Technology is used in this study. The dependence of photoinduced surface relief on the holographic recording parameters, chemical composition of photopolymer and on physical parameters of the photopolymer layer were studied. A model explaining the mechanism of surface relief grating formation is proposed. Electrically switchable diffraction gratings and polarization rotators were fabricated by filling these grooves with liquid crystals using the capillary filling technique.

In the second approach, holographic switchable diffraction gratings were fabricated using a novel PDLC, which was also developed in the Centre for Industrial and Engineering Optics. PDLCs consist of microscopic liquid crystalline droplets embedded in a polymer matrix. Preliminary results for the recording parameters and the physical parameters of the PDLC layer needed to fabricate gratings are presented. The redistribution of LCs was observed by using techniques such as phase contrast microscopy and Raman spectroscopy.

The electrically switchable diffraction gratings were characterized using linearly polarized light by measuring the dependence of the intensity in the first diffracted order on the applied electric field. The polarization rotator was characterized by studying the influence of the applied electric field on the twist angle and the variation of intensity in the zero and the first orders of diffraction. The capabilities of the photoinduced surface relief effect in the photopolymer and of a newly developed PDLC material for the fabrication of liquid crystal devices are demonstrated.

Declaration

I certify that this thesis which I now submit for examination for the award of Doctor of Philosophy, is entirely my own work and has not been taken from the work of others save and to the extent that such work has been cited and acknowledged within the text of my work.

This thesis was prepared according to the regulations for postgraduate study by research of the Dublin Institute of Technology and has not been submitted in whole or in part for an award in any other Institute or University.

The work reported on in this thesis conforms to the principles and requirements of the Institute's guidelines for ethics in research.

The Institute has permission to keep, to lend or to copy this thesis in whole or in part, on condition that any such use of the material of the thesis be duly acknowledged.

Signature_____ Date_____

Candidate

Acknowledgements

I would like to take this opportunity to thank a number of people who gave suggestions, who encouraged me and who helped with their valuable advices and assistance.

First of all I would like to thank my supervisors Dr. Vincent Toal and Dr. Izabela Naydenova for their valuable suggestions and constant encouragement all through my project work. I would also like to thank my other supervisor Dr. Robert Howard for his helpful suggestions during my project.

I would like to thank Dr Suzanne Martin, IEO Manager for helpful suggestions during my project. Also I would like to thank my husband and my colleague, Dr. Raghavendra Jallapuram for supporting and encouraging me through out my project work.

I would like to thank the Faculty of Science Scholarship Scheme for funding this project, School of Physics, Dublin Institute of Technology. FOCAS is greatly acknowledged for providing the excellent and state of the art laboratory facilities.

I would like to thank all my colleagues who have helped me during my project from Centre for Industrial and Engineering Optics, Focas and School of Physics.

I would like to thank Physics technicians Joe Keogh and Anne Scully for their assistance during my project work.

Finally, I would like to thank my parents for their constant encouragement all through my studies.

CONTENTS

LIST OF FIGURES

INTRODUCTION

Liquid crystals (LC) have attracted increasing interest due to their unique physical properties. These are soft materials with properties intermediate between solids and liquids [1, 2]. LCs have become natural candidates for use in electro-optic and data storage devices [2-6] for their ability to change the orientation of the director, which is the direction of preferred orientation of molecules, with the application of electric field and exhibiting large variation of refractive index [1-4]. Optical properties such as birefringence [1-4, 7, 8], dichroism [9, 10], fluorescence [11-13] and light scattering [14-17] have proved useful for the development of new opto-electronic devices.

The main aim of this research is to fabricate LC opto-electronic devices, such as electrically switchable diffraction gratings and polarizing components by using the holographic surface relief effect in a photopolymer and by developing new polymer dispersed liquid crystals (PDLCs). The LC devices have applications in integrated optics [18], information processing and optical communication [4, 19-21]. They have a large ability to control the direction and/or polarization states of light beams in optoelectronic circuits and in advanced interferometers [22]. A brief discussion on LCs, including different types of LCs and classification and different alignment techniques is given in chapter 1.

Uniform alignment of LCs is an essential requirement to fabricate LC devices. Liquid crystal displays (LCD) are the most common applications of LC technology. Commercially the current technique chosen to align LC molecules for large–scale production of LC devices is to create grooves by the rubbing of polyimide layers. This

technique has some disadvantages such as creation of static electricity and dust which are highly undesirable for active matrix LCDs [23, 24]. To overcome these problems several alignment methods have been developed and they are explained in detail by Hasegawa et al [23]. These methods can be divided into two categories. One uses surface alignment caused by the anisotropy of the surface. The other method aligns the LC based on an electric or magnetic field. When the electric or magnetic field is removed, the aligned LCs on the surface aligns the bulk of the LCs. Some of the alignment methods are summarized in chapter 1. In the present work the fabrication of LC opto-electronic devices was carried out by using holographic technique and exploiting the surface relief effect in the photopolymer as an alternative to the rubbing technique [23-28].

Holography is a technique of reproducing a 3-dimensional image of an object by means of interference of light waves in a photosensitive recording medium [29]. It is a widely used technique, which has a variety of applications in optical information processing [30], data storage [31], optical elements [32] and computer-generated holograms [33]. There are different holographic materials used for recording holograms among which photopolymers have reached a primary position [34, 35]. The advantage of being self developing when exposed to light pattern makes them a practical alternative to other conventional recording materials [36-40]. In this work an acrylamide based dry photopolymer developed in the Centre for Industrial and Engineering Optics (IEO), Dublin Institute of Technology [39, 40] was used for the production of surface relief gratings. A brief discussion on the basic principles of holography, types of holograms and maximum achievable diffraction efficiencies is given in chapter 2 which also gives

information about different recording materials for holography along with photopolymers and the mechanism of recording in IEO photopolymer.

A diffraction grating is the simplest possible hologram. It is created by exposing photosensitive material to an interference pattern created by two plane beams of light of suitable wavelength. If a variation of thickness of photosensitive material is produced then it is called a surface relief grating. The surface relief gratings observed on photopolymer layers have the ability to align LCs and take the place of the grooves generated using rubbing [41-43]. There are two methods of creating surface relief on the photopolymer layer, lithographic [44] and holographic photo patterning [23, 24, 42]. In this work holographic recording of patterns in photopolymer layers is emphasized. So it was important to characterize the photoinduced surface modulation observed in the photopolymer layer. The optical recording of surface relief gratings is based on the photopolymerization reactions caused in bright regions of the interference pattern. The photopolymerization processes are explained in chapter 2.

The composite materials in which LC droplets are embedded in a polymer matrix are known as polymer dispersed LCs (PDLC) [45-54]**.** Though there are a number of impressive reports describing the performance parameters of these materials [45-54] there is still a growing need to produce materials that offer high diffraction efficiencies (DE), low switching fields and fast response and decay speeds. Chapter 2 also describes a new PDLC material developed in the IEO which was used to fabricate switchable diffraction gratings.

The **first objective** of this research was to study the dependence of surface relief amplitude modulation on the holographic recording parameters such as spatial frequency, exposure intensity, total exposure, post exposure treatments and on the chemical composition of photopolymer layers and also on the physical characteristics of the layers such as thickness and temperature. Good optical quality layers play an important role in holographic recording. In this work good optical quality samples were prepared by two different coating techniques, spin coating and gravity setting. Detailed explanation of these methods will be given later in the thesis. The amplitude modulation of surface relief gratings was measured using a white light interferometer MicroXAM S/N 8038 (WLI) (ADE Phase Shift, Arizona). These results are presented in chapter 3. In holographic technique there is more flexibility in controlling the surface relief amplitude modulation by changing recording parameters and/or chemical composition of photopolymer and/or physical parameters of photopolymer layer; that is the height and shape of the grooves can be controlled whereas in rubbing technique there is very little possibility of controlling height of the grooves. Based on the above studies a mechanism for the formation of the surface relief in the photopolymer, which is the **second objective** of this research, is described in chapter 3.

As already stated the main aim of this project was to fabricate LC optoelectronic devices. For this it was important to identify which LCs are suitable for fabrication of these devices, which is the **third objective** of this project. High optical anisotropy (Δn) and dielectric anisotropy ($\Delta \varepsilon$) are important when choosing LCs as they result in higher diffraction efficiency (DE) and lower switching fields [45].

Among different phases of LC, nematic LCs are mostly used for the fabrication of LC optoelectronic devices. LCs are very sensitive to temperature changes and are in fact used for measuring temperature. The nematic to isotropic (N-I) transition temperature of the LC also plays an important role in choosing the LCs. LCs are birefringent and characterized by two refractive indices, ordinary and extra ordinary. The LCs are chosen in such a way that their ordinary refractive index n_o matches the refractive index of host photopolymer which is important for the operation of LC devices. In this work E7, E49, ZLI-3700-000 LCs and BL LCs from Merck Company (Merck KGaA, 64271 Darmstadt, Germany) were used.

This **fourth objective** of the project was divided into two parts; *first* to fabricate the devices such as switchable LC diffraction gratings and twisted nematic LC devices by using surface relief effect in the photopolymer and a new PDLC material, and *second* to test these devices.

For switchable LC diffraction gratings using the surface relief effect, the LC cells were fabricated by sandwiching LCs between conducting ITO coated glass plates in which one of two plates was coated with a photopolymer layer a few micrometers thick. This photopolymer layer was then holographically patterned to form a surface relief grating. Electrical contacts were made to the conductors by using silver loaded epoxy resin. There are two different methods for introducing LC between the grating and the adjacent plate to form a cell, the one drop filling method and the capillary method [2]. These are explained in chapter 4. Firstly birefringence was measured to know whether the LCs were aligned in the surface relief gratings or not. Ellipticity and azimuth of the

LC were also measured. The methodology of measurement and the results are presented in chapter 4.

To test whether the diffraction gratings are switchable, electric field was applied to the cell. The diffraction efficiency (DE), defined as the ratio of intensity of the first order diffracted beam to the incident intensity, of the device was measured at different voltages. DE results demonstrating electrical switching of such diffraction gratings are presented in chapter.4.

Another device fabricated using surface relief effect is a twisted nematic LC device, which consists of two parallel photopolymer layers with sinusoidal surface relief profiles on ITO coated glass plates, oriented so that the wave vectors of the two gratings are orthogonal. The main difference between the device presented in this work and a twisted nematic LC cell fabricated by standard rubbing technique is the existence of limited number of additional switchable diffraction orders. This is due to the nature of the two surfaces used to orient the LCs. The fabrication technique is described in chapter 5. The electro optical switching behaviour in the diffracted orders is characterized along with that in the zero order. The influence of the applied electric field on the twist angles in the zero order and in the first order of diffraction of the grating was studied. The variations of intensity in the zero and first orders with applied voltage were measured with the twisted nematic LC device placed between crossed polarizers and results are presented in the chapter 5.

In the second approach switchable diffraction gratings were optically recorded in a PDLC material. A novel PDLC material is developed at IEO. Details of the fabrication

and preliminary results of the characterization of PDLC diffraction gratings are presented in chapter 6. The redistribution of LCs was observed by using phase contrast microscopy and Raman spectroscopy. Results of electro-optical switching behaviour of PDLC diffraction gratings are also presented in chapter 6.

Finally, conclusions from this work are presented in chapter 7. The results show that the surface relief effect in an acrylamide based photopolymer and a new PDLC material developed at IEO centre are promising for the fabrication of LC optoelectronic devices. The results are published in various international journals [57-59].

References

1. P. J. Collings, “Liquid crystals: Nature’s delicate phase of matter.” Princeton University press, 2002
2. B. Bahadur, “Liquid crystals: Applications and uses.” Vol.1, World Scientific publisher, 1990.
3. M. J. Bradshaw, “Liquid crystal devices.” Phys. Educ., 18, 20-26, 1983.
4. R. S. McEwen, “Liquid crystals, displays and devices for optical processing.” J.Phys.E:Sci.Instrum., 20, 364-377, 1987.
5. A. S. Matharu, S. Jeeva and P. S. Ramanujam, “Liquid crystals for holographic optical data storage.” 36, 1868-1880, 2007.
6. J. Ashley, M. P. Bernal, G. W. Burr, H. Coufal, H. Guenther, J. A. Hoffnagle, C. M.Jefferson, B. Marcus, R. M. Macfarlane, R. M. Shelby and G. T. Sincerbox, “Holographic data storage.” IBM J.Res.Develop. 44(3), 341-368, 2000.
7. http://www.sharpsma.com/Page.aspx/americas/en/982f3cf5-ee6e-427d-a20e-bad3f8a7a15f 1-3-2006
8. http://plc.cwru.edu/tutorial/enhanced/files/textbook.htm 1-3-2006
9. S. Chandrasekhar, “Liquid Crystals.” Cambridge University ,26 Nov 1992
10. D. Katsis, P. H. M. Chen, J. C. Mastrangelo and S. H. Chen, “Vitrified chiral-nematic Liquid crystalline films for selective reflection and circular polarization.” Chem. Mater., 11(6), 1590-1596, 1999.
11. R. G. Howard, “Liquid crystalline polymers for nonlinear optics and polarised fluorescence.” Doctoral thesis, Trinity college Dublin, 1997

12. J. Seo, S. Kim, S. H. Gihm, C. R. Park and S. Young Park, “Highly fluorescent columnar liquid crystals with elliptical molecular shape: oblique molecular stacking and excited-state intramolecular proton-transfer fluorescence.” J. Mater. Chem., 17, 5052-5057, 2007.
13. K. Abe, A. Usami, K. Ishida, Y. Fukushima and T. Shigenari, “Dielectric and fluorescence study on phase transitions in liquid crystal 5CB and 8CB.” J. Korean. Phys. Soc., 46(1), 220-223, 2005.
14. P. G. De Gennes and J. Prost, “The physics of Liquid Crystals.” 2nd edition, 1993.
15. M. Yoneya, Y. Utsumi, and Y. Umeda, “Depolarized light scattering from liquid crystals as a factor for black level light leakage in liquid-crystal displays.” J. Appl. Phys., 98, 016106, 2005.
16. A. D. Kiselev, O. V. Yaroshchuk and L. Dolgov, “Ordering of droplets and light scattering in polymer dispersed liquid crystal films.” J. Phys.:Condens. Matter. 16, 7183-7197, 2005.
17. L. McKenna, L. S. Miller and I. R. Petereson, “Polymer dispersed liquid crystal films for modulating infra-red radiation.” Polymer, 45, 6977-6984, 2004.
18. G. Zou, H. Gro¨nqvist and J. Liu, “Integrated inductors on liquid crystal polymer substrate for RF applications.” Circuit World, 32-1, 41-44, 2006.
19. T. R. Wolinski, S. Ertman, P. Lesiak, A. W. Domanski, A. Czapla, R. Dabrowski, E. N. Kruszelnicki and J. Wojcik, “Photonic liquid crystal fibers- a new challenge for fiber optics and liquid crystal photonics.” Opto-Electron. Rev., 14(4), 329-334, 2006.
20. L.G. Commander, S.E. Day and D.R. Selviah, “Variable focal length microlenses.” Opt. Commu., 177, 157–170, 2000.

21. M. Hain, R. Glockner, S. Bhattacharya, D. Dias, S. Stankovic and T. Tschudi, “Fast switching liquid crystal lenses for dual digital versatile disc pickup.” Opt. Commun., 188, 291-299, 2001.
22. B. Bowe, S. Martin, V. Toal, A. Langhoff and M. Whelan, “Dual in-plane electronic speckle pattern interferometry system with electro-optical switching and phase shifting.” Appl.Opt., 38(4), 666-673, 1999
23. K. Takatoh, M. Hasegawa, M. Koden, N. Itoh, R. Hasegawa and M. Sakamoto, “Alignment technologies and applications of liquid crystal devices.” Taylor & Francis, 2005.
24. M. O’Neill and S. M. Kelly, “Photoinduced surface alignment for liquid crystal displays.” J.Phys.D.Appl.Phys.33, 67-84, 2000.
25. X. T. Li, A. Natansohn and P. Rochon, “Photoinduced liquid crystal alignment based on a surface relief grating in an assembled cell.” Appl. Phys. Lett., 74, 25, 3791- 3793, 1999.
26. K. Sakamoto, K. Usami, M. Watanabe, R. Arafune and S. Ushioda, “Surface anisotropy of polyimide film irradiated with linearly polarized ultraviolet light.” Appl. Phys. Lett., 72(15), 1832-1834, 1998.
27. V. V. Lazarev, M. I. Barnik and N. M. Shtykov, “Liquid crystal alignment by photo-processed polymer films.” Mol. Materials, 8, 235-244, 1997.
28. T. Ikeda, “Photomodulation of liquid crystal orientations for photonic applications.” J.Mater.Chem, 13, 2037-2057, 2003.
29. P. Hariharan, “Optical holography: Principles techniques and applications.” 2nd Edition, Cambridge monographics on physics, Cambridge University Press, 1996.

30. B. D. Genther, C. R. Christensen, and J. Upatnieks "Coherent optical processing: another approach." IEEE J. Quant Elect. 15, 1348-1362, 1979.
31. A. Kozma, "Holographic storage." Proc.SPIE, 53,77-83, 1974.
32. S. Guntaka, V. Toal and S. Martin, "Holographically recorded diffractive optical elements for holographic and electronic speckle pattern interferometry." Appl. Opt., 41(35), 7475-7479, 2002.
33. Y. Boiko, V. Slovjev, S. Calixto and D. Lougnot, "Dry photopolymer films for computer-generated infrared radiation focusing elements." Appl. Opt., 33(5), 787-793, 1994.
34. B. L. Booth, "Photopolymer materials for holography." Appl.Opt., 14(3), 593-601, 1975.
35. A. M. Weber, W. K. Smothers, T. J. Trout, and D. J. Mikish, "Holographic recording in DuPont's new photopolymer material." Proc SPIE 1212, 30-39, 1990.
36. B. M. Monroe, W. K. Smothers, D. E. Keys, R. R. Krebs, D. J. MicKish, A. F. Harrington, S. R. Schickers, M. K. Armstrong, D. M. T. Chan and C. I. Weathers, "Improved photopolymers for holographic recording." part 1. J. Imaging Sci. 35, 19-25, 1991.
37. G. Zhao and P. Mouroulis, "Diffusion model of hologram formation in dry photopolymer materials." J.Mod. Opt. 41, 1929-1939, 1994.
38. V. L. Colvin, R.G. Larson, A.L Harris and M.L Schilling, "Quantitative model of volume hologram formation in photopolymer materials." J. Appl. Phys., 81, 5913-5923, 1997.

39. S. Martin, “A new photopolymer recording material for holographic applications: photochemical and holographic studies towards an optimized system.” Doctoral thesis, University of Dublin, 1995.
40. R. Jallapuram, **“**Optimization of an acrylamide-based photopolymer for reflection holographic recording.” Doctoral thesis, Dublin Institute of Technology, 2005.
41. C. C. Barghorn and D. Lougnot, “Use of self-processing dry photopolymers for the generation of relief optical elements: a photochemical study.” Pure Appl. Opt., 5, 811-825, 1996.
42. D. Dantsker, J. Kumar and S. K. Tripathy, “Optical alignment of liquid crystals.” J. Appl. Phys, 89(8), 4318-4325, 2001.
43. T. Smirnova and O. Sakhno, “A mechanism of the relief-phase structure formation in self-developing photopolymers.” Optics and Spectroscopy, 3 (1), 126-131, 2001.
44. B. Maune, M. Lončar, J. Witzens, M. Hochberg, T. Baehr-Jones, D. Psaltis, A. Scherer and Y. Qiu, “Liquid-crystal electric tuning of a photonic crystal laser.” Appl. Phys. Lett. 85(3), 360-362, 2004.
45. T. J. Bunning, L. V. Natarajan, V. P. Tondiglia and R.L Sutherland “Holographic Polymer-Dispersed Liquid Crystals (H_PDLCs).” Annu. Rev. Mater. Sci., 30, 83-115, 2000.
46. J. W. Doane, “ Polymer Dispersed Liquid Crystal Displays” in Liquid crystal: Applications and uses, B. Bahadur, World Scientific , 1990.
47. R. L. Sutherland, L. V. Natarajan, V. P. Tondiglia, and T. J. Bunning, “ Bragg Gratings in an acrylate polymer consisting of periodic polymer-dispersed liquid crystal planes.” Chem. Matter. , 5, 1533-1538, 1993.

48. R. A. Ramsey and S. C. Sharma, “Switchable holographic gratings formed in polymer-dispersed liquid crystal cells by use of a He-Ne laser.” Opt. Lett., 30(6), 592-594, 2005.
49. D. E. Lucchetta, L. Criante and F. Simoni, “Optical characterization of polymer dispersed liquid crystals for holographic recording.” J.Appl.Phy, 93(12), 9669-9674, 2003.
50. G. Zharkova, I. Samsonova, S. Streltsov, V. Khachaturyan, A. Petrov and N. Rudina, “Electro-optical characterization of switchable Bragg gratings based on nematic liquid crystal-photopolymer composites with spatially ordered structure.” Microelectronic Engineering, 81**,** 281-287, 2005.
51. K. Beev, L. Criante, D. E. Lucchetta, F. Simoni and S. Sainov, “Recording of evanescent waves in holographic polymer dispersed liquid crystals.” J. Opt. A:Pure Appl. Opt., 8, 205-207, 2006.
52. M. S. Malcuit, M. E. Holmes and M. A. Rodriguez, “Characterization of PDLC holographic gratings.” Lasers and Electro-Optics, 395-396, 2002**.**
53. J. Qi and G. P. Crawford “Holographically formed polymer dispersed liquid crystal displays.” Displays, 25, 177-186, 2004.
54. G. Cipparrone, A. Mazzulla and G. Russo, “Diffraction gratings in polymer-dispersed liquid crystals recorded by means of polymerisation holographic technique.” Appl. Phy. Lett., 78(9), 1186-1188, 2001.
55. M. Jazbinsek, I. D. Olenik, M. Zgonik, A. K. Fontecchio and G. P. Crawford, “Characterization of holographic polymer dispersed liquid crystal transmission Gratings.” J. of Appl. Phys., 90(8), 3831-3837, 2001.

56. S. Harbour L. Simonyan and T. Galstian, “Electro-optic study of acrylate based holographic polymer dispersed liquid crystals with broad band photosensitivity.” Opt. Commun., 277, 225-227, 2007.

57. K Pavani, I Naydenova, S Martin and V Toal, “Photoinduced surface relief studies in an acrylamide-based photopolymer” J. Opt. A: Pure Appl. Opt. 9, 43-48, 2007.

58. K. Pavani, I. Naydenova, S. Martin, R. Jallapuram, R. G. Howard, V. Toal, “Electro-optical switching of liquid crystal diffraction gratings by using surface relief effect in the photopolymer.” Optics Communication**,** Vol. 273, 367-369, 2007.

59. K. Pavani, I. Naydenova, S. Martin, R. G. Howard, V. Toal, “Fabrication of switchable liquid crystal devices using surface relief gratings in photopolymer.” Published online in the Journal of Material Science (materials in electronics) (JMSE) DOI 10.1007/s10854-007-9537-5, 2008.

1. LIQUID CRYSTALS

1.1 Introduction

Liquid crystals are an intermediate state between crystalline solids and amorphous liquids [1, 2]. The liquid crystalline phase was first observed by an Austrian botanist Friedrick Reinitzer in 1888 when he was working with cholesteryl benzoate, an organic compound. He observed that, when heated, it showed two melting points. At 145 °C the solid turned into a cloudy liquid and on further heating to 179°C the cloudy liquid became clear. Shortly afterwards a German physicist, Otto Lehmann, determined the cloudy liquid to be an intermediate state of matter between solid crystalline and liquid phases [3]. He suggested the name LC for this cloudy liquid as it shows properties of both liquids and solids.

LCs are complex molecular systems which are of increasing interest in technological applications such as photonic components, including LCDs due to their unique properties such as self organizing nature, fluidity with long range order, cooperative motion, anisotropy of various physical properties (optical, electrical and magnetic) and change in alignment with applied external fields [4]. The molecules (mesogens) are asymmetric, typically rod-shaped, and on average their long molecular axes are oriented parallel to a preferred direction specified by a unit vector $\hat{n}$ called ***the director*** [5].

LCs can be divided into thermotropic and lyotropic LCs [2, 6]. Thermotropic LCs exhibit a phase transition into the LC phase as the temperature is changed whereas lyotropic LCs exhibit phase transitions as a function of concentration. The reactions of

lyotropic LCs, which are used in the manufacture of soaps and detergents, depend on the type of solvent they are mixed with. Thermotropic LCs are mainly of interest for optical device technologies. Many thermotropic LCs exhibit a variety of phases as temperature is changed. The LCs are characterized by positional and sometimes orientational order. Depending upon the amount of order in the material, there are different types of LC phases. The degree of ordering in the material is quantified by a parameter called the order parameter (S) given as

$$S = 1/2\left\langle 3\cos^2\theta - 1\right\rangle \text{ ---------- (1.1)}$$

where θ is the angle between the director and the long axis of the each molecule. The brackets denote an average over all of the molecules in the sample [1, 2, 6].

1.2 Liquid crystal phases

In 1922, a French scientist, George Friedel classified the LCs into three different phases known as nematic, cholesteric and smectic based on their structure [3, 5, 7, 8]. The properties of these phases will be explained below.

1.2.1. Nematic phase

The nematic phase LCs show the least ordered mesogens having average alignment of the long molecular axis along the director ($\vec{n}$) as shown in figure 1.1. These have no long range of positional ordering. The extent of alignment along the director, $\vec{n}$ in figure 1.1, is characterized by the order parameter (S). In the nematic state S normally varies from 0.6-0.8 at low temperatures to 0.3-0.4 near the transition to the isotropic state [9]. Most of the nematics are uniaxial.

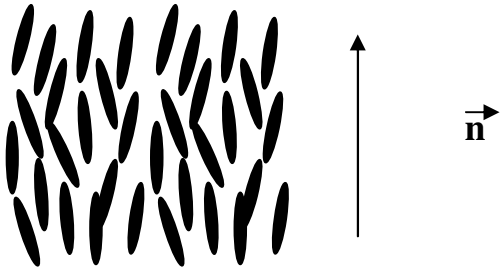

Figure 1.1 Structure of nematic phase.

1.2.2. Cholesteric phase

The cholesteric phase is generally considered a chiral nematic phase where the director is subject to helical distortion as shown in figure 1.2.

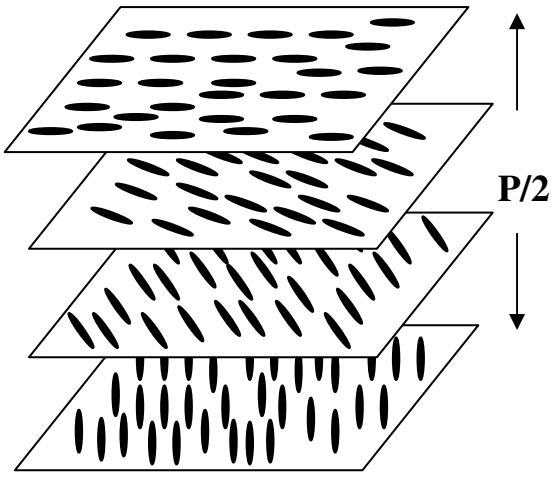

Figure 1.2: Structure of cholesteric phase.

The average molecular director is perpendicular to the helical axis and turns around it in a regular way. The distance along the director over which the mesogens twist by 2π radians is called the cholesteric pitch (P). Cholesteric LCs show the peculiar phenomenon of selective reflection of light. Since the pitch is temperature dependent this enables their use a number of applications such as in thermometers [6].

1.2.3. Smectic phase

Smectics are characterized by ordering in the layers. In this phase along with orientation in a preferred direction, the mesogens form a layered structure as shown in figure 1.3. Smectic phases occur at lower temperatures than nematic phases and are more viscous as the easiest mode of flow is for the layers to slip over one another. Depending on the orientation of the director relative to the layer normal and the degree of ordering within the layer smectics are subgrouped from **A** to **H** [5].

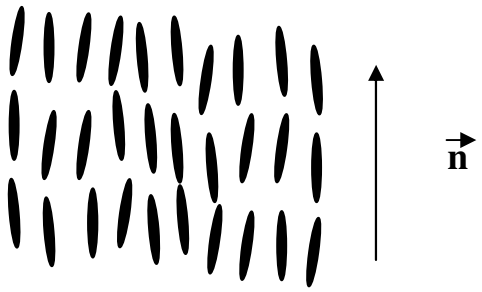

Figure 1.3 Structure of smectic phase.

In general the more ordered phases occur at lower temperatures and, as the temperature increases, LCs pass through the smectic phase first then the nematic/cholesteric and finally the isotropic phase liquid state. This is shown schematically below where $T_1 < T_2 < T_3$.

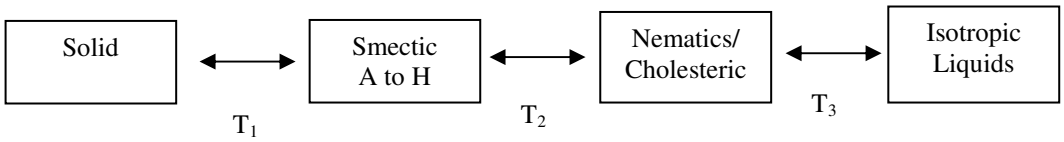

From the commercial point of view nematic LCs have attracted more attention than other phases. They are most commonly used in information displays and optical

communication. The reason is that nematics show rod shaped, long range of orientational order and no positional order. The mesogens align in a particular direction called the director when an external electromagnetic field is applied, which allows control of optical properties, as LCs are birefringent.

A material that has different properties for different directions is called an anisotropic material. As a result of orientational order, nematic LCs exhibit anisotropy in many of their properties such as dielectric, optical, elastic and viscosity. The existence of these anisotropic properties of LCs gives rise to different phenomena which are interesting for the fabrication of electro optical devices [1, 2].

The anisotropy of the dielectric permittivity ($\Delta\varepsilon$) is defined as $\Delta\varepsilon = \varepsilon_{\parallel} - \varepsilon_{\perp}$ ($\varepsilon_{\parallel}$ is the permittivity parallel to the director and $\varepsilon_{\perp}$ is the permittivity perpendicular to the director) and can be either positive or negative. The value of $\Delta\varepsilon$ ranges from -6 to +50 [2]. In electro optical applications, an electric field is applied to an LC device to control the orientation of the LC molecules. LCs with positive dielectric anisotropy tend to align parallel to the applied electric field while LCs with negative dielectric anisotropy align perpendicular to the electric field. Depending on the switching principle (parallel or perpendicular to the electric field), both types of LCs can be used for LC devices. If low switching voltage is desired, LCs with a large value of dielectric anisotropy should be used.

Anisotropic materials possess more than one index of refraction. This phenomenon is known as double refraction or birefringence or optical anisotropy [1]. Optical anisotropy is defined as $\Delta n = n_e - n_o$ where n_e is the extra ordinary refractive index and n_o is the

ordinary refractive index. Depending on the values of n_e and $n_{o,}$ birefringence can be positive or negative. The birefringence effect is observed when a beam of polarised light propagates through such an anisotropic medium. The refractive indices are different for the two orthogonally plane polarised components of the beam. Phenomena such as reflection or transmission or absorption in anisotropic media depend on the polarization of the incident light beam. Because of this behaviour birefringent materials can be used to fabricate a polarizer which can transmit a light component which is plane polarised parallel to the optical axis of the material or can be used as an analyzer to determine the state of polarization of light.

The anisotropy of nematic LCs causes the components of light with electric fields perpendicular and parallel to the director to traverse the LC with different velocities, resulting in a phase difference between the two components. This phase difference depends on the thickness of the material. When the thickness is adjusted to obtain a phase difference of 90°, the incident linearly polarised light emerges as circularly polarised light or vice versa. The phase difference can be used to fabricate the devices such as phase retarders or polarization rotators. By adjusting the external electric field, the properties of the propagating light such as state of polarization can be altered. In this work nematic LCs are used to fabricate the optoelectronic devices.

Another physical property of LCs which influences the dynamical behaviour of the system is viscosity. LCs shows five anisotropic viscosity coefficients depending on the orientation of the director with respect to the flow of the material. For nematic phase LCs show three different translational viscosities $\eta_{1,}$ $\eta_{2,}$ and $\eta_{3,}$ defined as follows,

η_1: The director is perpendicular to the flow pattern and parallel to the velocity gradient.

η_2: The director is parallel to the flow pattern and perpendicular to the velocity gradient.

η_3: The director is perpendicular to the flow pattern and perpendicular to the velocity gradient.

These viscosities are called Miesowisz viscosities. When the director is perpendicular to the flow the translational viscosity is at its maximum that is, $\eta_3 > \eta_1 > \eta_2$.

There is also a specific case which is also possible and small is η_{12} and is defined as,

η_{12}: The director is suspended at an angle of 45^o with both the flow pattern and the velocity gradient.

An important parameter considered when discussing reorientation of LCs in an electric or magnetic field is the rotational viscosity (γ).When the director is not held in its place it will be affected by a torque, creating a hydrodynamic torque and as a result rotational viscosity is experienced. The dynamic response of the LC devices depends mainly on the rotational viscosity [2].

The elastic constants of LCs are the material parameters which determine the restoring torque which arises when the system is perturbed from its equilibrium configuration. When an electric field is applied to reorient the molecules to control the effective birefringence in an electro optical device, it is the balance between the electric and elastic torque that determines the static deformation of the LC director. Any deformation can be divided into a combination of the three deformations namely splay, twist and bend [1, 2].

Using Oseen-Frank elastic theory, the deformation free energy density can be written as [2],

$$F = \frac{1}{2}[k_{11}(\nabla \cdot n)^2 + k_{22}(n \cdot \nabla \mathrm{x}\ n)^2 + k_{33}(n \mathrm{x} \nabla \mathrm{x}\ n)^2] \text{ --- ---------- (1.2)}$$

where k_{11} is the splay elastic constant, k_{22} is the twist elastic constant, and k_{33} is the bend elastic constant, all with order of magnitude 10^{-11} N.

The voltage needed to reorient the LC molecules is related to the elastic constants as well as the dielectric anisotropy. When the applied voltage is minimum the LCs remain undeformed but when voltage is increased to a certain threshold voltage, deformation begins and increases with the increase in the voltage. The minimum voltage needed to reorient the LC molecules in a parallel structure is given by

$$V_{th} = \pi\sqrt{\frac{k_{11}}{\varepsilon_0 \Delta\varepsilon}} \text{ ---------- (1.3)}$$

1.3. Alignment methods

In nematic LCs there are basically three alignments which are widely used for different applications. They are homogenous (parallel), homeotropic (perpendicular) and twist alignments [2].

In homogeneous alignment the director of the LC is parallel to the substrate surfaces and aligned in a specific direction. Homogeneous alignment can be obtained by the oblique evaporation of SiO or MgF_2 on to the surfaces or by the unidirectional rubbing of a surface coating of a polymer such as polyvinyl alcohol or polyimide [2, 7, 8]. But these methods have a number of drawbacks. The process of rubbing is hard to control and produces static electricity which is undesirable for the production of the active matrix LC-displays [11]. Alignment by oblique evaporation of metal oxides requires

quite expensive special vacuum equipment. Photoalignment of LCs is attractive as an alternative to these methods [3, 11-13]. There are a number of advantages of photoalignment methods over the common rubbing technique such as no electrostatic charge generation or dust contaminating the alignment surface and simplified fabrication technology. A general property of all photo-processed films is that being optically isotropic before polarized light treatment, they become anisotropic and cause a homogeneous alignment of LCs after photo processing [14]. Surface relief gratings fabricated in photopolymers through holographic recording can be filled with LCs to align them uniformly [11-13]. In this work surface relief gratings in an acrylamide based photopolymer are filled with LCs. The nematic LCs were aligned along the grating grooves and so switchable LC devices were fabricated.

In homeotropic alignment, the director of the LCs is perpendicular to the surfaces. Homeotropic alignment is achieved by coating the glass surfaces with a thin surfactant layer such as lecithin or by applying an external field normal to the surface [2, 10].

In the twist alignment method, two substrates are treated in the same way as in parallel alignment but with the alignment direction of the upper substrate at an angle to that of the lower. A cell showing this type of alignment is called twisted nematic (TN) cell. If the twist angle is greater than 90° the cells are called super twist nematic (STN) cells.

The operation, method of determination of the director and the twist angle of a TN device will be explained in chapter 5. When a monochromatic light wave propagating along the helical axis of a TN layer can be described by two elliptically polarized optical modes (Eigen modes), then only at a limit known as Mauguin limit, the

combination of these Eigen modes become linearly polarized, and this linearly polarized light follows the twist structure during transmission (wave guiding).

The Mauguin limit is defined as $d\Delta n >> \phi\lambda/\pi$ where d is the thickness of the LC layer, Δn is the birefringence of the LCs, ϕ is the twist angle and λ is the light wavelength. For a 90^o twisted nematic cell this condition reduces to $d\,\Delta n >> \lambda/2$.

The optical properties of a TN cell were calculated by Gooch and Tarry [2, 3]. The normalized transmittance (T) in the OFF state in a normal white mode (explained in chapter 5) is given by

$$T_{TN} = \frac{1}{2}\left(1 - \frac{\sin^2(\pi/2)\sqrt{1+u^2}}{1+u^2}\right) \quad \text{---------- (1.4)}$$

Where $u = 2\,d\Delta n/\lambda$ where d is the thickness of the LC layer. For faster response a lower value of u is selected.

The director of LCs in ON state tends to reorient parallel to the electric field by the Freedericksz effect. The threshold voltage V_{th} of the TN cell is given by the following equation.

$$V_{th} = \pi\sqrt{\frac{k_{11} + \frac{1}{4}\left(k_{33} - 2k_{22}\right)}{\varepsilon_o \cdot \Delta\varepsilon}} \quad \text{---------- (1.5)}$$

The response time from OFF state to ON state is given by τ_{on} and from ON state to OFF state is given by τ_{off} given respectively by following equations.

$$\tau_{on} = \frac{\gamma \cdot d^2}{\varepsilon_o \cdot \Delta\varepsilon\left(V^2 - V_{th}^2\right)} \quad \text{---------- (1.6)}$$

$$\tau_{off} = \frac{\gamma \cdot d^2}{\pi^2 \left(k_{11} + \frac{k_{33} - 2k_{22}}{4} \right)} \quad \text{---------- (1.7)}$$

This section gives overview on the electro optics of the nematic and twisted nematic devices. Switchable LC devices can also be fabricated by mixing LCs with the photopolymer and these are known as polymer dispersed liquid crystals. The next section gives an over view on PDLC and electro optics of PDLCs.

1.4. Polymer dispersed liquid crystals (PDLCs)

PDLCs are a relatively new class of materials that are emerging as promising for holographic recording materials and have potential applications in diffractive optical elements and many applications in optoelectronic devices [15-19]. PDLC films consist of micron-sized nematic droplets dispersed in a polymer matrix. Several methods have been developed to create LC dispersions. There are three methods of preparing PDLC layers depending on the factor causing phase separation: solvent-induced phase separation (SIPS), thermally-induced phase separation (TIPS) and polymerization-induced phase separation (PIPS) [3, 6]. These methods are explained clearly in chapter 6.

In the absence of a field the directors of the droplets within the layer are randomly oriented. As a result, incident light probes a range of refractive index values between n_o and n_e, which are the ordinary and extraordinary refractive indices of LCs. Since nematic LCs are optically uniaxial, indices encountered by incident light cannot be all

equal to the polymer refractive index n_p and so incoming light is scattered by the micro droplets; this is the opaque state (OFF state). When a sufficiently large electric field is applied, the LC molecules in the droplets are collectively reoriented with their directors parallel to the applied field. Hence, under this condition $n_p = n_o$ resulting in optically clear state (ON state), that is light is transmitted with no scattering. Because of this behavior PDLCs have potential for a variety of electro optic applications such as displays and light shutters.

The electro optical response of a PDLC layer depends on different factors such as the nematic director configuration, size and shape of the droplets and most importantly on resistivity (ρ) and dielectric properties of the LCs and polymer. The electric field inside an LC droplet is not the same as the electric field applied to the PDLC layer between two ITO electrodes [2].

Assuming that there is only one spherical droplet in a polymeric material in a uniform electric field (E), the electric field (E^d) inside the droplet is given by,

$$E^d = \frac{3E}{\varepsilon_{lc}/\varepsilon_p + 2} \quad \text{---------- (1.8)}$$

where ε_{lc} and ε_p are the dielectric constants of the LCs and polymer respectively.

The dielectric constant for materials with nonzero conductivities can be written as

$\varepsilon = \varepsilon' + j/\rho\omega$ where ε' is the real component, ρ is the resistivity and ω is the frequency of the applied voltage.

In the resistive regime ($\varepsilon' \rho\omega << 1$) the field inside the droplet can be expressed as,

$$E^d = \frac{3V}{d(\rho_{lc}/\rho_p + 2)} \quad \text{---------- (1.9)}$$

where V is the voltage applied to the electrodes and d is the thickness of the layer.

However there are cases where resistivity of the polymer or the LCs of the PDLC material are very high where the dielectric constants of LCs and polymer need to be considered to solve the above equations.

Another parameter to be determined for an electro optic PDLC switch is its threshold voltage which depends on the configuration of the droplets. The most common configurations are radial or axial and bipolar and are shown in figure 1.4 [6].

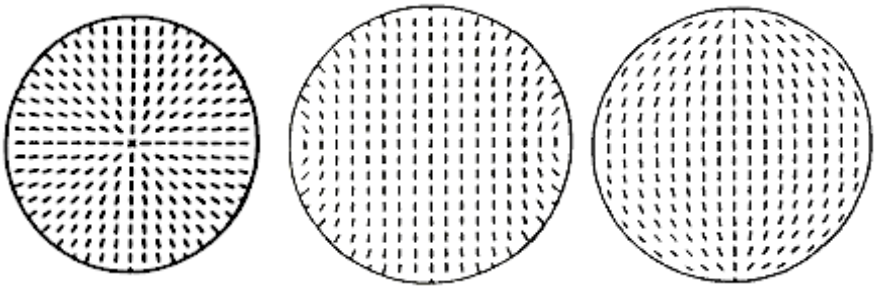

Figure 1.4 Schematic representation of droplet configurations of (a) radial (b) axial and (c) bipolar[6].

The radial configuration is observed when the LC molecules are anchored with their long axes perpendicular to the droplet wall. This configuration shows one point defect at the centre of the droplet as shown in figure 1.4(a). The axial configuration of the LC droplets also occurs when the molecules are oriented perpendicular to the droplet wall, but only when there is weak surface anchoring. This configuration creates a line defect

that runs around the equator of the spherical droplet, as seen in figure 1.4(b). When an electric field is applied to a radial droplet, the molecules adopt the axial configuration. This is the switching transition for a PDLC layer from opaque to clear. When an electric field of $E^{dR} \approx \sqrt{K/\Delta\varepsilon\varepsilon_o/2d_e}$ is applied to PDLC layer this switching transition occurs. The radial configuration is restored when the field is removed. Applying equation (1.9) the threshold voltage for the radial droplets is expressed as,

$$V_{thR} \approx \frac{1}{40}\frac{d}{d_e}\left(\frac{\rho_p}{\rho_{lc}}+2\right)\left[\frac{k}{\varepsilon_o\Delta\varepsilon}\right]^{1/2} \text{----------(1.10)}$$

where d_e (surface extrapolation) = k/W_o (W_o is the anchoring strength).

The switching voltage can be reduced by choosing materials with lower ρ_p/ρ_{lc} or a small thickness PDLC layer. Larger droplets could also be used to obtain lower threshold voltage since they do not require such a small d_e value, but making the droplets too large results in more scattering.

The bipolar configuration is obtained when the LC molecules are anchoring tangentially to the droplet walls as shown in figure 1.4(c). This creates two point defects at the poles of the droplet. The electric field used to orient elongated bipolar droplets is given as,

$$E^{dB} = \frac{1}{a}\left[\frac{k\left(l^2-1\right)}{\varepsilon_o\Delta\varepsilon}\right]^{1/2} \text{----------(1.11)}$$

Where $l = a/b$, the ratio of the length of the semi-major axis (a) to the length of the semi-minor axis (b). Applying equation (1.9) the threshold voltage for the bipolar droplets is expressed as,

$$V_{thB} = \frac{d}{3a}\left(\frac{\rho_p}{\rho_{lc}} + 2\right)\left[\frac{k\left(l^2 - 1\right)}{\varepsilon_o \Delta\varepsilon}\right]^{1/2} \quad \text{----------(1.12)}$$

The switching voltage can be reduced as explained by choosing materials in radial configuration with lower ρ_p/ρ_{lc} or a small thickness PDLC layer.

The response time of the device is also an important parameter for an electro optical PDLC device. It is divided into two parts: the time for a droplet director to reorient in an applied field (ON state) and the subsequent relaxation time to restore the original director alignment after the field is removed (OFF state).

The response time of the droplet director to an applied electric field i.e, ON state is obtained by balancing all three torque densities, electric, elastic and viscous. It is expressed as,

$$\tau_{ON}^{-1} = \frac{9\varepsilon_o \Delta\varepsilon E^2}{\gamma_1\left(\rho_p/\rho_{lc} + 2\right)^2} + \frac{k\left(l^2 - 1\right)}{\gamma_1 a^2} \quad \text{----------(1.13)}$$

The relaxation time i.e, OFF state is obtained by balancing two torque densities, elastic and viscous and ignoring the inertial term. It is expressed by

$$\tau_{off} = \frac{\gamma_1 a^2}{k\left(l^2 - 1\right)} \quad \text{----------(1.14)}$$

The performance of an electro-optical PDLC device also depends on light scattering properties of the PDLC film [2, 20]. The transmitted light intensity I_t of a parallel beam of linearly polarized light of intensity I_o incident at a specific angle φ, on a PDLC cell in OFF state is given by

$$I_t = I_0 e^{-\beta t \sigma} \quad \text{----------(1.15)}$$

where β = volume density of the droplets, t = path length through the layer, defined as

$t = d\cos\varphi$ with d the thickness of the layer and σ a measure of the scattering capability of a droplet. For a nematic LC droplet of radius R, σ is defined as,

$$\sigma = 2\sigma_o (KR)^2 \left[\frac{n(\varphi)}{n_p} - 1 \right]^2 \quad \text{----------(1.16)}$$

Where $K=2\pi/\lambda$, σ_o is the geometrical cross section and $n(\varphi)$ is the refractive index of the LC droplet.

A brief discussion on LCs and the methods used to fabricate switchable LC optoelectronic devices is presented in this chapter. Electro optics of nematic LCs, TNLC devices and PDLC materials are also presented. In the present work surface relief gratings filled with LCs to fabricate LC switchable devices are reported. A novel PDLC material for holographic recording was also developed and used to fabricate switchable devices. These switchable LC devices were fabricated by exploiting holographic technique. A brief discussion of holography is given in the next chapter.

References

1. P. J. Collings, “Liquid crystals: Nature’s delicate phase of matter.” Princeton University press, 2002
2. B. Bahadur, “Liquid crystals: Applications and uses” Vol.1, World Scientific publishers, 1990.
3. K. Hubert, S. Desmond and A. Nandana, “Liquid crystal: Nature’s Perfect light switch.” Spectra Switch inc., http://www.spectraswitch.com/news_events/articles/FiberOpticNewsJul2001/fopn701.htm 5-2-2006.
4. T. Ikeda, “Photomodulation of liquid crystal orientations for photonic applications.” J.Mater.Chem., 13, 2037-2057,2003.
5. M. J. Bradshaw, “Liquid crystal devices.” Phys.Educ., 18, 20-26,1983.
6. Polymer and Liquid crystals: virtual text book, http://plc.cwru.edu/tutorial/enhanced/files/textbook.htm 5-2-2006.
7. H. Gleeson, “Introduction to liquid crystals.” Manchester University, 1998. http://reynolds.ph.man.ac.uk/pdf/intro_to_lcs.pdf 5-2-2006.
8. R. S. McEwen, “Instrument Science and Technology: Liquid crystals, displays and devices for optical processing.” J. Phys. E: Sci. Instrum. 20, 364-377, 1987.
9. R. G. Howard, “Liquid crystalline polymers for nonlinear optics and polarised fluorescence.” Doctoral thesis, University of Dublin, 1997.
10. J. Cognard, “Alignment of nematic liquid crystals and their mixtures.” Mol. Crys. Liq. Crys., supplement 1, 1-78, 1982.
11. M. O’Neill and S. M. Kelly, “Photoinduced surface alignment for liquid crystal displays.” J.Phys.D.Appl.Phys.3, 67-84, 2000.

12. D. Dantsker, J. Kumar and S. K. Tripathy, “Optical alignment of liquid crystals.” J. Appl. Phys, 89(8), 4318-4325, 2001.
13. X. T. Li, A. Natansohn and P. Rochon, “Photoinduced liquid crystal alignment based on a surface relief gratings in an assembled cell.” Appl. Phys Lett. 74(25), 3791-3793, 1999.
14. V. V. Lazarev, M. I. Barnik and N. M. Shtykov, “Liquid crystal alignment by photo-processed polymer films.” Mol. Materials, 8, 235-244, 1997.
15. J. Qi and G. P. Crawford “Holographically formed polymer dispersed liquid crystal displays.” Displays, 25, 177-186, 2004.
16. M. S. Malcuit, M. E. Holmes and M. A. Rodriguez,” Characterization of PDLC Holographic Gratings.” Lasers and electro optics, 395-396, 2001.
17. D. E. Lucchetta, L. Criante and F. Simoni, “Optical characterization of polymer dispersed liquid crystals for holographic recording.” J.Appl.Phy., 93(12), 9669-9674, 2003.
18. D. E. Lucchetta, R. Karapinar, A. Manni and F. Simoni, “Phase-only modulation by nanosized polymer-dispersed liquid crystals.” J.Appl.Phys, 91(9), 6060-6065 2002.
19. T. J. Bunning, L. V. Natarajan, V. P. Tondiglia and R. L. Sutherland “Holographic Polymer-Dispersed Liquid Crystals (H_PDLCs).” Annu. Rev. Mater.Sci, 30, 83-115, 2000.
20. S. J. Cox, V. Yu. Reshetnyak and T. J. Sluckin, “Effective medium theory of light scattering in polymer dispersed LC films.” J. Phys. D:Appl. Phys. 31, 1611-1625, 1998.

2. HOLOGRAPHY AND RECORDING MATERIALS

2.1. Introduction

Holography is a technique for reproducing a three dimensional image of an object by using interference of light waves recorded in a photo sensitive medium. In photography, which is a conventional imaging technique, a two dimensional image of a three dimensional object is recorded. Only the intensity distribution of light from the original object is recorded. All information about relative phases of light coming from different points of the object (that means the optical path differences between light from different points of the object) is lost. But in holography the complete information about an object is recorded which means that both amplitude and phase of light waves scattered or reflected from the object are recorded. Holography is also sometimes known as lensless photography [1, 2].

The idea of holographic imaging was first proposed by Dennis Gabor in 1948 [1, 2]. His aim was to improve the resolution in electron microscopy. He was awarded a Nobel prize in 1971 for his invention. In Gabor's experiment, the object was a transparency consisting of a clear background with a few fine opaque lines on it. When this transparency was illuminated with a collimated beam of monochromatic light, the Fresnel diffraction pattern of the transparency was recorded on a photographic plate. When this hologram was illuminated once again with a collimated monochromatic beam, two diffracted waves were obtained, one corresponding to the original scattered wave from the object and the other, with the same amplitude but with its variations in phase having opposite sign. This second wave was the phase conjugate of the original

wave from the object and formed a real, conjugate, image in space. Gabor's technique of recording holograms is also called in-line holography. There were some drawbacks in his method of hologram recording where the normal and conjugate images, so called twin images, were observed during reconstruction in the same direction. After Gabor's work, several attempts were made to record holograms. However it was not until the invention of the laser, which provided a coherent light source of sufficient intensity, that holography found any real application.

The first successful method for separating the twin images was developed by Leith and Upatnieks in mid 1960s [3-4]. They used a separate reference beam derived from the same laser source to record the hologram. This reference beam was incident onto the photosensitive plate at an angle offset to the object beam. As the object and reference beams are incident at an angle to one another this method of hologram recording is called the "off-axis method". They showed that three-dimensional images can be generated by illuminating a recorded hologram with laser light. Almost at the same time Denisyuk introduced the recording of reflection holograms [5]. A reflection hologram is recorded when the reference beam and the object beam are incident on the photosensitive medium from opposite sides. When these holograms are illuminated with a point source of white light or the sun, they reconstruct images of acceptable quality, similar to those obtained with monochromatic illumination in transmission holograms.

Holography is now a widely used technique whose range of applications has extended considerably from a method of producing three dimensional images to non-destructive testing [6], optical information processing [7], data storage [8], holographic optical elements [9] and security holograms [10].

2.2 Types of holograms:

A hologram recorded on the photo sensitive material is generally equivalent to a diffraction grating with a spatially varying transmittance and/or refractive index (or thickness) or birefringence and spatial frequency. Holograms are classified based on recording geometry, thickness and method of modulation of optical properties.

Recording geometry is either transmission or reflection.

2.2.1 Transmission holograms:

In a transmission hologram the object beam and reference beam (recording beams) are incident from the same side of the photo sensitive medium and interfere in the recording medium (Figure 2.1). The image of the object is reconstructed by diffraction of the reference beam by the recorded hologram. Usually transmission holograms are reconstructed with monochromatic light. When $\alpha = \beta$, the hologram is unslanted and when $\alpha \neq \beta$ it is slanted.

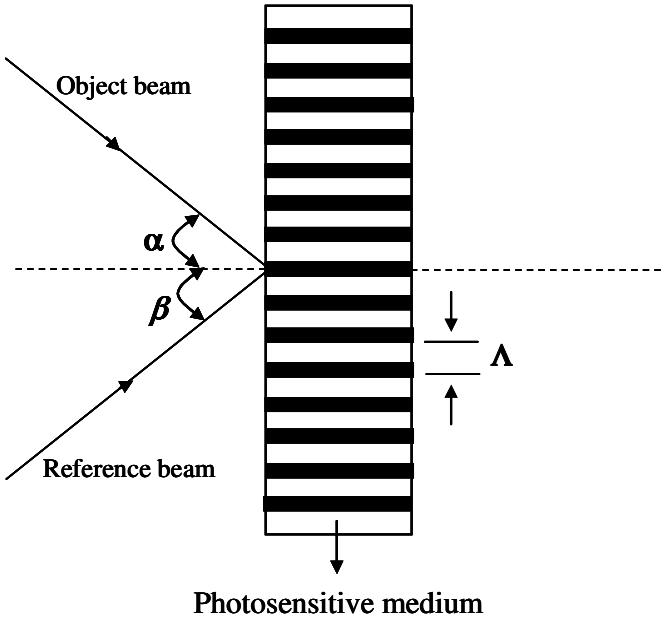

Figure 2.1Interference pattern in transmission hologram where α and β are angles of incidence for object beam and reference beam and Λ is fringe spacing.

2.2.2 Reflection holograms:

In a reflection hologram the two recording beams (object beam and reference beam) are incident from the two opposite sides of the photosensitive medium. The interference fringes are formed nearly parallel to the surface of the recording medium. During reconstruction, the hologram is illuminated by light from the same side of the photosensitive medium as the observer and the image is reconstructed in reflection from the hologram. These holograms can be reconstructed by using white light because they also act as spectral filters and so are also called white light holograms. The geometry of the experimental setup for recording reflection holograms is shown in figure 2.2.

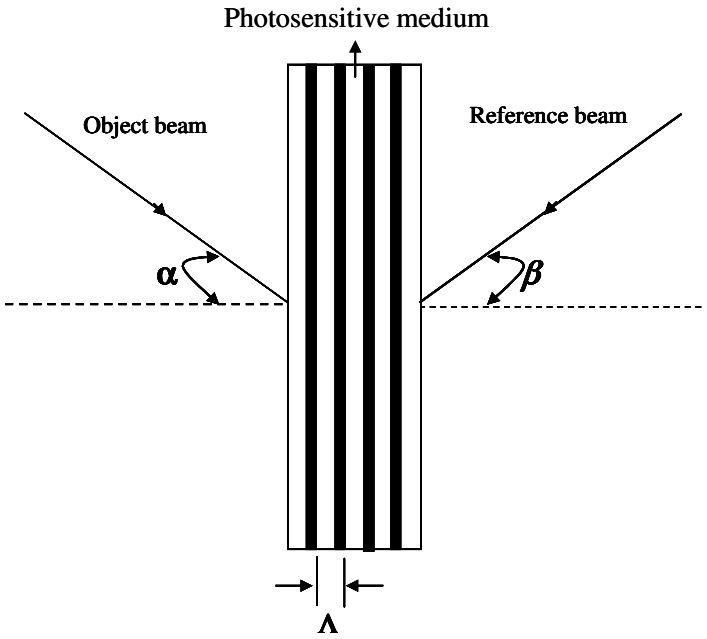

Figure 2.2 Interference pattern in reflection hologram where α and β are angle of incidence for object beam and reference beam and Λ is fringe spacing.

When $\alpha = \beta$, the hologram is unslanted and when $\alpha \neq \beta$ it is slanted. Slanted holograms require careful consideration if the recording material is liable to dimensional changes (for instance shrinkage).

2.2.3 Thick and thin holograms

Holograms are also of two types, thin and thick (volume). Kogelnik used the value of the *Q*-factor to distinguish between thin and thick holograms [11]. *Q*-factor is defined as

$$Q = \frac{2\pi\lambda d}{n\Lambda^2} \quad \text{---------- (2.1)}$$

where, λ is the wavelength of the incident reference beam, n is the refractive index of the recording medium, Λ is fringe spacing of the holographic grating and d is the thickness of the layer on which hologram is recorded.

A thin hologram is one whose Q-factor is < 10.
A thick hologram is one with $Q > 10$.

2.2.4 Amplitude and phase holograms

Holograms may also be of amplitude and phase types depending on what property of the recording medium is modulated during the recording process.

An amplitude hologram is recorded as a spatial variation in the amplitude transmissivity of the photosensitive medium.
Phase holograms are recorded as a spatial variation in the refractive index and/or thickness of the recording layer.

To summarize, holograms can be thin or thick depending on the thickness of recording medium and the fringe spacing. Thick holograms can either be reflection or transmission holograms. Thin holograms are necessarily transmission holograms. Finally each of these three types of holograms may be recorded as either a phase or amplitude hologram.

Diffraction efficiency is the main characteristic of the hologram and in non-scattering materials is normally defined as the ratio of the intensity of the diffracted light beam to

the intensity of the incident beam. The maximum theoretical diffraction efficiency of various types of holograms is given in table 2.1 [11, 12].

Table 2.1: Maximum efficiencies of various types of holograms

Amplitude holograms			Phase holograms		
Thin transmission	Thick transmission	Thick reflection	Thin transmission	Thick transmission	Thick reflection
6.25 %	3.7 %	7.2 %	33.9 %	100 %	100 %

From the table it is seen that the efficiency of amplitude holograms is less than efficiency of the phase holograms. This is due to the fact that amplitude holograms rely on absorption of the light and thus some of the energy of the reading beam is wasted during reconstruction whereas phase holograms are nearly transparent and use the reconstructing light more effectively.

2.3. Polarization holograms

With scalar holographic techniques, the amplitude and phase of the object wavefront are recorded. However, information about its state of polarization is lost.

When orthogonally polarized object and reference waves interfere, in the region of overlap standing waves with a spatially varying state of polarization are recorded. Such a recording when illuminated by coherent polarized wave can reconstruct the polarization state of the original object wave in addition to its amplitude and phase. This type of hologram is known as a polarization hologram.

2.4. Holographic recording media

There are different types of holographic recording materials such as silver halide photographic emulsions, dichromated gelatin, photoresists, thermoplastics, photochromics, photorefractive materials and photopolymers [11, 12].

Table 2.2 Recording materials for holography.

Recording material	Advantages	Disadvantages
Silver halide photographic emulsions (SHPE)	High sensitivities, high resolution, high diffraction efficiencies	Wet chemical processing, shrinkage
Dichromated gelatin	High resolution, high DE, lower sensitivity (compared with SHPE), high optical quality, grainless	Wet chemical processing
Photoresists	Low granularity, high resolution	Low sensitivities, usually UV sensitive, chemical processing
Photochromics	No post processing, easy to prepare	Low sensitivity, low DE, degradation
Photorefractives	No post processing, reversible, high DE, sensitivity, high thicknesses	Stability
Photo thermoplastics	High sensitivity, high DE, no wet chemical processing, re-usable	Low spatial resolution
Photopolymers	High sensitivity, high DE, self processing, high resolution	Stability varies with composition of material.
Polymer composite (PDLCs)	High index modulation, unique anisotropic nature, electro optical behaviour	Scattering, Complicated sample preparation

Specific materials have significant advantages for particular holographic applications. To record holograms the recording material should have properties like sensitivity to recording wavelength, a linear transfer characteristic, high resolution and low noise [11].

Table 2.2 shows different types of holographic recording materials and their advantages and disadvantages. Since the work reported uses photopolymers, a detailed explanation of the recording process in photopolymers is given below.

2.5. Photopolymers

There are several organic materials called photopolymers, which can be activated by a photosensitizer to produce refractive index modulation due to photopolymerization when exposed to light. Photopolymers are attracting attention for holographic applications because of their unique properties like self development, ease of preparation and low cost compared to other recording materials [15]. Photopolymers are volume phase recording materials, which have applications in real-time holographic interferometry [9], holographic optical elements [13], and holographic data storage [14] and holographic sensors [15, 16].

There are two types of photopolymers: crosslinking photopolymers and polymerizable photopolymers. In crosslinking photopolymeric materials the phase change in the hologram is caused by modification of the local refractive index modulation when crosslinks between the polymer strands are broken or formed so that the molecular polarizability of these bonds is altered. The second type of photopolymer recording material is photopolymerizable material. Like photocrosslinking photopolymer materials, the sensitivity of photopolymerizable materials is lower than silver halide emulsions but varies greatly depending on different formulations. Photopolymers can be

generally classified as liquid or solid dry photopolymers, the difference being the inclusion of a binder for the dry layer format.

The photopolymerizable layer usually consists of a polymerizable monomer, an initiator and a sensitizer. If the layer is solid then there will also be a polymeric binder. The mechanism of recording in photopolymerizable photopolymer recording materials can be described as follows. When light of appropriate wavelength is incident on the photosensitive medium, the dye sensitizer molecule absorbs a photon and enters into a excited singlet state. The excited singlet state dye molecule enters into a excited triplet state through intersystem crossing and reacts with the electron donor to generate a free radical. These free radicals in the presence of monomer initiate the polymerization reaction resulting in a local change of the molecular refractivity due to the conversion of C=C into C-C. In addition, as monomer is depleted by polymerization, diffusion of monomer occurs from dark to bright regions resulting in a spatially modulated density. This redistribution of material results in refractive index modulation corresponding to the interference pattern produced by the incident light beams, resulting in a phase hologram. The main advantage of these materials is that they are self-developing, capable of recording 100 % diffraction efficiency gratings, and can be prepared in much greater thicknesses for volume holographic multiplexing. These materials can be sensitized to different wavelengths by using different dyes and can also be prepared with ease.

There are high performance, commercially available photopolymers, DuPont OmniDex, Polaroid DMP 128 (Aprilis photopolymer) and Inphase. These photopolymers are expensive and their compositions are proprietary [17-21]. As photopolymers are

promising materials for holography, many research groups are working to improve their performance [22-27]. The photopolymer used in this work is acrylamide based photopolymer [29].

2.6. Optical recording in an acrylamide based photopolymer

The acrylamide based photopolymer used in this work was developed and formulated at the Centre for Industrial and Engineering Optics [25-28]. It has been used for different holographic applications such as holographic data storage, interferometry and for fabricating optical elements. It consist of two polymerizable monomers (acrylamide and N, N'-methylene bisacrylamide), an electron donor (triethanolamine), a photosensitive dye (erythrosine B) and a binder (polyvinyl alcohol). Optical recording in this material is based on photopolymerization.

In this section the photochemical processes that occur in an acrylamide-based photopolymer when illuminated by of light of suitable wavelength are discussed. The main objective in this work is to record surface relief gratings and fill them with LCs to fabricate LC optoelectronic devices.

The simplest transmission hologram that can be recorded is a diffraction grating. There are different theoretical models explaining formation of holograms in photopolymer material [23, 24] due to mass transport from dark to bright regions. From the diffusion studies of acrylamide based photopolymer [25-28] it was observed that the mass transport from dark to bright regions is faster than in other photopolymer systems [20, 31].

When a hologram is recorded in a photopolymer, a refractive index modulation or variation of thickness of the layer is produced, as a result of several processes as explained in section 2.6.1. If a variation of thickness of photosensitive material is produced then it is called a surface relief grating.

2.6.1 Photopolymerization

Polymerization is defined as the process in which many small molecules (monomers) are combined to form a large molecule called a polymer. The most common polymerization is free radical polymerization [26]. In this process light is absorbed by an appropriate dye, which reacts with an electron donor to produce the free radical necessary for initiation of polymerization.

In the work erythrosine B, a xanthene dye was used as a photoinitiator. When a photosensitive dye (erythrosine B) is exposed to a light of appropriate wavelength the dye (XD) absorbs a photon of the light and enters into an excited singlet state (^{1}XD*) [25, 26].

$$XD + h\nu \rightarrow {}^1XD^* \text{ ---------- (2.2)}$$

This may either revert to the ground state by emission of a photon (fluorescence) or by radiationless energy transfer to another molecule e.g. the electron donor, ED, (fluorescence quenching)

$$^1XD^* \rightarrow XD + h\nu \quad \text{(fluorescence)---------- (2.3)}$$

$$^{1}XD^{*} + ED \rightarrow XD + ED \quad \text{(fluorescence quenching)} \text{ ---------- (2.4)}$$

or it may cross over to the more stable long lived lower excited triplet state ($^{3}XD^{*}$) (intersystem crossing).

$$^{1}XD^{*} \rightarrow {}^{3}XD^{*} \text{ (intersystem crossing)} \text{ ---------- (2.5)}$$

The excited triplet state dye molecules may revert to the ground state by radiationless transfer (triplet quenching) or by phosphorescence or fluorescence. At high dye concentrations, concentration quenching can also occur.

$$^{3}XD^{*} + XD \rightarrow 2XD \quad \text{(concentration quenching of triplet state)} \text{ ---------- (2.6)}$$

Oxygen quenching is also an important process that may lead to the reduction of triplet and singlet state quantum yields and usually causes an 'inhibition period' at the beginning of the polymerization [32]. During the holographic exposure the oxygen present in the photopolymer layer is used up before starting the polymerization.

$$^{3}XD^{*} + {}^{3}O_{2} \rightarrow XD + {}^{3}O_{2}^{*} \quad \text{(Oxygen quenching)} \text{ ---------- (2.7)}$$

$$^{1}XD^{*} + {}^{3}O_{2} \rightarrow XD + {}^{1}O_{2}^{*} \quad \text{(Oxygen quenching)} \text{ ---------- (2.8)}$$

However, the main pathway to polymerization is thought to be the formation of a free radical.

Triethanolamine donates an electron to the excited triplet state of the dye molecule leaving the latter with one unpaired electron and an overall negative charge.

$$^{3}XD^{*} + (HOCH_2CH_2)_3N: \rightarrow XD^{\bullet -} + (HOCH_2CH_2)_3N^{\bullet +} \quad \text{----------(2.9)}$$

The triethanolamine radical cation then loses a proton and becomes an uncharged free radical.

$$(HOCH_2CH_2)_3N^{\bullet +} \rightarrow (HOCH_2CH_2)_2NCH^{\bullet}CH_2OH + H^{+} \quad \text{---------- (2.10)}$$

The triethanolamine radicals produced in the above reaction are the initiating species for the polymerization process.

This free radical in the presence of monomer molecule (acrylamide) can react in two ways. It can react either with a dye radical to form a leuco (bleached or colourless) form of the dye (thereby using up the dye radicals) or it can react with a monomer to initiate free radical polymerization [32]. Therefore, the bleaching rate in the presence of monomer could be less than in the absence of monomer.

$$TEA^{\bullet} + M\ (\text{monomer}) \rightarrow TEA - M^{\bullet} \quad (\text{initiation}) \quad \text{----------(2.11)}$$

$$TEA^{\bullet} - M^{\bullet} + M \rightarrow TEA - (M)2^{\bullet} \quad (propagation) \quad \text{----------(2.12)}$$

Bleaching of the dye is also a very important step for final transparency of holograms. Furthermore if the bleaching process is irreversible, then, there will not be any further photosensitization on light illumination when the dye is completely bleached.

The polymerization reaction continues until all the monomer is consumed or a termination reaction occurs. There are two ways in which a termination reaction could occur, either combination and/or disproportionation reaction. When the termination occurs by combination, two free radicals meet and share their single odd electron forming a covalent bond resulting in single polymer chain. In a disproportionation termination reaction, termination occurs when a hydrogen atom is abstracted from one of the growing polymer chains to the other, leaving a double bond on one of the terminated polymer chains.

During the process of recording a holographic diffraction grating, the rate of growth of diffraction efficiency depends on several physical and chemical factors. The one of the factor is the rate of polymerization, but this depends on the rate of initiation and propagation which in turn depends on the concentrations of the monomer and initiator. The local concentration of the monomer at any time will depend not only on the percentage conversion, but also on the diffusion of monomer from the unpolymerized dark fringe region into polymerized bright fringe regions. This polymerization process continues until all the monomer is consumed. As a result of these processes the refractive index changes and the grating is recorded. In addition to the refractive index changes some surface relief changes are induced during the holographic recording.

The surface relief gratings recorded in this material were filled with LCs to fabricate LC optoelectronic devices. A detailed investigation of the dependence of photo induced surface relief gratings on recording and physical parameters is explained in the next chapter. It also explains the advantage of using holographic technique to fabricate these devices.

2.7 Novel PDLC material

Another promising holographic material used in this work is a new PDLC material developed in IEO centre which has the advantages of the photopolymers and LCs. It consists of monomers (acrylamide and N, N'-methylene bisacrylamide), coinitiator (TEA), photosensitizer (erythrosine B), LCs and a reactive diluent (n-vinyl-2-pyrrolidinone). The use of acrylamide and N, N'- methylenebisacrylamide as monomers in HPDLC formulations are used for the first time in this work. Optical recording in this PDLC material is based on polymerization induced phase separation which is explained in chapter 6. This results in spatially periodic structures with alternating polymer and LC rich planes in the volume of the layer. A diffraction grating is created as a result of refractive index modulation between polymer and LC rich planes. A detailed discussion of these devices is given in chapter 6.

References

1. D. Gabor, “A new microscopic principle.” Nature, Vol.161, 777-778, 1948.
2. D. Gabor, “Microscopy by reconstructed wavefronts.” Proc.Royal Society A, Vol.197, 454-487, 1949.
3. E. N. Leith and J. Upatnieks, “Wavefront reconstruction with diffused illumination and three dimensional objects.” J.Opt.Soc.Am., Vol.54, 1295-1301, 1964.
4. E. N. Leith and J. Upatnieks, “Holographic imagery through diffusing media.” J.Opt.Soc.Am., Vol.56, 523, 1966.
5. Y. N. Denisyuk, “On the reproduction of the optical properties of an object in its own scattered radiation field.” J.Opt.and Spec. Vol.15, 279-284, 1963.
6. R. K. Erf, “Holographic non-destructive testing.” Academic Press, New York 1974.
7. B. D. Genther, C. R. Christensen and J. Upatnieks, “Coherent optical processing: another approach.” IEEE J.Quant Elect. Vol.15,1348-1362, 1979.
8. A. Kozma, “Holographic storage.” Proc.SPIE, Vol.53, 77-83, 1974.
9. S. Guntaka, V. Toal and S. Martin, “Holographically recorded diffractive optical elements for holographic and electronic speckle pattern interferometry.” Appl.Opt. Vol.41, No.35, 7475-7479, 2002.
10. S. K. Kaura, D. P. Chhachhia and A. K. Aggarwal, “ Interferometric Moire pattern encoded security holograms.”, J. Opt. A: Pure Appl. Opt., 8, 67-71, 2006.
11. P. Hariharan, “Optical holography: Principles techniques and applications.” 2nd Edition, Chapter 4, 45-67, Cambridge monographics on physics, Cambridge University Press, 1996.

12. J. F. Ready, “Industrial applications of lasers.” 2nd edition, Elsevier, 1997.
13. S. R. Guntaka, V. Toal and S. Martin, “Holographic and Electronic Speckle-Pattern Interferometry using a Photopolymer Recording Material” Strain, Vol.40, No.2, 79-81, 2004.
14. H. Sherif, I. Naydenova, S. Martin, C. McGinn and V.Toal “Characterisation of an acrylamide-based photopolymer for data storage utilizing holographic angular multiplexing.” J.Opt.A: Pure and Appl.Opt. Vol.7, 255-260, 2005.
15. I. Naydenova, R. Jallapuram, V. Toal and S. Martin, “Visual indication of environmental humidity using a colour changing hologram recorded in a self-developing photopolymer.” Appl. Phys. Lett., 92, 031109, 2008
16. A. J. Marshall, J. Blyth, C. Davidson and C. R. Lowe, “pH-Sensitive holographic sensors.” Analyt. Chem., 75 (17), 4423-4431, 2003.
17. B. L. Booth, “Photopolymer materials for holography.” Appl.Opt., 14(3), 593-601, 1975.
18. R.T. Ingwall and M. Troll, “Mechanism of hologram formation in DMP-128 photopolymer.” Opt. Eng., 28, 586-591, 1989.
19. W. K. Smothers and A. M. Weber, “Photopolymers for holography.” Proc. SPIE 1212, 351-160, 1990.
20. A. M. Weber and W.K. Smothers, T.J. Trout, and D.J. Mikish, “Holographic recording in DuPont’s new photopolymer material.” Proc SPIE 1212, 30-39, 1990.
21. “Inphase technologies achieves benchmark in digital recording media density; New holographic technique enables terabyte disc recording.” http://findarticles.com/p/articles/mi_m0EIN/is_2005_April_18/ai_n13628099 4-3-2006.

22. B. M. Monroe, W. K. Smothers, D. E. Keys, R. R. Krebs, D. J. MicKish, A. F. Harrington, S. R. Schickers, M. K. Armstrong, D. M. T. Chan and C. I. Weathers, “Improved photopolymers for holographic recording.” part 1. J. Imaging Sci. 35, 19-25, 1991.
23. G. Zhao and P. Mouroulis, “Diffusion model of hologram formation in dry photopolymer materials.” J.Mod. Opt., 41, 1929-1939, 1994.
24. S. Piazzolla and B. Jenkins, “First-harmonic diffusion model for holographic grating formation in photopolymers.” J.Opt.Soc.Am.B., 17(7), 1147-1157, 2000.
25. S. Martin, “A new photopolymer recording material for holographic applications: photochemical and holographic studies towards an optimized system” Doctoral thesis, Dublin Institute of Technology by, 1995.
26. R. Jallapuram, “Optimization of an acrylamide-based photopolymer for reflection holographic recording.” Doctoral thesis, Dublin Institute of Technology, 2005**.**
27. I. Naydenova, S. Martin, R. Jallapuram, R. Howard and V. Toal,” Investigations of the diffusion processes in self-processing acrylamide-based photopolymer system”, Applied Optics, 43 (14), 2900, 2004.
28. C. A. Feely, S. Martin, V. Toal, A. Fimia and F. Mateos, "Optimization of a red sensitive photopolymer." Holographic Materials III, SPIE Photonics west, San Jose, USA, Proc. SPIE 2688, 1995.
29. J. R. Lawrence, F. T. O’ Neill and J. T. Sheridan, “Photopolymer holographic recording material”, Optik, 112(10), 449-463, 2001.
30. V. L. Colvin, R.G. Larson, A.L Harris and M.L Schilling, “Quantitative model of volume hologram formation in photopolymer materials”, J. Appl. Phys. 81, 5913-5923, 1997.

31. V. Moreau, Y. Renotte and Y. Lion, “Characterization of dupont photopolymer: determination of kinetic parameters in a diffusion model.” Appl. Opt., 41(17), 3427-3435, 2002.
32. J.B. Birks, “Organic Molecular Photophysics”, Chap.2, 153-154, John Wiley and Son, New York, 1975.
33. A. Giz, H. Giz, J.L. Brousseau, A. Alb and W.F. Reed, “Kinetics and mechanism of acrylamide polymerization by absolute, online monitoring of polymerization kinetics”, Macromolecules, 34(5), 1180-1191, 2001.

3. PHOTOINDUCED SURFACE RELIEF STUDIES IN AN ACRYLAMIDE-BASED PHOTOPOLYMER

3.1 Introduction

Photopolymers are of considerable interest for the development of holographic applications because of their unique property of self development when exposed to light. However, not all of the photopolymers are completely self-developing. The commercially available DuPont photopolymer needs uniform UV post exposure and heat treatment to achieve maximum diffraction efficiency. Photopolymers which can record photoinduced surface relief gratings are attractive for application in diffractive optical elements [1, 2], optical data storage [3], recording of computer generated holograms [4] and the alignment of LCs [5-8]. There has been extensive growth of technological applications of LCs, such as photonic components and LCDs in the last two decades. To fabricate these devices, uniform alignment of the LCs is essential. Recently, for the alignment of LCs non rubbing techniques have been investigated to avoid creation of static electricity and dust which are not desirable. An alternative approach for LC alignment would be to utilize the periodical surface relief structures inscribed in photopolymerizable materials. When the photosensitive material is exposed to an interference pattern of light of suitable wavelength, a surface relief grating, that is a variation of the thickness of the material, is produced. This effect is often called surface relief amplitude modulation. Light induced surface relief gratings in photopolymer have the potential to align LCs [5-8]. In order to control their properties it is important to investigate the mechanism of the formation of surface relief gratings and the dependence of surface relief amplitude and profile on recording parameters and on the physical properties of the layers.

An investigation of the photoinduced surface relief modulation in thick layers (50-250μm) of an acrylamide-based photopolymer system [9-11] was reported earlier [13]. Although the resolution of the material needs to be high in order to record volume holograms, surface relief gratings can only be made at low spatial frequencies. However it is anticipated that LC devices may be fabricated by exploiting the effect even at quite low spatial frequency (~100 lines/mm). To study their properties the photoinduced surface relief profiles were obtained with a white light interferometer (WLI) [14, 15] after recording.

The main goal of this chapter is to report the dependence of surface relief amplitude modulation on recording parameters such as spatial frequency, intensity, exposure energy, uniform UV post exposure and on the thickness of the layer (2-80 μm), composition of photopolymer and the effect of heating the grating. Crossed gratings were also recorded using two orthogonal interference patterns. Preliminary results of the fabrication and dependence of the crossed gratings on the time of exposure are also discussed in this chapter.

3.2 Theory

Optical recording in an acrylamide based photopolymer is based on photopolymerization reactions caused in the areas illuminated by light, as discussed in chapter 2. Due to polymerization there is a change in the density and the molecular polarizability, which in turn changes the local photopolymer refractive index and a

grating is recorded. If the thickness of the layer is also modulated then a surface relief grating is recorded. There are different theoretical models proposed in order to explain the formation of holograms in photopolymer recording material.

There are two main models describing the surface relief formation in photopolymers. The first explains the relief formation by shrinkage of the photopolymer depending on the intensity of light. This model is applicable to systems where the peaks of the surface relief appear in the non-illuminated areas [20, 22]. The second model, based on the assumption that redistribution of system components by diffusion is responsible for the relief formation, suits systems such as ours where experimental observation shows the surface relief peaks appearing in the illuminated areas [1, 2, 13, 22]. The causes proposed for diffusion of the components are a monomer chemical potential gradient [1], concentration gradient of monomer [2] and local shrinkage of a polymer layer [21]. All of the proposed causes consider the change in the surface free energy during the relief formation as the main reason for the restricted resolution of the inscribed relief structures [1, 2, 20, 21].

Previous studies in acrylamide-based photopolymer report that the main mechanism of surface relief formation is the mass transport or diffusion of monomer from the dark to bright regions [16, 17]. From the diffusion studies of an acrylamide based photopolymer [12] it was observed that the monomer diffusion is faster than in other commercially available photopolymer systems [18, 19] and this is in agreement with the surface relief amplitude dependence at low spatial frequencies.

Some of these models consider the possibility of counter diffusion of material from bright to dark fringe areas [23] and its influence on the formation of surface relief gratings [13, 24]. In the analysis of the surface relief formation in thin photopolymer layers a new factor must be considered in addition to those mentioned above. When the thickness of the layers approaches few micrometers the interaction between the photopolymer and the substrate appears to play an important role in determining the ultimate surface relief amplitude and shape [22].

3.3 Experimental

3.3.1 Sample preparation

The material used here is a self-developing, acrylamide based, water soluble photopolymer. The general composition of this material is acrylamide, N, N'-methylenebisacrylamide monomers, triethanolamine initiator, polyvinyl alcohol (PVA) binder and Erythrosin B sensitizing dye [9-13]. The above components were mixed well by using a magnetic stirrer and the dye was added finally. Good optical quality photopolymer layers were prepared by using spin coating and gravity settling methods.

Spin coating: Spin coating involves the rapid evaporation of solvent by high speed spinning to get good quality dry layers. Thickness of layers ranging from one micron to about ten microns with very high viscosity liquids can be obtained.

After mixing the components, the solution was spin coated on a thin glass plate of 1"x1" to get thin layers of photopolymers. By changing speed of rotation (V), time of rotation

(T) and quantity of photopolymer solution (Q) dropped on the glass, the thickness of the sample can be controlled. In preliminary investigations, it was observed that photopolymer solutions prepared with 10 % w/w PVA stock solution did not produce good optical quality layers. To improve the quality of the layers the concentration of PVA stock solution was changed to 20 % w/w as spin coating needs viscous liquid. After preparation, samples were allowed to dry at room temperature for 17 hours. They were exposed to record surface relief gratings but the measured amplitude modulation was very low. To get better results samples were dried for 3 to 4 hours at room temperature. These investigations also showed that if the thickness of the sample is less than 2 μm, the amplitude modulation was not measurable though it can be seen that there is a grating with the WLI. To get better results the thickness of the photopolymer layer was maintained at 2 to 2.5 μm. The speed of rotation was chosen to be 2750 rpm, for 10 sec and for a 1 ml of photopolymer solution dropped on glass plate to get this thickness. Samples of different thicknesses were prepared by changing V, T, and Q.

Gravity settling: Gravity settling is a simple method of layer coating. A known amount of photosensitive mixture is spread on a leveled glass substrate and allowed to dry by evaporation. With this method much thicker samples can be prepared.

The photopolymer solution was gravity settled on a 5x5 cm^2 or 2.5x3 cm^2 glass plates. To prepare samples with different thicknesses, the photopolymer solution was diluted with deionised water. They were allowed to dry under ambient room conditions for 17 hours. Good optical quality samples were prepared from 2.5 μm to 80 μm thickness. The thickness of the sample depends on the amount of dilution and on the amount of

solution spread on the glass plate. After the samples were dried, a cut was made on the sample and its thickness was measured by using the white light interferometer.

3.3.2 Holographic recording

Surface relief gratings were optically recorded at different spatial frequencies. Two different optical recording systems were used to record surface relief gratings.

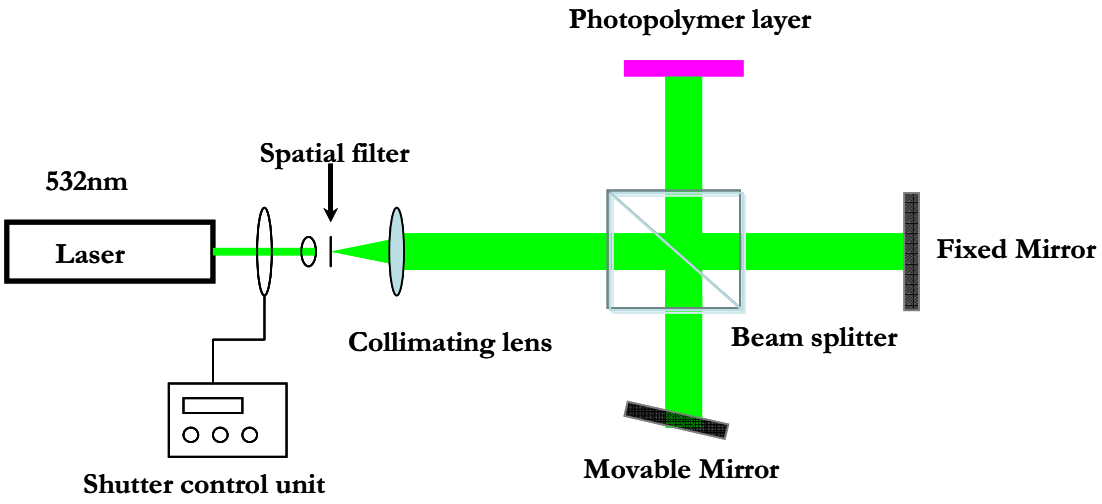

Figure 3.1 Experimental set up to record low spatial frequency patterns.

The Michelson interferometer optical setup (figure. 3.1) was used to record surface relief transmission diffraction gratings at less than 70 lines/mm. The spatial frequency was adjusted by rotating one of the mirrors shown in figure 3.1.

A two-arm holographic optical setup which is shown in figure 3.2 was used to record surface relief gratings at spatial frequencies above 100 lines/mm. A s- polarized laser beam with wavelength 532 nm was used to record the transmission diffraction gratings because the photosensitive dye used in this work has sensitivity at this wavelength.

The spatial frequency was calculated by using the Bragg equation

$$2\Lambda \sin\theta = \lambda \quad \text{----------} \quad (3.1)$$

where Λ= fringe spacing, 2θ = inter beam angle and λ = wavelength.

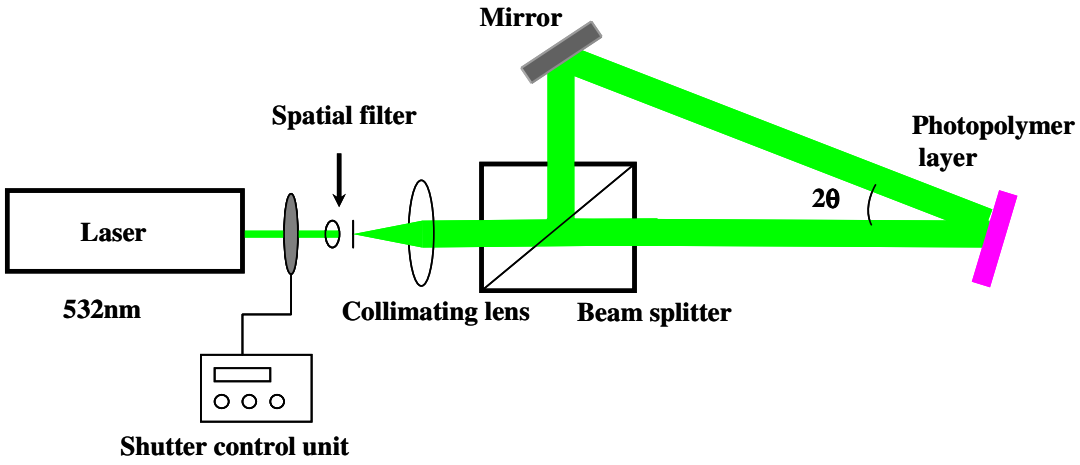

Figure 3.2 Experimental set up to record high spatial frequency patterns.

The surface relief gratings were recorded on the photopolymer samples of various thicknesses under different recording conditions. These samples were scanned typically an hour after recording using a white light interferometer. White light interferometry is an extremely powerful technique for surface profile measurement. This technique is based on the principle that interference fringes can only be obtained when the optical path difference is less then the coherence length of the light source. It has significant advantages in measuring surface profiles as the measurement is non-contact with very high vertical resolution of ~ 1 nm and vertical scanning range of 100 μm.

3.4 Results and discussion

3.4.1 Positions of the surface relief peaks

In order to determine the positions of the surface relief peaks, holographic gratings with low spatial frequency of 2 lines/mm were recorded in spin coated layers with thickness of 2 μm. The recording time was varied between 5 and 10 sec and the intensity of the recording laser beam was between 10 and 30 mW/cm^2. The sample surface was examined with a Dektak_3 profiler equipped with a camera. This facilitates observation of the position of the measuring tip on the surface during the scan. The illuminated and non-illuminated areas of the photopolymer surface are well distinguished as white and pink stripes (Erythrosine B causes the unexposed stripes to appear pink). The position of the tip with respect to the bleached and unbleached areas can be easily correlated to the measurement in the vertical direction. The results from this measurement are presented in figure 3.3. It was observed that the surface relief peaks appear in the areas where the light was absorbed. This is in agreement with previous results from investigation of surface relief modulation in thick acrylamide photopolymer films after light exposure through a mask [9]. The observation of the surface relief peaks in the areas illuminated by light implies that mass transport must be the main mechanism of surface relief formation. It is also known that free radical polymerization is usually accompanied by shrinkage of the material. Such shrinkage could be expected in holographic recording as well. If the surface relief modulation occurred due to photopolymer shrinkage only, the relief peaks would be observed in the dark fringe areas. It is possible that in the beginning of the surface relief formation the peaks are indeed positioned in the dark fringe areas and shortly after that due to mass transport from the dark to bright fringe areas these initial peaks disappear and new peaks grow in

the bright fringes. The latter are observed during the scan with Dektak_3 profiler. It should be kept in mind that the measurements presented here of the surface relief modulation are not real time measurements. With the present technique we can not observe what happens in the initial stage of surface relief formation. Although the intensity and time of the recording were varied in order to find exposure conditions at which the initial shrinkage was not yet entirely compensated by diffusion, no surface relief peaks localized in the dark fringe areas were observed.

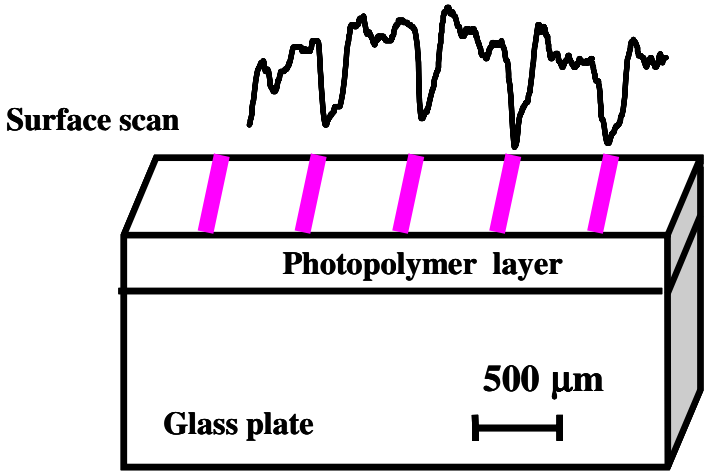

Figure 3.3 Position of the surface relief peaks when a diffraction grating with spatial frequency of 2 lines/mm is recorded. Light illumination leads to well-distinguished alternating bleached and unbleached stripes (pink).

3.4.2 Effect of recording parameters on surface relief modulation

3.4.2.1 Dependence on spatial frequency

The dependence of surface relief amplitude modulation on the spatial frequency of recording is shown in figure 3.4. Photopolymer layers of thickness 2.5 µm were exposed to interference patterns of intensity 10 mW/cm^2 for 100 sec for different spatial frequencies up to 300 lines/mm. As seen from the graph with the increase in spatial frequency there is a decrease in the amplitude modulation. Similar behaviour of the

spatial frequency dependence was observed in the layers with different thicknesses and recorded at different recording conditions [22]. This decrease at constant exposure may be explained by the increased role of surface tension forces at high spatial frequency. In other photopolymers it was observed that [21] there is a decrease in amplitude as the spatial frequency decreases. This decrease in amplitude modulation could be due to lower diffusion of mass over these larger distances whereas in the photopolymer used in this study, no such decrease in the amplitude modulation is observed with decrease in spatial frequency. This implies that the diffusion is faster in this photopolymer system [11, 12] compared to others [20, 21].

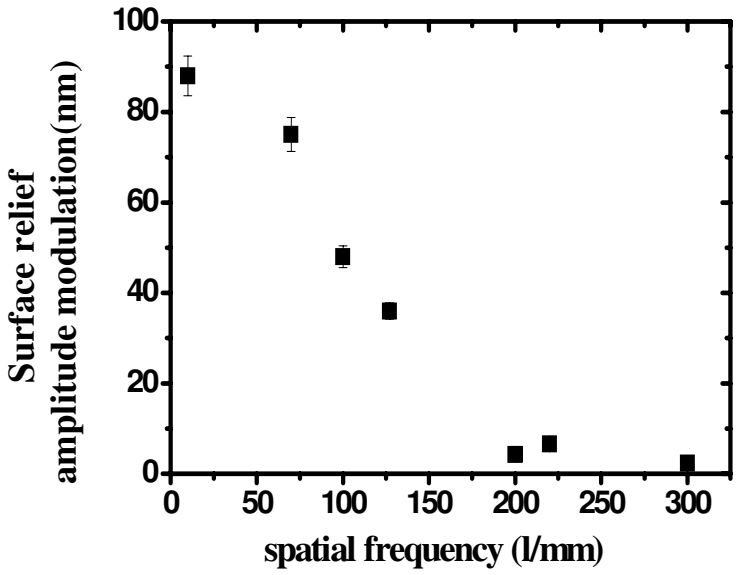

Figure 3.4 Dependence of surface relief of amplitude modulation on the spatial frequency at constant exposure of 1 J/cm^2 in the layers of thickness between 2 and 2.5 μm.

With the increase in the spatial frequency, a decrease in the surface relief amplitude modulation was also observed at different recording intensities as explained in section 3.4.2.3.

3.4.2.2 Dependence on exposure

Experiments were carried out to investigate the influence of exposure on the surface relief amplitude. Figure 3.5 shows how the surface amplitude changes with increase in exposure at intensity 10 mW/cm^2 at a spatial frequency of 18 lines/mm.

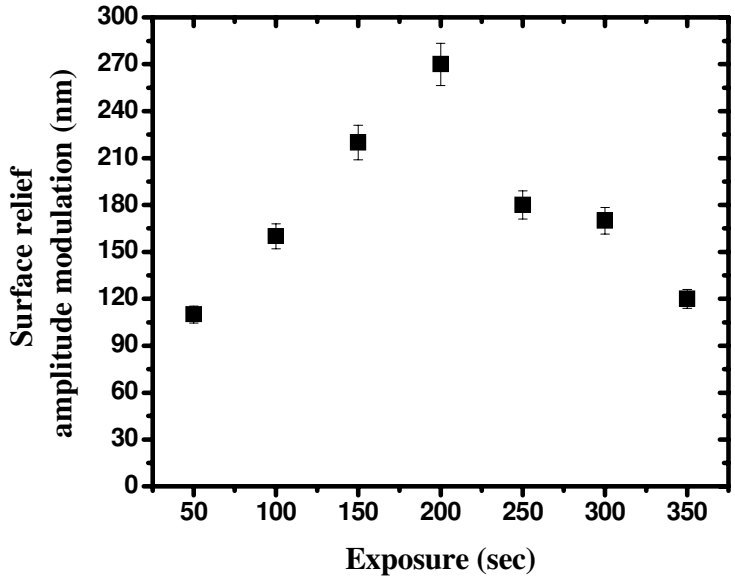

Figure 3.5 Dependence of surface relief on exposure at constant intensity 10 mW/cm^2 in layers of thickness 2 to 2.5 μm at spatial frequency 18 lines/mm.

It was observed that at constant intensity there is an optimum exposure for achieving maximum surface relief amplitude. The reduced surface modulation amplitude at higher exposure could be due to lower permeability of the layer in the polymerized regions which decreases the diffusion of monomer and the further increase in the surface relief amplitude modulation is not observed. However, there is a possibility that the monomer polymerizes at the edge of the bright region and there is a chance that the polymer chain grows into the dark region decreasing the surface relief amplitude modulation.

3.4.2.3 Dependence on intensity and exposure

The intensity dependence of the surface relief modulation was studied at two different spatial frequencies 10 lines/mm and 100 lines/mm in layers of 2 to 2.5 μm thickness. As we see from figures 3.6(a) and 3.6(b) at higher spatial frequency there is a reduced surface relief modulation for both intensities of recording. At both spatial frequencies the modulation depth increases with the increase in the recording intensity. The two recording intensities were 10 mW/cm^2 and 5 mW/cm^2.

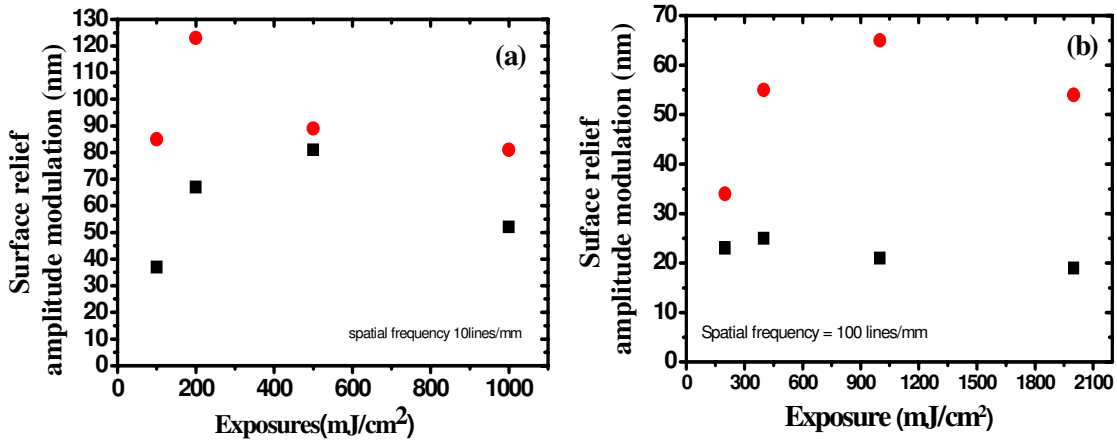

Figure 3.6 Intensity dependence of surface relief amplitude modulation at intensities 5 (black) and 10 mW/cm^2 (red) in the layers of thickness 2 to 2.5 μm for spatial frequencies 10 lines/mm (a) and 100 lines/mm (b).

When the intensity is low, the number of incident photons is low and thus the concentration of free radicals leading to slower polymerization and termination rates. In this case higher number of monomer molecules per single photon will be polymerized and larger concentration gradient will be created leading to more monomer molecules diffusing into the bright regions and thus contributing to the surface relief amplitude. Thus we should observe higher amplitude modulation at low intensity but the observed amplitude modulation is low which shows that there are other factors which are influencing the monomer diffusion. These might include the interaction forces between

substrate and the photopolymer layer. After that time of exposure where maximum amplitude modulation is observed, there is a decrease in amplitude modulation and this may be due to lower permeability of the layer in the polymerization regions, which decreases the mass transport to contribute to further increase in amplitude modulation and also there is a possibility that the monomer polymerizes at the edge of the bright region and there is a chance that the polymer chain grows into the dark region decreasing the surface relief gratings.

As the intensity increases the polymerization process speeds up and so consumption of diffused monomer is greater, which increases the surface relief amplitude modulation up to a certain time of exposure. After that there is a decrease in the amplitude modulation which could be explained as there is a possibility that polymer chains could extend into dark regions. Also at higher intensities there is a possibility of forming short chain polymer molecules, which can easily diffuse from bright to dark regions resulting in the decrease of surface relief amplitude. However, the decrease in the surface relief amplitude modulation is not observed here. This might be due to the influence of interaction forces between the substrate and the photopolymer layer.

Dependence of the amplitude modulation of the surface relief gratings on the intensity of recording is 17 μm shown in figure 3.7. From the thickness dependence studies (figure 3.9) it is observed that 17 μm is the thickness where the thickness dependence is strong below this thickness and there is no dependence above this thickness. Layers of thickness 17 μm were illuminated at different intensities at a spatial frequency of 100 lines/mm. The effect observed was different from that seen in very thin (2.5 μm) and thick photopolymer layers (above 50 μm) in this recording spatial frequency [22, 13]. In layers

of 2.5 μm thickness it was observed that with increase in the recording intensity, surface relief amplitude modulation increased. In layers of thickness above 50 μm, it was observed that there is no dependence of surface relief amplitude modulation on the recording intensity.

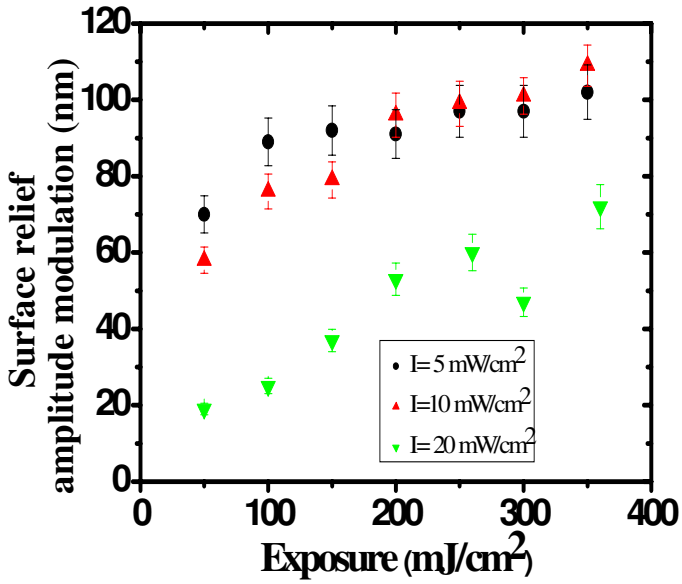

Figure 3.7 Dependence of surface relief amplitude on the intensity of recording in samples of thickness 17 μm at spatial frequency 100 lines/mm.

Intensities of recording of 5, 10 and 20 mW/cm^2 were studied. It is seen from figure 3.7 that at constant intensity with increase in exposure time, surface relief amplitude modulation increases. There is not much difference in surface relief amplitude modulation at intensities 5 and 10 mW/cm^2 with increase in exposure time. When the intensity was increased to 20 mW/cm^2, the observed surface relief modulation was smaller. So it is concluded that, for such thicknesses of the photopolymer layers, 5-10 mW/cm^2 is an optimum intensity.

The reason for higher surface relief amplitude modulations at lower intensities could be that fewer photons per unit time are absorbed by the photopolymer layer and so the polymerization process is slower in the illuminated regions. The monomer molecules which diffuse into bright regions have more time to diffuse and form longer polymer chains and termination will occur at slower rate at low intensity which increases surface relief amplitude modulation. Therefore one would observe higher surface relief amplitude modulation at low intensity. As the intensity increases the number of photons absorbed by the photosensitive layer will be higher and so the polymerization process will be faster. When polymerization is fast, the rate of consumption of diffused monomer is higher which should increase the surface relief amplitude modulation. However, at higher intensities it is likely that shorter polymer chains are formed. These could diffuse out of the illuminated regions more easily resulting in a decrease in the surface relief amplitude modulation. Diffusion of short polymer chains at high intensities of recording from bright to dark regions was also observed in volume gratings recorded in the same material [22]. Also it is possible that at higher recording intensities, polymerization is fast in the bright regions and the material comes less permeable making it more difficult for the monomers to diffuse. This decreases amplitude modulation at high intensities.

3.4.2.4 Dependence on uniform UV post exposure

The influence of uniform UV post exposure is shown in figure 3.8. After recording a surface relief grating on the photopolymer layer of thickness 17 μm at intensity 10 mW/cm^2 and spatial frequency 100 lines/mm, the sample was exposed to uniform UV intensity of 16 W for 45 min and then the amplitude modulation was measured after a further 30 min. If the photopolymer layer is thin it needs less time of uniform UV post

exposure to completely polymerize the remaining unpolymerized material. It was observed that after post exposure with UV light there was an average of 30 % increase in the amplitude modulation. Similar dependence was observed in thicker layers (above 50 μm) and thin layers (2.5 μm) [13, 22].

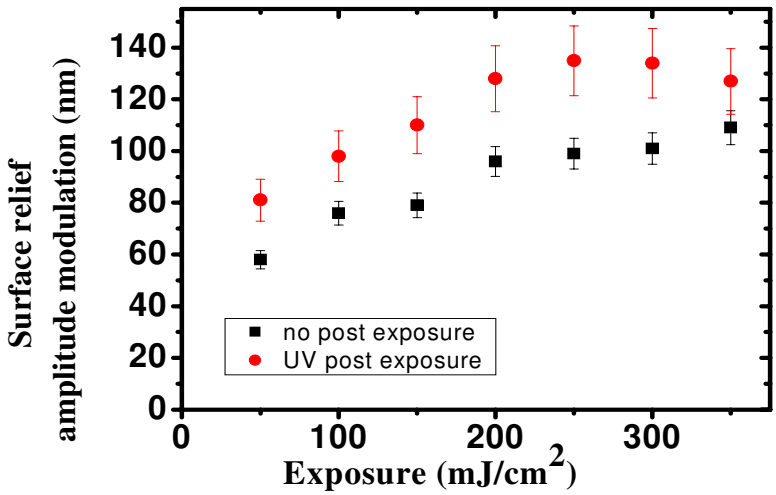

Figure 3.8 Dependence of surface relief amplitude on uniform UV post exposure in the layers of thickness 17 μm at spatial frequency 100 lines/mm.

It was previously observed by using a Dektak profilometer [13, 22] that the surface relief peaks appear in the bright regions of the interference pattern. When exposed to uniform UV light intensity, there will be no effect in bright regions as the monomer there is already polymerized but the unconsumed monomer in dark regions polymerizes. Monomer absorbs in the UV region so polymerization proceeds even if it does not contain dye for photopolymerization. The photosensitizer, erythrosin B also absorbs in UV region and so polymerization is possible with dye present as well. The increase in surface relief amplitude modulation with uniform UV post exposure could be due to shrinkage upon further photopolymerization in the dark regions.

From the above studies of the influence of the recording parameters on the surface relief amplitude modulation it can be concluded that the surface relief amplitude modulation can be controlled by changing the recording conditions. At higher spatial frequencies the overall surface relief amplitude decreases and similar behaviour was observed at different layer thicknesses. As the intensity increases, amplitude modulation decreases in layers of thickness 17 μm which is different from the behaviour of thin (2.5 μm) and thick (50 μm) layers [13, 22]. There is an optimum exposure to obtain maximum amplitude modulation. An increase in the surface relief amplitude modulation was observed with UV post exposure.

3.4.3 Effect of physical characteristics of the photopolymer layer on surface relief modulation

3.4.3.1 Dependence on the thickness of sample

Figure 3.9 shows surface relief for different thicknesses. These samples were exposed at 5 mW/cm^2 intensity for 40 sec. As has already been shown in figure 3.7, at 10 mW/cm^2, the surface relief amplitude modulation is not much different than at 5 mW/cm^2. The spatial frequency of recording was 100 lines/mm. It is seen from the figure that above 15 μm thicknesses there is not much change in the amplitude modulation.

The observed thickness dependence could be explained as follows. When the sample is exposed to a light pattern, polymerization starts in bright regions. As monomer diffuses into the polymerization region from dark regions, this increases surface relief amplitude modulation. One possible reason for the existence of strong thickness dependence below 15 μm could be the existence of interaction forces acting between the substrate and the

photopolymer layer [2] to oppose the diffusion of the monomer and this effect would be more pronounced when the layers are thinner. When the sample is thick enough the diffusion assisted surface relief formation which takes place closer to the photopolymer surface would not be influenced by the substrate and would proceed normally.

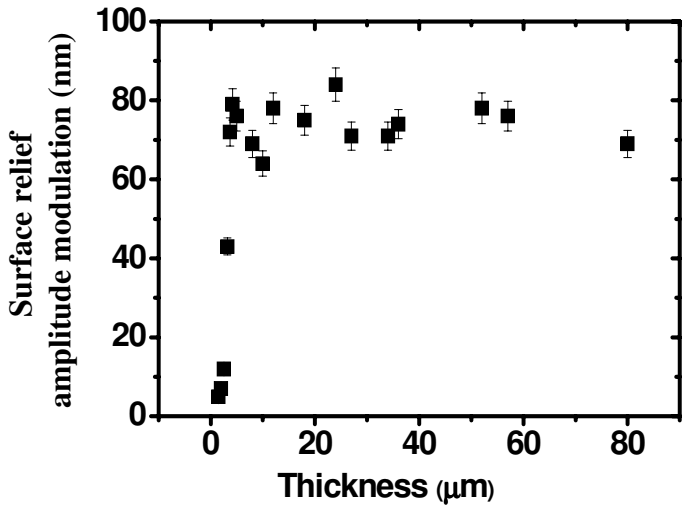

Figure 3.9 Dependence of surface relief amplitude on the thickness of the layers at spatial frequency 100 lines/mm and constant exposure.

Another possible explanation of the thickness dependence of the photoinduced surface relief is that the polymerized area extends through the depth of the layer. In thicker layers the amount of diffusing material would be greater and a simple proportionality between the amplitude modulation and the layer thickness could be expected. Indeed thicker layers produce a greater surface relief amplitude modulation. Above a certain thickness there is not much additional increase in the surface relief amplitude modulation, possibly because of the inability of the surface to deform further due to increased surface tension upon polymerization. As the influence of the surface tension increases with the increase in the spatial frequency, one should observe that the surface relief amplitude modulation reaches saturation at smaller thickness when recording at

high spatial frequency than the thickness at which the surface relief amplitude modulation reaches saturation at low spatial frequencies. Such dependence of the thickness of the layer at which the saturation occurs, on the spatial frequency of recording was indeed observed and reported by Naydenova et al [22].

The existence of a plateau in the surface relief modulation could also be explained as follows. When the thickness of the layer increases, there will be more monomer to diffuse into the bright region contributing to increase in surface relief amplitude modulation as shown in figure 3.10 but polymerization in the bright regions causes the material to become more viscous, inhibiting diffusion of the monomer.

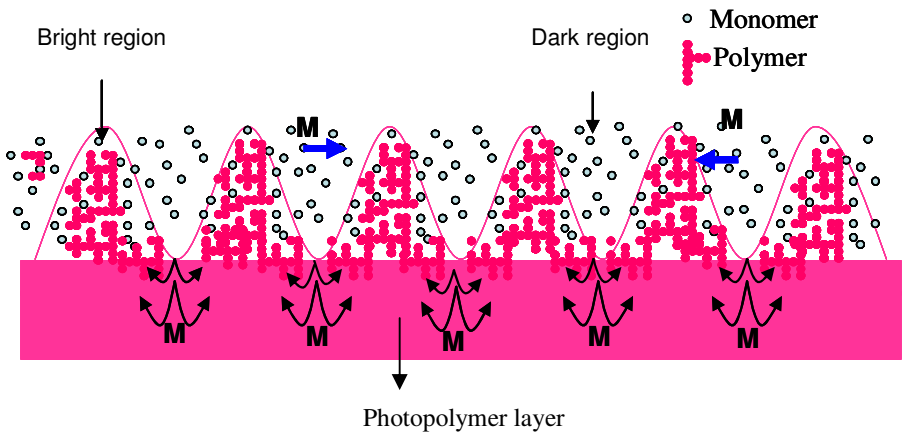

Figure 3.10 Recording mechanism.

The diffraction efficiency (DE) of these layers was measured as given by equation 4.1. Figure 3.11 shows the variation of DE with increase in the thickness of the layer. It is observed that DE increases with increase in the thickness. It was seen that above a certain thickness though there is not much change in surface modulation, the DE increases with increase in thickness. This is due to the contribution of the volume grating along with the surface relief grating.

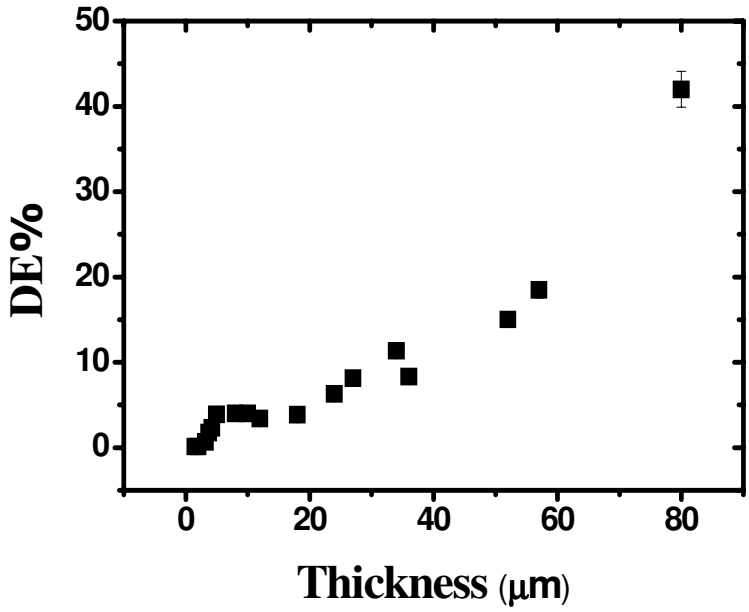

Figure 3.11 DE % verses the thickness of layers at spatial frequency 100 lines/mm and constant exposure.

Similar behaviour of surface relief amplitude modulation dependence and DE dependence on the thicknesses of the layers at different spatial frequencies were observed.

Increase of the surface relief amplitude modulation with layer thickness up to a maximum was also observed at 10 lines/mm. However, unusual surface relief profiles (splitting of the peak into two) were observed at 10 lines/mm but not at 100 lines/mm. Experiments were carried out to study this surface relief effect at low spatial frequencies. Samples of different thicknesses were prepared and exposed to an interference pattern of intensity 10 mW/cm^2.

Figure 3.12 shows experimentally observed surface relief grating profiles, recorded at 10 lines/mm. It is observed that splitting is pronounced in layers of thickness 17 μm as

if there is a change in the spatial frequency of recording. It is observed that the surface relief amplitude modulation also decreased along with splitting.

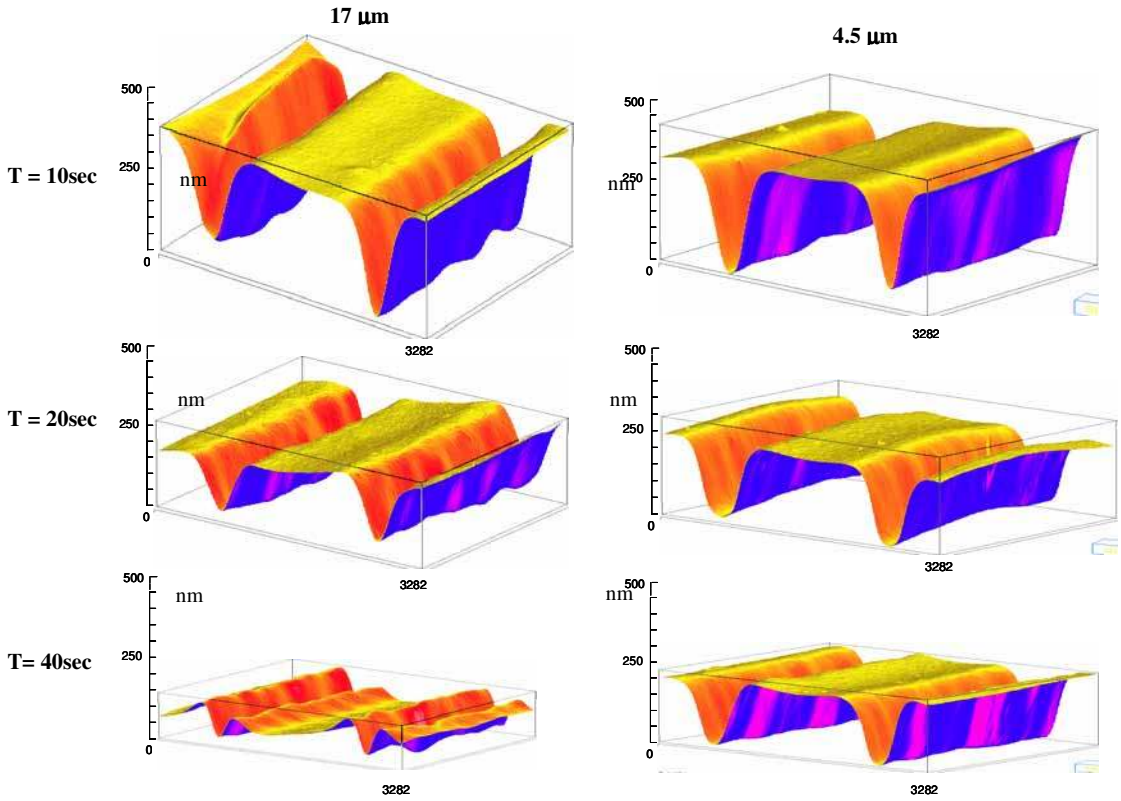

Figure 3.12 Surface relief gratings at 10 lines/mm in layers of different thickness.

It is also observed that splitting depends on thickness and exposure time. The splitting effect is observed after 5 sec exposure in layers of thickness 4.5 µm and 17 µm. This could be due to generation of higher order diffracted beams. In 17 µm thick layers the splitting is greater and the intensity of the second order beams is expected to be higher. These are preliminary experimental observations and more detailed investigations would need to be carried out.

3.4.3.2 Dependence on the chemical composition of photopolymer layer:

In order to increase the surface relief amplitude modulation the influence of the chemical composition was studied. In the photopolymer, triethanolamine (TEA) is an electron donor (coinitiator), which plays an important role in the generation of the free radicals. It also acts as a plasticizer, which favours the solution and stability of other components in the matrix, which in turn influences the performance of the material. A high concentration of TEA produces stable layers without precipitation of monomer on the surface.

Experiments were carried out to study the dependence of surface relief amplitude modulation on chemical composition of the photopolymer material by changing the concentration of TEA.

Three different stock solutions (TEA1, TEA2 and TEA3) of photopolymer were prepared containing 1.5 ml, 2 ml and 2.5 ml TEA respectively, and used in the standard photopolymer composition [17]. The typical thickness of TEA1 was 15 ± 3 μm, TEA2 was 17 ± 3 μm and TEA3 was 19 ± 3 μm. The thickness and optical quality of the layer were repeatable. These samples, after drying, were exposed to an interference pattern of intensity 10 mW/cm^2 for 35 sec at 100 lines/mm spatial frequency.

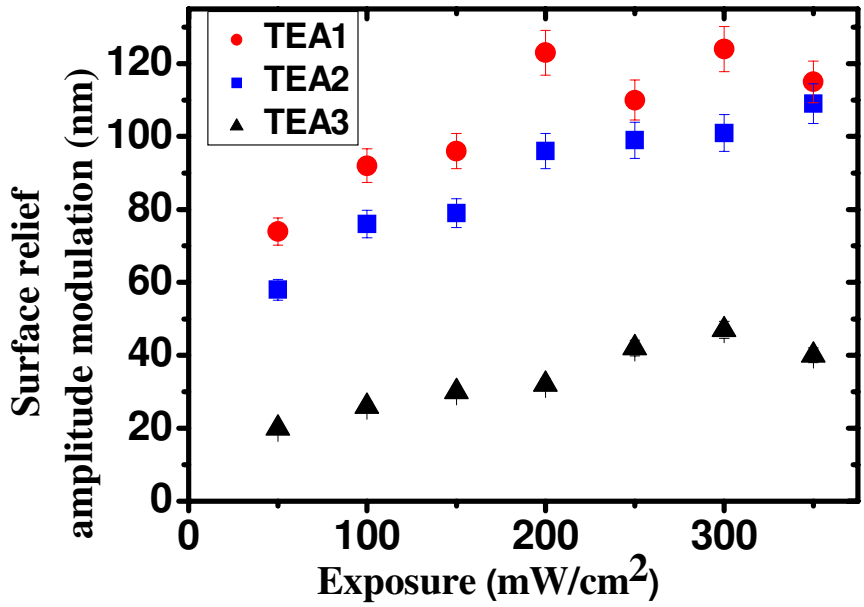

Figure 3.13 Dependence of surface relief amplitude modulation on chemical composition of the photopolymer layer at 100 lines/mm.

From figure 3.13 it is observed that an increase in TEA concentration decreases the surface relief amplitude modulation. In order to determine the reason for this we have carried out some estimation of the relative concentrations of the two co-initiating species – the dye molecules and the TEA molecules. 2.6 mM concentration of dye molecules contains 6.16×10^{18} dye molecules, and the sample with the smallest concentration of TEA (1.5 ml) contains 7.4×10^{21} TEA molecules, that is, for each dye molecule there are 1000 TEA molecules available even at this lowest TEA concentration. So, the decrease in amplitude modulation could be related to the role of TEA as plasticizer rather than its role as coinitiator of the photopolymerization reaction. Another possible explanation could be that with the increase in TEA concentration (TEA3), the monomer concentration is decreased to 23 % of the initial monomer concentration (TEA1). This decrease in the monomer concentration decreases the

number of monomer molecules that diffuse and contribute to the final surface relief amplitude modulation. But when compared to the total mass of the layer, the difference of the monomer concentration between TEA1 and TEA3 is only 4 %. This 4 % difference in monomer concentration can hardly be responsible for a more than 4 times decrease in the surface relief amplitude modulation seen in figure 3.13. Also it should be noted that with the increase of the TEA concentration the thickness of the layers slightly increases. According to the previously observed dependence of the surface relief amplitude on the thickness of the photopolymer layers (figure 3.9) this would imply that the effect of the TEA concentration is even greater as, instead of an increase in the surface relief amplitude modulation, a decrease is observed.

The most probable reason for the strong dependence of the surface relief modulation on the TEA concentration is perhaps TEA's plasticizing role. With the increase of the number of TEA molecules the layers become less viscous with the possibility of diffusion of short polymer chains into dark regions [23] which in turn decreases amplitude modulation. A separate investigation of diffusion processes with variation of the TEA concentration in this photopolymer material would be beneficial for understanding of the observed effect.

3.4.3.3 Dependence on the temperature

Experiments were carried out to study the influence of temperature on the surface relief amplitude modulation. Samples of thickness 5 to 5.4 μm were exposed to intensity 10 mW/cm^2 for 35 sec and spatial frequency 100 lines/mm. To study the temperature dependence, after recording, the surface relief grating was heated for 1 min at a

particular temperature and cooled to room temperature. Then they were scanned with the white light interferometer to measure surface relief amplitude modulation.

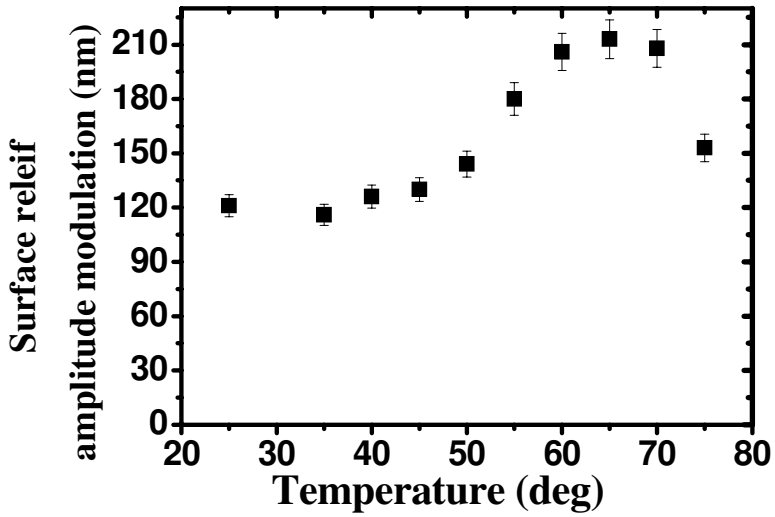

Figure 3.14 Dependence of surface relief amplitude modulation on temperature.

Figure 3.14 shows surface relief amplitude modulation increasing to a maximum and then decreasing. This shows that there is an optimum temperature for maximum surface relief amplitude modulation. When the temperature increases, monomer diffuses more easily from dark to bright regions and consequently surface relief amplitude modulation is greater [2]. Polymerization of the monomer in dark regions could also occur due to heating, thus increasing the surface relief amplitude modulation. The decrease in the amplitude modulation above a certain temperature could be as a result of short polymer chains diffusing into dark regions.

From the above studies of the influence of physcial characteristics of the photopolymer it can be observed that by changing the thickness of the layer, composition of the layer

and the temperature of the layer, the magnitude and shape of the suraface relief amplitude modulation can be controlled.

3.4.4 Crossed gratings

Crossed gratings could be used for the fabrication of electrically controllable lenslet arrays. The peaks and troughs from a 2D array of depressions can be filled with LCs to form a lenslet array. For this it is important to study the influence of recording parameters and physical characteristics of the layer on the magnitude and shape of the surface relief profile.

A crossed grating was recorded on the layer by changing the orientation of the sample by 90° between two successive recordings as shown in figure 3.15 [22].

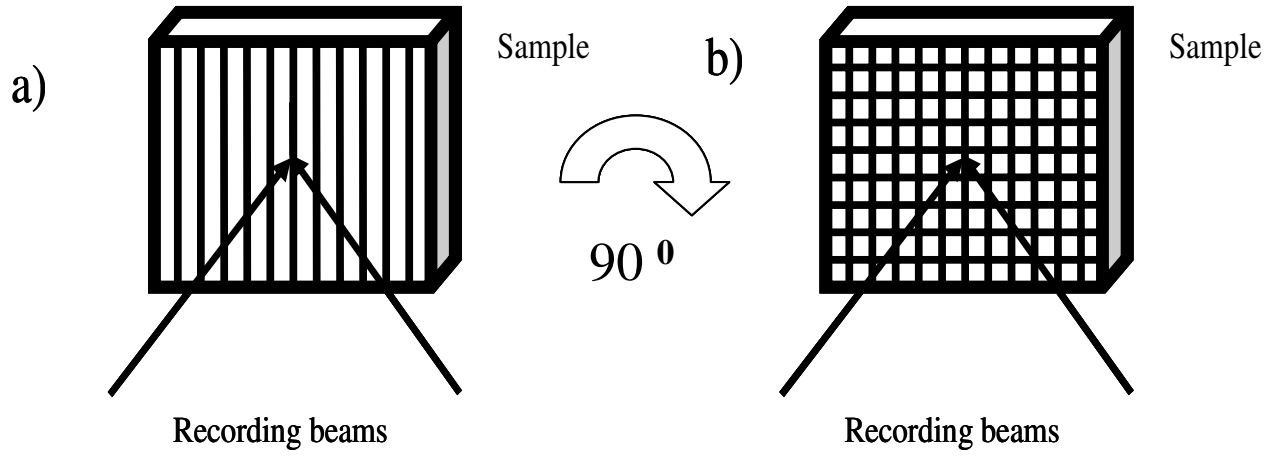

Figure 3.15 Recording mechanism of cross gratings.

Earlier crossed gratings were recorded in thin and thick layers at different recording intensities and spatial frequencies [13, 22]. Here the dependence of the holographically

recorded 2D relief pattern on exposure time at constant spatial frequency and recording intensity are presented.

The optical setup used to record these gratings is shown in figure 3.1. The gratings (100 lines/mm) were recorded in 10 μm thick photopolymer layers with 5 mW/cm^2 intensity. The recording exposure time was varied. The exposure times used for each of the two recordings on a crossed grating were same. From the results it was observed that the crossed grating does not appear when the first grating is recorded for more than 30 sec. This could be due to consumption of all material during the first exposure. Figure 3.16 shows profiles obtained at t = 5 sec, 40 sec and 60 sec respectively.

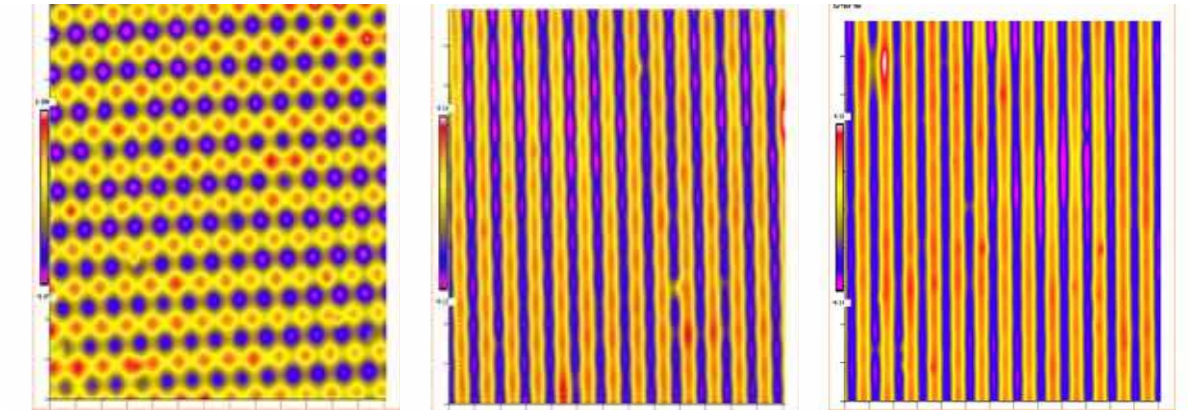

Figure 3.16 Holographic patterns recorded at 5, 40 and 60 sec of exposure time.

3.5. Conclusions

Photoinduced surface relief gratings in acrylamide based photopolymer were investigated. The outstanding advantage of this material is the absence of any chemical post treatment. From the studies of dependence of surface relief on intensity, thickness

and composition it is concluded that diffusion of monomer from dark to bright region is the main mechanism which governs the formation of surface relief gratings.

As the intensity increases, amplitude modulation decreases in layers of thickness 17 μm which is different from the behaviour of thin (2.5 μm) and thick (above 50 μm) layers [13, 22]. Post exposure of the exposed gratings to uniform UV light leads to more than 30 % increase in the surface relief amplitude. As the TEA content increases surface relief amplitude modulation decreases. It was observed that when the thickness of the photopolymer layer increases, the modulation depth increases up to certain point and after that there is not much change at constant exposure, at a given spatial frequency. With increase in temperature there is an optimum temperature to obtain maximum surface relief amplitude modulation. At low spatial frequency non sinusoidal profiles are observed which depend on thickness and exposure time, which shows that shrinkage is also involved in the formation of surface relief gratings. From the preliminary work done on the crossed gratings it is observed that no crossed grating can be obtained above 30 sec initial exposure. So it can be concluded that, surface relief amplitude modulation and shape can be controlled by changing recording parameters and physical characteristics.

The next phase in this research involved filling these surface relief gratings with LCs to fabricate LC devices. These will be discussed in the following chapters. Fabrication and characterization of electrically switchable LC diffraction gratings using these optically recorded surface relief gratings in an acrylamide based photopolymer will be discussed in the next chapter.

References

1. Y. Boiko, V. Slovjev, S. Calixto and D. Lougnot, “Dry photopolymer films for computer-generated infrared radiation focusing elements.” Appl. Opt., 33 (5), 787-793, 1994.
2. C. C. Barghorn and D. Lougnot, “Use of self-processing dry photopolymers for the generation of relief optical elements: a photochemical study.” Pure Appl. Opt., 5, 811-825, 1996.
3. M. E. Potter, K. Goss, M. A. Neifeld and R. W. Ziolkowski, “Nanostructure surface relief profiles for high density optical data storage.” Opt. Comm., 253**,** 56–69 , 2005.
4. J. Neumann, K. S. Wieking and D. Kip, “Direct laser writing of surface reliefs in dry, self developing photopolymer films.” Appl. Opt., 38(25) 5418-5421, 1999
5. X. T. Li, A. Natansohn and P. Rochon, “Photoinduced liquid crystal alignment based on a surface relief grating in an assembled cell.” Appl.Phys.Lett., 74, 25, 3791- 3793, 1999.
6. D. Dantsker, J. Kumar and S. K. Tripathy, “Optical alignment of liquid crystals.” J. Appl. Phys, 89(8), 4318-4325, 2001.
7. V. V. Lazarev, M. I. Barnik and N. M. Shtykov, “Liquid crystal alignment by photo-processed polymer films.” Mol. Materials, 8, 235-244, 1997.
8. F. Kaneko, T. Kota, A. Baba, K. Shinbo, K. Kato and R. C. Advincula, “Photo induced fabrication of surface relief gratings in alternate self assembled films containing azo dye and alignment of LC molecules.” Colloids and Surfaces A: Physicochem. Eng. Aspects., 198-00, 805-810, 2002.

9. S. Martin, “A new photopolymer recording material for holographic applications: Photochemical and holographic studies towards an optimized system”, Ph.D. Thesis, University of Dublin, 1995.
10. S. Martin, C. A. Feely and V. Toal, “Holographic recording characteristics of an acrylamide-based photopolymer.” Appl. Opt., 36(23), 5757-5768, 1997.
11. R. Jallapuram, I. Naydenova, S. Martin, R. Howard, V. Toal, S. Frohmann, S. Orlic and H. J. Eichler, “Acrylamide based photopolymer for micro-holographic data storage.” Opt. Mat. 28 1329-1333, 2006.
12. I. Naydenova, R. Jallapuram, S. Martin, R. Howard and V. Toal,” Investigations of the diffusion processes in self-processing acrylamide-based photopolymer system.” App. Opt., 43 (14), 2900, 2004.
13. I. Naydenova, E. Mihaylova, S. Martin and V. Toal, “Holographic patterning of acrylamide–based photopolymer surface.” Opt. Express., 13 (13), 4878-4889, 2005.
14. B. Bowe and V. Toal, “White light interferometric surface profilers.” Optical Engineering, 37, 1796-1799, 1998.
15. A. Hirabayashi, H. Ogawa and K. Kitagawa, “Fast surface profiler by white-light interferometry by use of a new algorithm based on sampling theory.” Appl. Opt. 41(23) 4876-4883, 2002.
16. G. Zhao and P. Mourolis, “Diffusion model of hologram formation in dry photopolymer materials”, J. Mod. Opt., **41**, 1929-1939, 1994.
17. S. Piazzolla and B. Jenkins, “First harmonic diffusion model for holographic grating formation in photopolymers”, J. Opt. Soc. Am. B, **17**, 1147-1157, 2000.

18. V. Moreau, Y. Renotte and Y. Lion, “Characterisation of DuPont photopolymer: determination of kinetic parameters in a diffusion model”, Appl. Opt. **41**, 3427-3435, 2002.
19. V. Colvin, R. Larson, A. Harris and M. Schilling, “Quantitative model of volume hologram formation in photopolymers”, J. Appl. Phys., **81**, 5913-5923, 1997.
20. J. Jenney, “Holographic recording with photopolymers”, JOSA, 60, 1155-1161, 1970.
21. T. Smirnova and O. Sakhno, “A mechanism of the relief-phase structure formation in self-developing photopolymers.” Optics and Spectroscopy, 3(1), 126-131, 2001.
22. I. Naydenova, K. Pavani, E. Mihaylova, K. Loudmer, S. Martin and V. Toal, “Holographic recording of patterns in thin film acrylamide-based photopolymer.” SPIE Proc., 5827-17 163-172, 2005.
23. S. Martin, I. Naydenova, V. Toal, R. Jallapuram and R. G. Howard, “Two way diffusion model for the recording mechanism in as self developing dry acrylamide photopolymer.” SPIE Proc. 6252 37-44, 2006.
24. K. Pavani, I. Naydenova, S. Martin and V. Toal, “Photoinduced surfce relief studies in an acrylamide-based photopolymer.” J. Opt. A: Pure Appl. Opt., 9, 43-48, 2007.

4. FABRICATION OF SWITCHABLE LIQUID CRYSTAL DIFFRACTION GRATINGS USING SURFACE RELIEF EFFECT IN PHOTOPOLYMER

4.1 Introduction

The applications of switchable holographic optical devices are in beam steering [1, 2], light intensity modulation (displays) [3], variable focal length lenses [4], reconfigurable waveguide interconnects [5] and fiber optic communication switches [6, 7]. Generally a switchable optical element uses a material that exhibits a change in the refractive index with applied electric field. LCs are attractive for the fabrication of switchable optical devices as they change their orientation with applied external field [8-10].

Uniform alignment of LCs is essential for the fabrication of LC optoelectronic devices. Non-rubbing techniques have been investigated for alignment of LCs [11-17]. These methods have advantages over the common rubbing method as they avoid electrostatic charge and dust which are not desirable as explained in earlier chapters. To avoid these problems photoinduced surface relief gratings in photopolymer layers are attractive for filling with LCs to align them so as to fabricate optoelectronic devices such as switchable gratings and polarization rotators [14-17]. The advantages of photoinduced surface relief gratings and their dependence on different parameters in an acrylamide based photopolymer were explained in chapter 3. The results reported in chapter 3 strongly indicate that, due to a concentration gradient, the mass transport of monomer from dark to bright regions is the main mechanism which governs the formation of surface relief gratings [18, 19].

LC diffraction gratings were fabricated by filling surface relief gratings in the photopolymer layer with LCs. E49 and E7 LCs from Merck were used in this study. The ordinary refractive index (n_o) of the LCs matches the refractive index of the photopolymer. A measurement of the variation of the first order intensity with applied voltage is presented. In this chapter a comparison between the behaviour of the switchable diffraction gratings using E7 (n_e= 1.74, n_o= 1.52) and E49 (n_e= 1.79, n_o= 1.53) LCs and the switching behaviour was demonstrated in each case. The orientation of the LCs in the surface relief gratings is determined by measuring the birefringence [20-22].

4.2 Methodology

4.2.1 Electro optical behaviour

LCs are birefringent in nature. They are characterised by ordinary, n_o and extraordinary, n_e refractive indices. The LCs used in this study were chosen to have large birefringence. The LC molecules were aligned such that the long axis of the LC molecules lay along the grating grooves. When linearly polarized light having its electric field plane of polarization parallel to the direction of the long axis of the LC molecules, is incident on the LC device, it propagates through the medium with a refractive index corresponding to the extraordinary axis of the LC molecules. When a voltage is applied to the LC device, the LC molecules re-align perpendicular to the substrate. Now the incident linearly polarized light has its electric field of polarization in the direction of the ordinary refractive index of the LCs.

Usually these LC gratings can be operated in two different ways [23]. In the first, the grating is fabricated such that there is no diffraction when the field is zero. This can be done by choosing the refractive indices of substrate and LCs to be equal when voltage is not applied. This is called 'OFF' state. When electric field AC or DC is applied, the LC molecules re-align such that there is a large difference in the refractive indices of substrate and LCs, resulting in strong diffraction of incident light. This state is called 'ON' state.

In the second way of operation, the LC diffraction grating is fabricated such that diffraction occurs when no electric field is applied. In this case the refractive indices of substrate and LCs are chosen to be unequal when voltage is not applied. This state is called 'ON' state. When electric field is applied AC or DC, the re-alignment of LCs is observed such that the refractive indices of substrate and LCs match, resulting in no diffraction of incident light. This state is called 'OFF' state.

In this work the second type of operation of the LC device is demonstrated and the model is shown in figure 4.1.

By measuring the intensity in the diffracted first order beam the diffraction efficiency (DE) is obtained. The DE (η) is defined as the ratio of the light intensity in the first diffraction order (I_1) and the incident beam intensity (I_0), expressed as a percentage. Thus

$$\eta = \frac{I_1}{I_0} \times 100 \quad \text{----------} \quad (4.1)$$

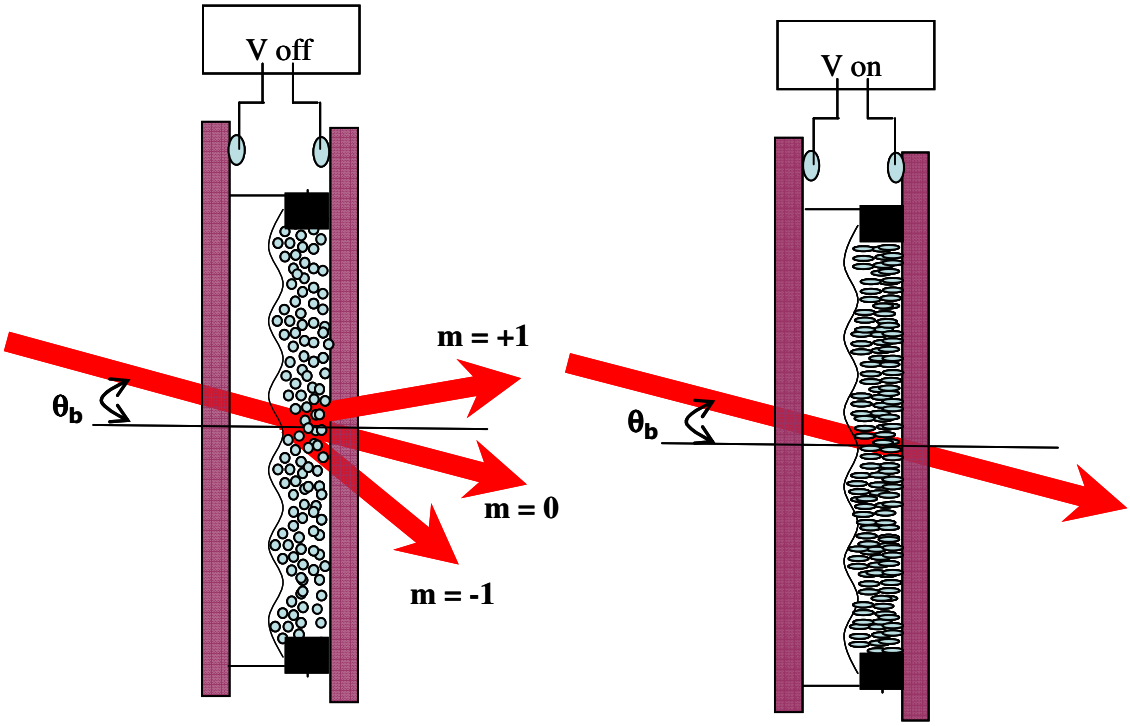

Figure 4.1 Operation of the LC diffraction grating.

4.2.2 Measurement of ellipticity and birefringence of a LC cell

Elliptically polarized light is generated when linearly polarized light is passed through birefringent material [24]. Depending on the orientation of the plane of polarization of incident light with respect to the LC principal axes and on the phase difference introduced by the LC layer due to the birefringence, the emergent light may be linearly, circularly or elliptically polarized. Monochromatic light is used to probe the sample.

Elliptically polarized light may be described by the electric field components,

$$E(x,t) = A\cos(\omega t - kz) \text{----------} (4.2)$$

$$E(y,t) = B\cos(\omega t - kz + \delta) \text{----------} (4.3)$$

Then the ellipticity χ is given by [19]

$$\sin 2\chi = \frac{2AB\sin\delta}{A^2 + B^2} \quad \text{----------} \quad (4.4)$$

Ellipticity can also be defined as inverse of the tangent of ratio of the fast component (I_{min}) of electric field to slow component (I_{max}). Therefore

$$\tan\chi = \left(\sqrt{I_{min}/I_{max}}\right) \quad \text{----------} \quad (4.5)$$

The birefringence of the material is characterised by the difference in the refractive indices. It is given by the formula

$$\Delta n = n_e - n_o = \frac{\delta\lambda}{2\pi d} \quad \text{----------} \quad (4.6)$$

Where δ = phase difference, λ = wavelength and d = thickness of the LC layer.

To measure the birefringence of LCs, first the ellipticity is calculated by measuring the intensities and substituting in equation (4.5). The phase difference (δ) is calculated by substituting the result in equation (4.4) where $A = \sqrt{I_{max}}$ and $B = \sqrt{I_{min}}$. Birefringence is calculated by substituting δ, λ and d in equation (4.6).

4.3 Experimental

4.3.1 Fabrication of switchable LC diffraction grating

ITO coated glass plates were cut into small pieces 3 cm x 2.5 cm. Electrical contacts were made on the corners of the plates with silver loaded epoxy resin and allowing it to dry. The plates were treated with NaOH solution for 30 minutes in an ultrasonic bath. An acrylamide based photopolymer was used here with composition as described in chapter 3. Good optical quality samples of photopolymer were prepared by the gravity settling method. The thickness of the photopolymer layer on ITO coated glass substrates was 10 μm after drying for 2 to 3 hours. These photopolymer layers were exposed to a light pattern to record gratings. The experimental set up used to record surface relief gratings is shown in figure 3.2. A spatially filtered and collimated laser with $\lambda = 532$ nm was used to record surface relief transmission diffraction gratings. As explained in section 3.4.2.1 greater surface relief amplitude modulation is obtained at low spatial frequency so gratings were recorded at 70 lines/mm and 100 lines/mm spatial frequencies. They were recorded with 10 mW/cm^2 recording intensity for 35 sec and then exposed to uniform UV light intensity of 16 W uniformly for 20 min to polymerize remaining monomer. Spacers of thickness 6 μm were placed at the four corners on the exposed layers and an ITO coated glass plate was placed on top. Two sides were glued keeping the sides open for filling with LC. This glue was allowed to dry for 15 min. Figure 4.2 shows the empty cell.

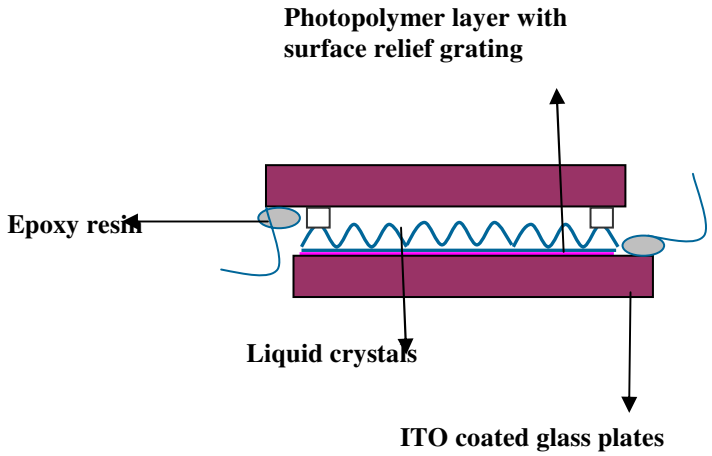

Figure 4.2 An empty cell used for the fabrication of switchable LC diffraction grating.

There are two methods of filling with LCs, the one drop method and capillary flow [25].

One drop fill method:

Spacers a few μm thick were placed on two sides of the surface relief grating and a very small amount of LC was dropped onto the grating. A second ITO coated glass plate was placed on the grating with small amount of mismatch so as to enable connection to the electrodes. Then the cell was glued on all four sides and allowed to dry. These filled cells were heated above critical temperature of the LC material and cooled so as to align the LCs.

Capillary flow:

The empty cell was placed in a container of LCs in a vacuum chamber and the pressure reduced using a vacuum pump. LCs then rise into the cell by capillary action. The inlet was glued immediately to avoid the formation of air bubbles. Alternatively, the empty cell was heated above the critical temperature of the LCs and a small amount of the LC

placed at one of the openings and so LC entered the cell. The openings were immediately glued to avoid the formation of air bubbles.

In this work a vacuum pump was used to fill the LCs uniformly into the cell. This filling method is also based on the capillary flow principle. In this method only two sides of the cell were glued before filling. One of the open sides was placed in the LC container and a vacuum pump was connected to the second opening. When the vacuum pump was turned on LCs were drawn into the cell. It took 15 to 20 minutes to fill the cell completely and uniformly.

4.3.2 Experimental set up

4.3.2.1 Measurement of birefringence

The experimental setup used to measure ellipticity and birefringence is shown in figure 4.3. A linearly s-polarized laser of wavelength 633 nm was used. The laser beam was incident normal to the cell. The polarizer (P) was adjusted such that its transmission axis was parallel to the plane of polarization of the light. The transmission axis of the analyzer (A) was kept perpendicular to the transmission axis of (P) so that no light was seen after (A). The half wave plate (HWP) was adjusted such that the plane of polarization was rotated by 45^{o}. The LC diffraction grating was placed between HWP and (A). The maximum (I_{max}) and minimum (I_{min}) intensities were measured by rotating the analyzer (A).

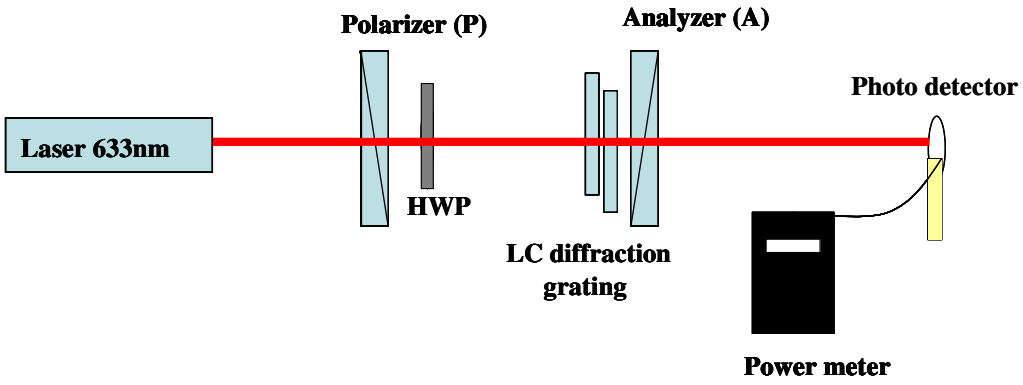

Figure 4.3 Experimental set up used to measure ellipticity and birefringence of LC.

4.3.2.2 Switching behaviour

The optical setup used to study electro optical switching behaviour of the diffraction grating is shown in figure 4.4. A linearly s-polarized laser beam of wavelength 633 nm was used to probe the device at the Bragg angle. The intensity in the first order was measured while applying an electric field (DC and AC).

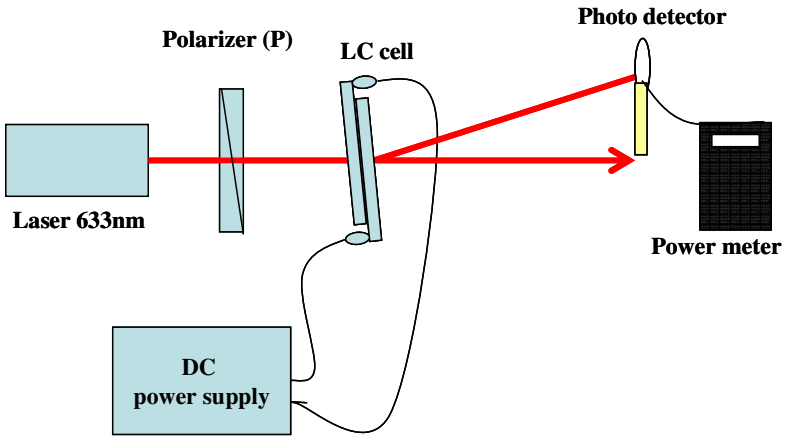

Figure 4.4 Experiment setup to study electro optical switching of LC diffraction grating.

4.4 Results

4.4.1 Birefringence measurement

The LC diffraction grating was placed between polarizer (P) and analyzer (A) as shown in figure .4.4. It was observed that there was some light after (A) which proves the birefringent nature of LC. Linearly polarized light was incident at 45^0 to director of LCs and by rotating (A), the maximum (I_{max}) and minimum (I_{min}) intensities were measured with a photodetector. The ellipticity (χ) was calculated by using equation (4.5). The values of χ, I_{min} and I_{max} were substituted in equation (4.4) to obtain the phase difference (δ). By finding δ and taking d = 6 μm, birefringence was calculated using equation (4.6) to be 0.016 for E7 LCs and 0.026 for E49 LCs. These results show that there is a weak initial alignment of LCs in the device. The LC device consists of two glass plates, one with a surface relief grating in the photopolymer layer and the second one with only an ITO coated glass plate without an alignment layer. The ITO coated glass cannot align LCs homogenously as depicted in figure 4.1. This explains the low birefringence observed. Although the devices show low birefringence they show good electro-optical switching behaviour as discussed in the next section.

When a LC cell was fabricated in which the photopolymer layer was only rubbed with velvet cloth it did not show any alignment of the LCs. This was also confirmed for TNLC devices as explained in the next chapter. The LC diffraction gratings fabricated with photoinduced surface relief gratings showed some alignment of LCs as explained above. In order to study the degree of alignment of the LCs, LC diffraction gratings were fabricated by using a method combining surface relief effect and rubbing because

this technique had enabled good alignment of LCs in fabrication of the TNLC devices [26]. The optically recorded grating was rubbed slightly with velvet cloth before filling with LCs. These gratings were fabricated with same thickness spacers. There was no significant difference in the birefringence value and they showed similar switching behaviour to that of the gratings fabricated with only surface relief gratings. The only difference found in these devices is that the switching time was faster in the devices with rubbed surface relief gratings. This effect could be explained as follows. Due to rubbing of the photopolymer layer the LCs need less energy to align along the applied electric field. Two things which are worth noting are that the LCs used to fabricate LC diffraction gratings are different from the LCs used to fabricate TNLC devices and there is no second alignment layer in the LC diffraction gratings.

4.4.2 Switching behavior

Surface relief gratings were recorded in dry photopolymer layers by exposing them to the interference pattern of the light at 70 lines/mm with similar exposure conditions as discussed in section 4.3.1. The surface relief amplitude modulation was measured to be 160 nm. The cell was fabricated and the DE was measured without LCs. It was found to be 13.5 %. After filling the surface relief grating with the LCs, the measured DE of the grating was found to be 4.5 %. This could be explained as follows. As the recorded grating is an surface relief grating (thin grating), the DE of the first order Raman-Nath diffraction is given by $DE = J_1^2(\Delta\rho)$ [27-29] where J_1 is a first order Bessel function, $\Delta\rho = \frac{2\pi}{\lambda}\Delta d(n_p - n)$ where n_p is the refractive index of photopolymer, n the is refractive index of air, Δd is the amplitude modulation and λ is probe beam wavelength.

When the surface relief gratings were filled with LCs, the refractive index difference n_p-n is replaced by the smaller refractive index difference between polymer and LC and so one would expect a decrease in the DE. The application of the electric field then decreases the apparent refractive index difference further so that the LC refractive index approaches that of the photopolymer. Before studying the electro-optical switching of the device, the intensity in the first order was measured for different azimuth angles of incoming linearly polarized light. It was observed that the intensity is constant for all azimuths of the probe beam. This also suggests that the alignment of LCs is weak and explains the low birefringence that is observed.

Figure 4.5 (a) shows the variation of intensity in the first order with applied DC voltage. The intensity in the diffracted first order beam decreases as the applied voltage increases and finally disappeared at around 3.8 V. This could be due to the refractive index of the LCs matching the refractive index of the photopolymer layer. It was also observed that switching behaviour is reversible. On decreasing the applied voltage, the intensity in the first order increased and no hysteresis was observed. Similar behaviour was observed with other switchable diffraction gratings fabricated with the E49 LCs. The diffraction patterns at 0 V and 3.8 V are shown in figure 4.5(b). From figure 4.5(b) it is clear that there is scattering and is more when voltage is applied which could be due to LC molecules in the bulk above the grating.

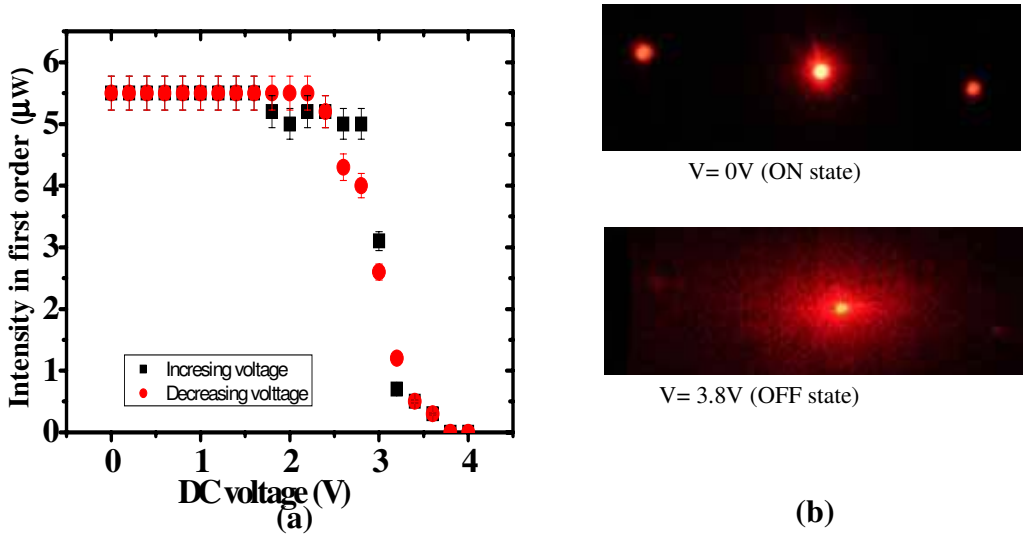

Figure 4.5 (a) Intensity of the first order of LC diffraction grating versus applied DC voltage (b) Diffraction patterns at 0 and 3.8 V.

Figure 4.6 shows the variation of intensity in the first order with applied AC voltage (square wave) at 1 KHz. It was observed that the first order of the diffraction disappears at lower DC voltage, around 2 V_{RMS}. It is also observed that the voltage at which switching is observed (threshold voltage) is lower when an AC instead of DC voltage is applied. This behaviour could be explained as follows. When a DC voltage is applied to the device, any impurity ions present in the cell will migrate towards the alignment layers under the influence of the electric field and be deposited at the cell surfaces. An electric field generated across the liquid crystal persists due to the captured charges and hinders switching. When an AC voltage (square wave) is applied, polarity is rapidly switched with certain frequency, t_t^{-1}, (t_t is the transient time for the injected charge carries) which prevents the migration of impurity ions and hence switching is faster [8, 29].

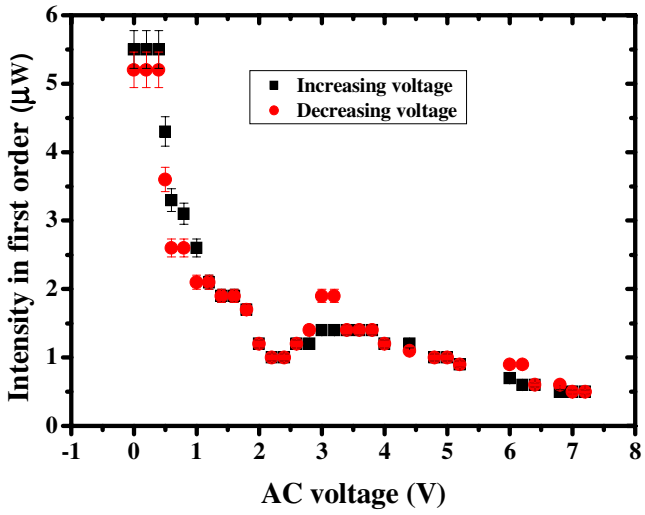

Figure 4.6 Intensity of the first order of LC diffraction grating verses applied AC voltage.

To study the influence of the LCs on the DE of the gratings, switchable diffraction gratings were fabricated with E7 and E49 LCs. The surface relief gratings were recorded at 100 lines/mm under similar recording exposure conditions as discussed in section 4.3.1. The surface relief amplitude modulation of the grating was measured and a value of 129 ± 8 nm was obtained. The diffraction efficiency (DE) of the gratings was 7 ± 0.5 % before filling with LCs. The gratings were filled with E49 or E7 LCs. The DE after filling was measured to be 0.4 % for E49 LCs and 0.15 % for E7 LCs. The decrease in the DE could be explained by the fact the refractive index difference between polymer and LCs along n_e (0.22 for E7 LCs and 0.29 for E49 LCs) is smaller than the refractive index difference between polymer and air (0.5) [10, 26]. Similarly, the DE values for E7 LC gratings were less than those for E49 LC gratings which could be explained by a higher difference between the average refractive index of E49 LCs and that of the photopolymer.

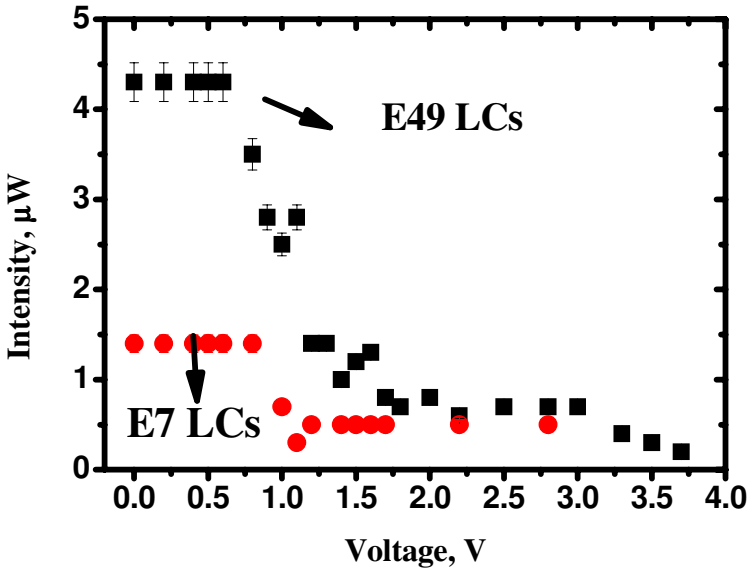

Figure 4.7 Switching behaviour of the LC diffraction gratings with E7 and E49 LCs.

Figure 4.7 shows the switching behaviour of the LC diffraction gratings. Both types show similar switching behaviour, switching OFF at around 1.5 V and 1 V, The switching time from ON to OFF state was around 10 sec and 60-70 sec from OFF to ON state. These switching times are quite slow and alternative methods for fabrication of such devices to improve the switching times need to be investigated.

4.5 Conclusions

LC diffraction gratings were successfully fabricated by filling surface relief gratings with E49 and E7 LCs and electro-optical switching was demonstrated. The gratings prepared with higher n_e LCs show higher DE. These studies show the potential of surface relief gratings in acrylamide based photopolymer for fabrication of electrically switchable LC optical components.

The next chapter discusses the fabrication and the characterization of a switchable LC polarization rotator. Photoinduced surface relief gratings in combination with rubbing were used to orient LCs for the successful fabrication of a twisted nematic LC device for rotating the plane of polarization of light.

References

1. A. Miniewicz, A. Gniewek and J. Parka, “Liquid crystals for photonic applications.” Opt. Material., 21, 605-610, 2002.
2. M. Johansson, S. Hard, B. Robertson, I. Manolis, T. Wilkinson and W. Crosland, “Adaptive beam steering implemented in a ferroelectric liquid-crystal spatial-light-modulator free-space, fiber-optic switch.” Appl. Opt., 41(23), 4904-4911,2002
3. S. Brugioni and R. Meucci, “Liquid crystal twisted nematic light modulator for the infrared region.” J. Opt. A: Pure Appl. Opt., 6, 6-9, 2004.
4. H. Ren, Y. H. Fan and S. T. Wu, “Liquid-crystal microlens arrays using patterned polymer networks.” Opt. Lett., 29(14), 1608-1610, 2004.
5. I. Fujieda, O. Mikami, and A. Ozawa, “Active optical interconnect based on liquid-crystal grating.”, Appl. Opt., 42(8), 1520-1525, 2003.
6. A. Ashmead, “Electronically switchable Bragg gratings for versatility”, A special report in Passive and Active components, http://optics.caltech.edu/switchable_b_gratings.pdf. 10-3-2006.
7. G. Zou, H. Grönqvist and J. Liu, “Integrated inductors on liquid crystal polymer substrate for RF applications.” Circuit World, 32-1, 41-44, 2006.
8. B. Bahadur, “Liquid crystals: Applications and uses” Vol.1, World Scientific Publisher, 1990.
9. R. S. McEwen, “Liquid crystals, displays and devices for optical processing.” J.Phys.E:Sci.Instrum.20, 364-377, 1987.

10. T. J. Bunning, L.V. Natarajan, V.P. Tondiglia and R.L. Sutherland “Holographic Polymer-Dispersed Liquid Crystals (H_PDLCs).” Annu. Rev. Mater.Sci. 30, 83-115, 2000.
11. M. O’Neill and S. M. Kelly, “Photoinduced surface alignment for liquid crystal displays.” J.Phys.D.Appl.Phys.33, 67-84, 2000
12. T. Ikeda, “Photomodulation of liquid crystal orientations for photonic applications.” J.Mater.Chem., 13, 2037-2057, 2003.
13. G. P. Crawford, J. N. Eakin, M. C. Radcliffe, A. C. Jones and R. A. Pelcovits, “Liquid crystal diffraction gratings using polarization holography alignment techniques.” J. App. Phys., 98, 123102, 2005.
14. M. L. Jepsen and H. J. Gerritsen, “Liquid crystal filled gratings with high diffraction efficiency.” Opt. Lett. 21(14), 1081-1083, 1996.
15. D. Dantsker, J. Kumar and S. K. Tripathy, “Optical alignment of liquid crystals.” J. Appl. Phys, 89(8), 4318-4325, 2001.
16. X. T. Li, A. Natansohn and P. Rochon, “Photoinduced liquid crystal alignment based on a surface relief grating in an assembled cell.” Appl.Phys.Lett., 74(25) , 3791, 1999.
17. F. Kaneko, T. Kota, A. Baba, K. Shinbo, K. Kato and R. C. Advincula, “Photo induced fabrication of surface relief gratings in alternate self assembled films containing azo dye and alignment of LC molecules.” Colloids and Surfaces A: Physicochem. Eng. Aspects 198-200, 805-810, 2002.
18. I. Naydenova, K. Pavani, E. Mihalova, K. Loudmer, S. Martin and V. Toal, “Holographic recording of patterns in thin film acrylamide-based photopolymer”. SPIE Proc. 5827-17, 163-172, 2005.

19. K. Pavani, I. Naydenova, S. Martin and V. Toal, “Photoinduced surface relief studies in an acrylamide-based photopolymer.” J.Opt.A: Pure Appl. Opt., 9, 43-48, 2007.

20. N. Ouellette and L. Larrimore, “Measuring the birefringence of a liquid crystal.” P116 Seminar 7 Experiment 1. http://www.sccs.swarthmore.edu/users/02/lisal/physics/labs/birefringence.pdf 10-2-2006.

21. O. KÖysal, S. E. San, S. Özder and F. N. Ecevit, “A novel approach for the determination of birefringence dispersion in nematic liquid crystals by using the continuous wavelet transform.” Meas. Sci. Technol. 14(6), 790–795, 2003.

22. Y. Yusuf, Y. Sumisaki and S. Kai, “Birefringence measurement of liquid single crystal elastomer swollen with low molecular weight liquid crystal.” Chemical Physics Letters 382, 198–202, 2003.

23. M. L. Jepsen and H.J. Gerritsen, “High efficiency liquid-crystal filled diffraction gratings.” SPIE Proc., 3011, 165-176, 1997.

24. M C K Wiltshire and M. R. Lewis, “A method for analyzing elliptically polarised light over a range of wave lengths.” J.Phys, E: Sci.Instrum.20, 884-887, 1987.

25. B. Bahadur, “Liquid crystals: Applications and uses.” Vol 1, World Scientific publishers, 1990.

26. K. Pavani, I. Naydenova, R. G. Howard, S. Martin and V. Toal, “Fabrication of switchable liquid crystal devices using surface relief gratings in photopolymer.”JMSE published online, 2007. *http://www.springerlink.com/content/94q743l002810lt9/*

27. M. L. Jepsen and H. J. Gerritsen, “Liquid-crystal-filled with high diffraction efficiency.” Opt. Lett., 21(14) 1081-1083, 1996.

28. A. K. Ghosh, Y. Takanishi, K. Ishikawa, H. Takezoe, Y. Ono and J. Kawamura, “Electrically controllable polarization-dependent phase grating from photocurable liquid crystals.” J. Appl. Phys., 95(9), 5241-5243, 2004.

29. P. Hariharan, “Optical holography: Principles techniques and applications.” 2nd Edition, Cambridge monographics on physics, Cambridge University Press, 1996.

30. S. Palmer, “The optical response of liquid crystal cells to a low frequency driving voltages.” Liquid Crystal Journal, 36(10), 1-8, 1998.

5. FABRICATION OF TWISTED NEMATIC LIQUID CRYSTAL DEVICES USING PHOTOPOLYMER SURFACE RELIEF GRATINGS

5.1 Introduction

Most widely used LCDs are based on twist nematic (TN) LCs for applications ranging from watches to computer monitors. Although the liquid crystal state was discovered in1888, the most widely used TN LCD mode was invented by Schadt and Helfrich in 1970 [1-4]. A comprehensive description of the importance of the nematic LCs in the TN LCD is given by Gray et al. [5]. The advantages of the TN mode are high contrast ratio, analog grey scale and low driving voltage. The concepts that led to TN mode were also formulated by Fergason, who established the International Liquid Xtal Company in Kent, OH [6].

Nematic LCs exhibits a helical twist when they are sandwiched between cross-grooved plates. This twist nematic structure is obtained either by rotating one of the substrates through 90º in its plane or by the action of two rubbed surfaces placed at an angle of 90º to each other [5]. Usually the latter method is used to obtain a twisted nematic structure [1, 2]. Linearly polarized light incident normal to the plates with its plane of polarization parallel to the grooves at the input plane emerges with its direction of polarization rotated along the helical twist. If the LCs are positive anisotropic, an applied electric field perpendicular to the plates reorients the long axis of the LCs parallel to the direction of the incident light and thus the rotation of polarization is eliminated. By using two polarizers, TNLC device can act as a light switch and can be controlled by electric field. Fergason described the concept of helical twist and

rotation of linearly polarized light in 1968 and reported the reorientation of nematic LCs by an electric field [6].

In optical systems the plane of polarization is often rotated by quartz retardation plates. The advantages of these quartz plates are that they are of high quality and have good transmission especially in the UV region. However the disadvantages of these plates are that they are expensive, they have only a narrow spectral bandwidth and have a small incidence acceptance angle, less than 2°. These disadvantages are overcome by replacing quartz by LCs. Nematic LCs are used to fabricate optoelectronic LC devices. The advantages of the LC nematic cells are large acceptance angle, operation over a large spectral range from VIS to NIR and lower price. Optionally, by applying voltage on the TN cell, the polarization rotation can be "switched off". Also in combination with two polarizers it can act as an optical shutter [7].

The alignment layer plays an important role in the fabrication of a TNLC device. Commercially a thin alignment layer such as polyimide is coated on the glass, and the surface is rubbed with velvet cloth (soft cloth) in the direction in which the LC molecules will be aligned. In order to obtain a twist angle between both glasses, rubbing directions are different from each other. The disadvantages of this method are the creation of dust and the static electricity highly undesirable for the LC displays [2, 8]. The advantage of this method is the perfect alignment of the LCs [8]. Another method for fabricating these devices is to use photoinduced surface relief gratings recorded in photopolymers. This is an attractive technique for fabrication of these devices as explained in chapter 1[2]. The advantage of this technique is that dust and static electric field are not generated as discussed in the introduction chapter. The

disadvantage is that in some photopolymers there is no photochemical generation of the surface anisotropy [8-12] thus the alignment of the LCs is weak. Initially the TNLC devices were fabricated by filling the surface relief gratings with LCs and without using any rubbing. Although, the device acted as switchable 2D diffraction grating the obtained twist angle and switching behaviour were not very encouraging. This chapter presents a novel technique for the fabrication of a twisted nematic LC device by using the combination of rubbing and non rubbing techniques where the disadvantages of the two techniques are eliminated.

Optically recorded surface relief gratings in an acrylamide based photopolymer were used in this work for the fabrication of the TNLC device, which consists of two parallel photopolymer layers with sinusoidal surface relief profiles, oriented so that the wave vectors of the two gratings are orthogonal. These surface relief gratings were rubbed for five times along the grooves with a velvet cloth. The main difference between the device presented here and a twisted nematic LC cell fabricated by standard rubbing technique is the existence of additional diffraction orders due to the nature of the two interfaces used to orient the LCs. Thus this device can have a dual role as an electro-optical polarization rotator and a switchable beam splitter. ZLI-3700-000 LCs from Merck (Merck catalogue) were used to fabricate TN devices and so these LCs were chosen to fabricate TNLC device. The optical anisotropy of the LCs is 0.101 with n_e =1.585 and n_o = 1.484.

A parameter that has a crucial influence on the performance of the device is the twist angle [13]. By using a simple method, the twist angle of the device was determined. Twist angle was measured in the zero and in the diffracted orders. The electro optical

switching behaviour in the diffraction orders was characterized along with the zero order by placing the TNLC device between crossed polarizers. Depending upon the configuration of polarizers and analyzer, whether their transmission axes are parallel (dark mode) or perpendicular (white mode) to each other, two cases are possible. In white mode, when the light azimuth is rotated by 90º the light is not blocked by the analyzer in the OFF state, while in dark mode, when light azimuth is rotated by 90º the light is blocked by the analyzer in the OFF state. In this work the polarization rotator was characterized by studying the influence of the applied electric field on the twist angle and the variation of intensity in the zero and the diffracted orders with the twisted nematic LC device placed between crossed polarizers (white mode) [1, 14]. The dependence of the polarization state of the light transmitted through the device (zero order) on the applied electric field was analysed by measuring the ellipticity.

5.2 Methodology

5.2.1. Determination of the director and twist angle

The ellipticity was measured at different azimuths of the linearly polarized probe beam as described in chapter 4. At the optical axis (along extraordinary axis and ordinary axis of the LCs) of the TNLC device the measured ellipticity reaches its minimum. The director in the twisted nematic LC device was determined as follows. Supposing the input plane of polarization makes a small, unknown angle δ, with the director at the input of the device. If the amplitude of the electric field at the input is A then the components parallel and perpendicular to the director are $A\cos\delta$ and $A\sin\delta$. Both components will be rotated by α, the twist angle and the

angle between the output director and the azimuth of the light immerging from the device will be δ.

Now suppose an analyzer is inserted at the output, with its transmission axis set at an unknown angle γ to the output director of the device. The output intensity is given by

$$I = (A \cos\delta \cos\gamma)^2 + (A \sin\delta \sin\gamma)^2 \quad \text{——————————————————————} (5.1)$$

$$= A^2 [(1- \sin^2\delta) \cos^2\gamma + \sin^2\delta \sin^2\gamma] \text{----------} (5.2)$$

$$= A^2 [\cos^2\gamma + \sin^2\delta(\sin^2\gamma - \cos^2\gamma)] \text{----------} (5.3)$$

When $\gamma = 0$, $I = A^2 \cos^2\delta$ (maximum) and when $\gamma = \pi/2$, $I = A^2\sin^2\delta$ (minimum).

It follows that when the output is maximum, the analyzer has its transmission axis parallel to the output director.

Further, when δ is zero, the intensity is A^2, so the half wave plate in front of the input director should be rotated about the optical axis to obtain an absolute maximum output. The input plane of polarization is now parallel to the input director. The twist angle is obtained from the settings of the half wave plate and the analyzer. It is the angle between the input light polarization direction and transmission axis of the analyzer.

5.2.2. Electro optical switching behaviour

The basic operation of the twisted nematic LC device as a polarization rotator is shown in figure 5.1 and is explained as follows. When no electric field is applied to the device (OFF state), the linearly polarized light propagates through the LC layer and its plane

of polarization is rotated by the twisted structure and the light emerges from the layer with its polarization plane parallel to the transmission axis of the analyzer. This is only true when Mauguin condition, $\Delta nd >> \lambda/2$, is satisfied and for TNLC device with 90^{o} twist [1]. When a voltage is applied across the device (ON state), the director (local optic axis) in the central portion of the LC layer orients parallel to the electric field and the twist is removed. The polarization plane of the light is no longer rotated and light passing through the cell is absorbed at the analyzer which is in the crossed position [1-6].

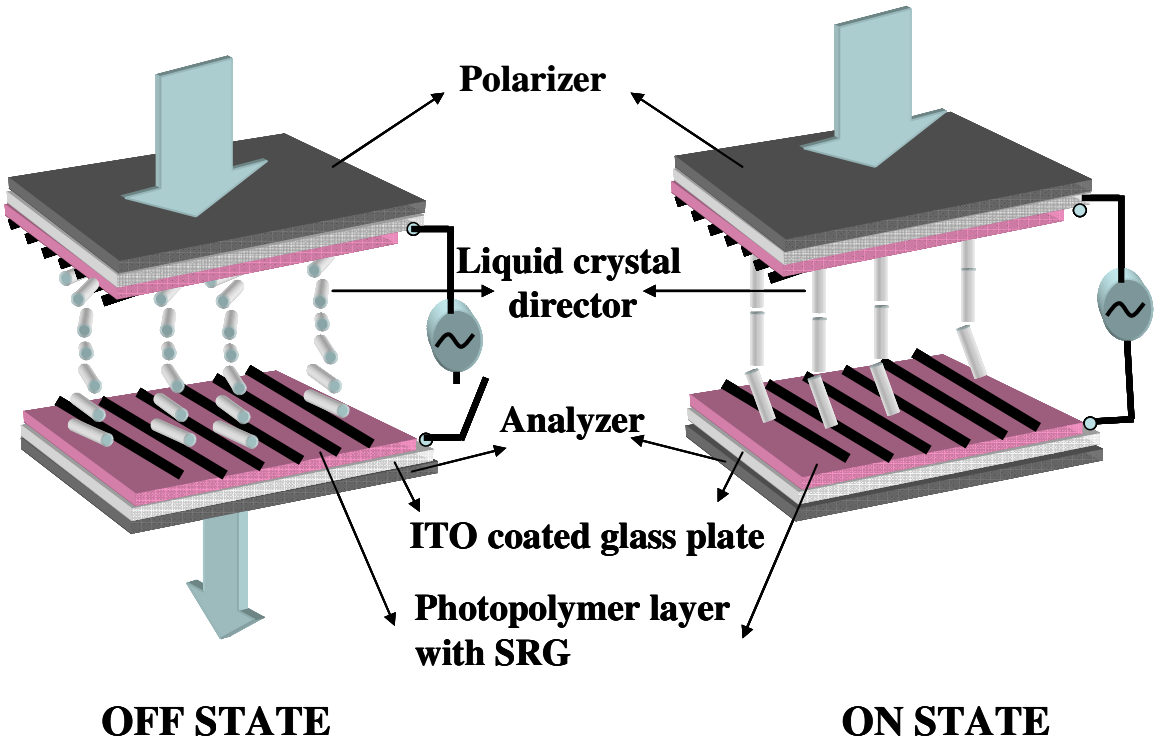

Figure 5.1 Operation of the twisted nematic LC device.

5.3 Experimental

5.3.1. Fabrication of the TNLC device

ITO coated glass plates were cut into small pieces 3 x 2.5 cm^2. Electrical contacts were made on the corners of the plates with silver loaded epoxy resin and allowed to dry. The plates were treated with NaOH solution for 30 min in an ultrasonic bath. Good optical quality samples of acrylamide based photopolymer were prepared by the gravity settling method. The thickness of the photopolymer layer on ITO coated glass substrates was 10 μm after drying for 2 to 3 hours. These photopolymer layers were exposed to an optical interference pattern to record surface relief transmission diffraction gratings of 100 lines/mm as described in chapter 3 using a spatially filtered and collimated laser with λ = 532 nm. These gratings were further exposed to uniform UV light intensity to completely polymerize the remaining monomer. The amplitude modulation of the surface relief grating was measured to be 140 ± 8 nm. Before assembly, the surface relief gratings were rubbed five times along the fringes with a velvet cloth. In general, when a polymer layer is rubbed in a particular direction, polymer chains are reoriented which gives anisotropic behaviour. The interaction of the polymer chains with LCs causes alignment [2, 14]. The TN device was assembled in such a way that the wave vectors of the two surface relief gratings were orthogonal as shown in the figure 5.1. The gratings were separated by 6 μm thick spacers. In this photopolymer such orientation of polymer chains showing anisotropic was not observed and was verified by measuring birefringence after rubbing. This could be because they were rubbed very lightly and for only five times. The assembled device was glued on two sides and the other two sides were kept open to fill the device with LCs. The device was filled with the LCs by using capillary action [1]. One of the open sides was placed in the LC container and a vacuum pump was connected to the second

opening. When the vacuum pump was turned on LCs were drawn into the cell. It took 15 to 20 minutes to fill the cell completely and uniformly. Considering thickness of the spacers and birefringence of the LCs used for fabrication of the TNLC device one can estimate that the Mauguin condition is satisfied.

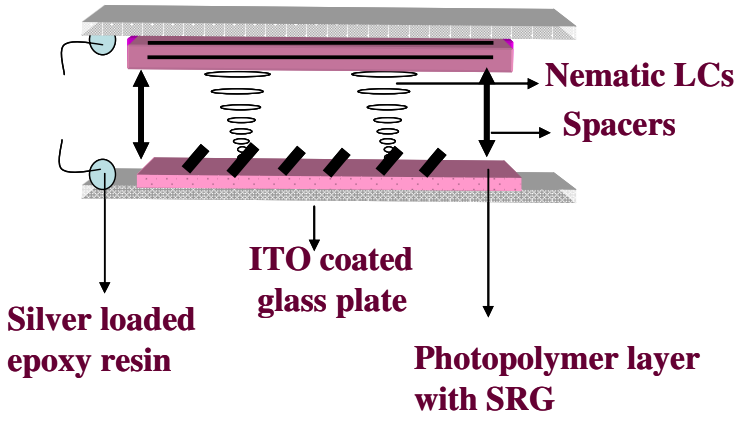

Figure 5.2 Fabrication of the TNLC device.

5.3.2. Characterization of TNLC device

The incident light on the LC material experiences two refractive indices, one is along n_o and other is along n_e. This introduces a phase difference between two light components and thus rotation of linearly polarized light is induced. A vertically polarized laser beam of wavelength 633 nm was used to characterize the TNLC devices and the experimental set up is shown in figure 5.3. To study the electro-optical switching behaviour the laser beam was incident normal to the device. A half wave plate is used to ensure that the plane of polarization of the incident light is parallel to the input director of the device and an analyzer is set with its transmission axis orthogonal to the plane of polarization of the input light beam.

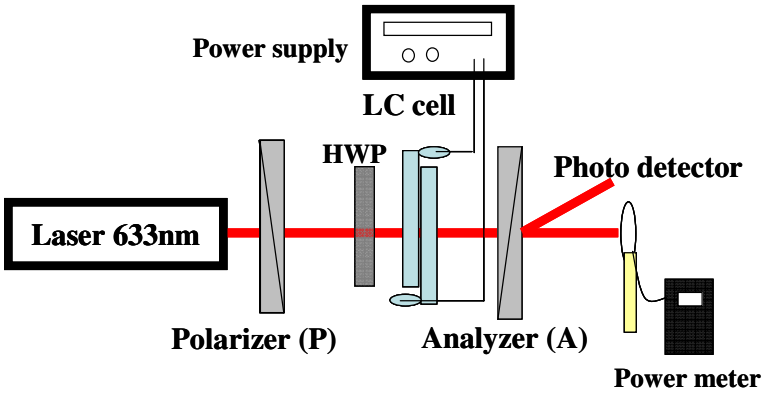

Figure 5.3 Optical setup used to characterize the twisted nematic LC device.

5.4 Results

5.4.1. Determination of director and twist angle

Figure 5.4 shows the variation of ellipticity in the zero order with incoming orientation angle of the plane of polarization of the probe beam. It can be seen that there are two minimum ellipticities which shows that the device has two optical axes which are along the extraordinary axis (director) and ordinary axis of the index ellipsoid for the LC molecules [16].

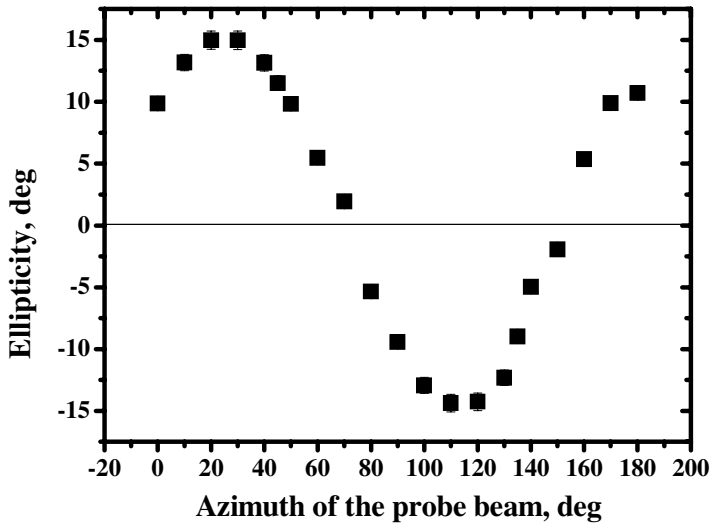

Figure 5.4 Ellipticity verses azimuth of the linearly polarized probe beam.

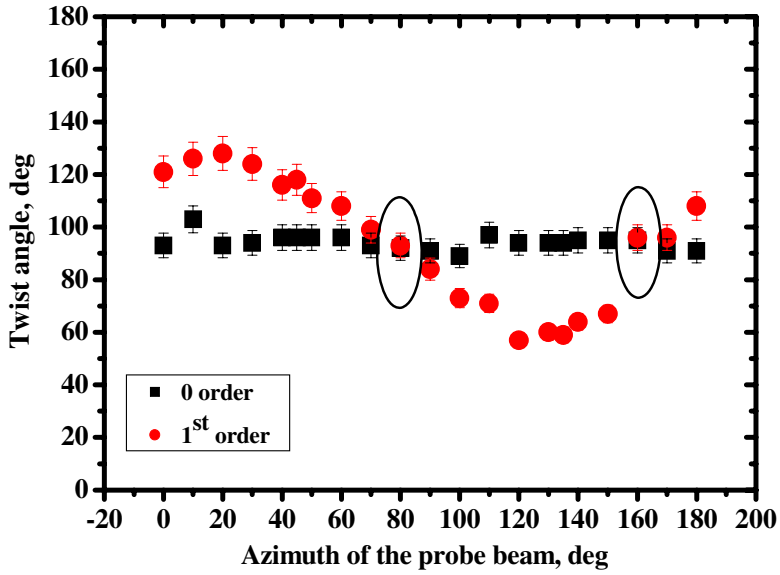

Figure 5.5 Variation of the twist angle in the zero and first orders with the azimuth of the linearly polarised probe beam.

Figure 5.5 shows the variation of twist angle in the zero and the first orders with the azimuth of the linearly polarized probe beam. It can be seen from the graph that there is no variation in the twist angle in the zero order while the twist angle varies in first order. No variation in the twist angle in zero order with azimuth of probe beam suggests that the LCs are perfectly aligned by the combination of photoinduced surface relief gratings and rubbing of photopolymer layer. The variation of the twist angle in the first order could be due to the oblique propagation of the diffracted beams in the twisted device. As we see from the graph (figure 5.5) the twist angle is same at the optical axes of the device.

To determine the director of the device, an absolute maximum output intensity was measured by rotating analyzer at these two orientations of the input polarization plane was measured by rotating the analyzer as described in section 5.2.1. At these positions

minimum ellipticity and same twist angle are observed. The director was adjusted at 160^0 to study the switching behaviour of this device.

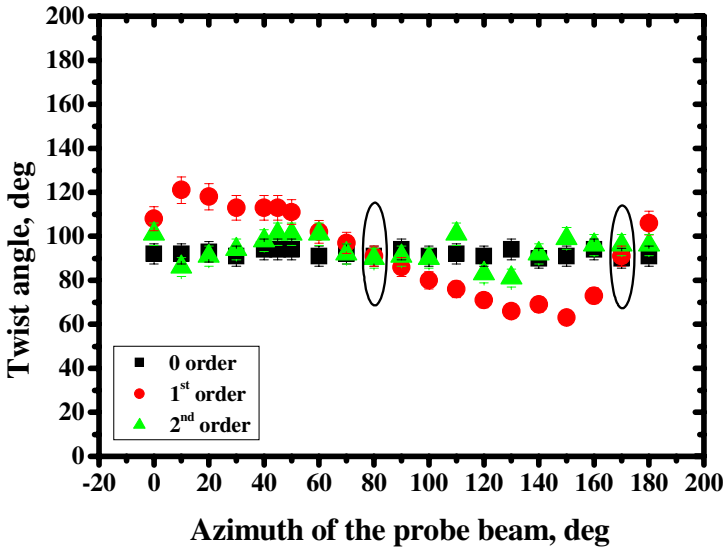

Figure 5.6 Variation of the twist angle in the zero and diffracted orders with the azimuth of the linearly polarised probe beam.

Figure 5.6 shows another example of the twist angle versus the azimuth of the linearly polarized probe beam in a different device in zero, first and second orders. As it is seen a similar behaviour is observed as in figure 5.5. It can be observed that the variation of twist angle is also observed in second order. This device also shows two optical axes and the director of the device was determined to be at 170^0 with respect to vertical axis. This variation of the twist angle with the azimuth of the linearly polarized probe beam was confirmed in five more devices.

5.4.2. Study of the electro optical switching behaviour

To study the electro optical switching behaviour of the TNLC device, the plane of polarization of the incident light was set parallel to the input director of the device and

an analyzer was set with its transmission axis parallel to the output director of the device. Figure 5.7 shows the variation of the normalised transmitted intensity with applied electric field when the device was placed between crossed polarizers. It can also be seen that the switching behaviour was reversible when the field was removed.

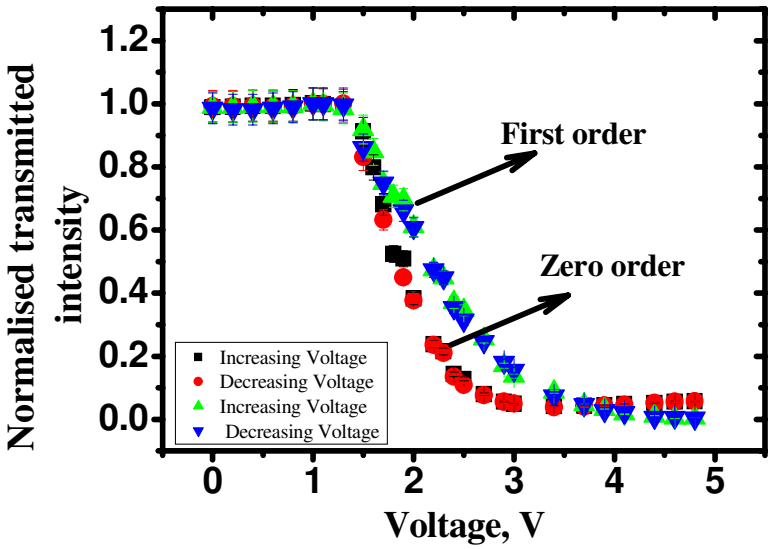

Figure 5.7 Intensity versus voltage.

Figure 5.8 shows the variation in the twist angle with applied voltage. The measured twist angle of this device was 92º. It is seen that at around 3.4 V the twist disappears due to orientation of LCs perpendicular to the substrates. The polarization plane of the light passing through the device is not rotated and the light is then absorbed at the analyzer. The time taken to switch from the OFF state to ON was around 6-8 sec and 12-15 sec from the ON to the OFF state. The switching behaviour of this device is shown in figure 5.9. As is seen from figure 5.9 (b) some light is passing through the analyzer even after applying voltage. This could be attributed to the ellipticity due to some scattering of the light as seen in figure 5.13.

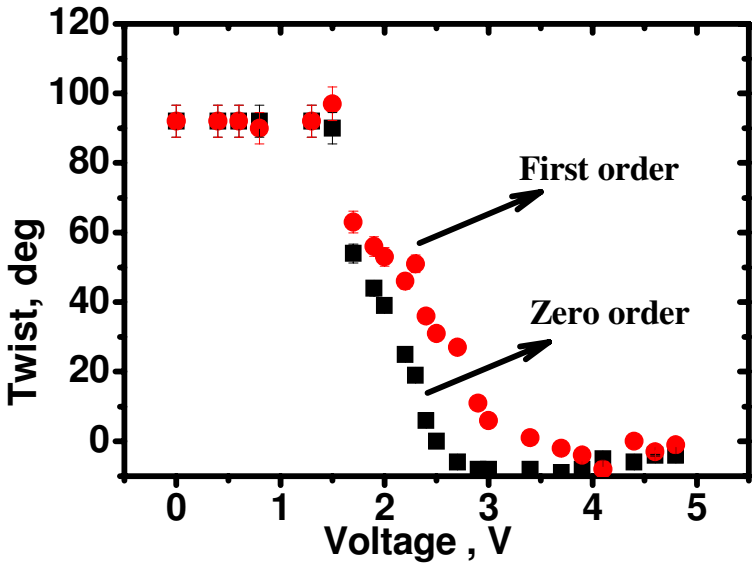

Figure 5.8 Twist angle versus voltage

Figure 5.9 Intensity of transmitted light between crossed polarizers with applied voltage.

In some TNLC devices a similar electro optical switching behaviour was observed at lower voltages, for example at around 2-2.5 V as shown in figures 5.10 and 5.11 respectively and showed a twist angle of 92º. However, there were some devices which had different twist angles, for example 82º and 102º. The reason for that is probably

some misalignment between the two surface relief gratings at the cell fabrication stage. Nevertheless, these devices also showed electro-optical switching behaviour. Figure 5.10 shows the decrease in the twist angle as the voltage is applied to the device. Figure 5.11 shows the variation of the transmitted light intensity with applied electric field when the device was placed between crossed polarizers. It is observed from the figures 5.10 that at around 2.5 V the twist disappeared in zero and diffracted orders which could be due to orientation of LCs along the electric field. From figure 5.11 it can be observed that at around same voltage the polarization plane of the light passing through the device is not rotated and the light is absorbed at the analyzer in all orders.

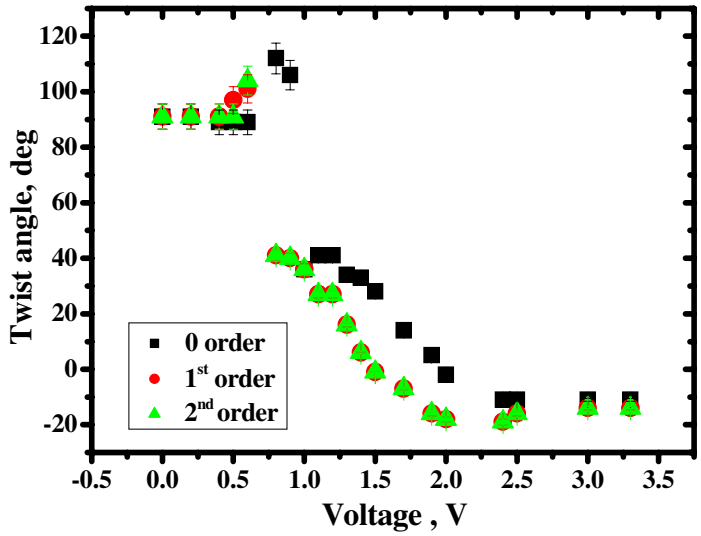

Figure 5.10 Twist angle versus Voltage.

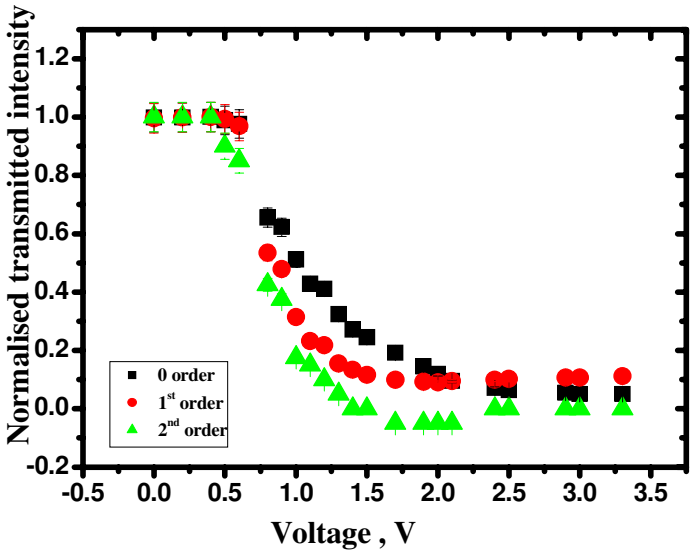

Figure 5.11 Intensity versus Voltage.

From these results it is observed that when no electric field is applied a twist of 92° ± 10º is obtained, and it can be decreased with applied voltage but the original twist angle is restored when the voltage is removed. Electro optical switching behaviour was also observed in diffracted orders along with the zero order which is an advantage of this device compared to commercially available devices. These results demonstrate the successful fabrication of the TNLC device. The next step was the analysis of the polarization state of light emerging from the device.

5.4.3. Analysis of the polarization state of light

Depending on the orientation of the plane of polarization of incident light with respect to the LC principal axes and on the phase difference introduced by the LC layer due to the birefringence, the emergent light may be linearly, circularly or elliptically polarized. By analyzing the ellipticity the state of the polarized light emerging from the device can be characterized.

Ellipticity (χ) was defined in equation (4.5) or it can also be defined as the ratio of two semi axes of the ellipse as shown in figure 5.12. From equation (4.5) it can be shown that an ellipticity of 0^o corresponds to linear polarization and ellipticity of 45^o corresponds to circularly polarized light.

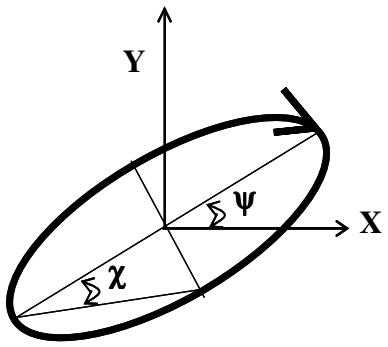

Figure 5.12 Ellipticity and azimuth.

The dependence of the polarization state of the emerging light on applied electric field was studied. The optical setup shown in the figure 5.3 was also used here. After applying an electric field to the device the analyzer was rotated to measure I_{min} and I_{max}. By using the equation (4.5) ellipticity was calculated and the result is shown in figure 5.13. The measurements were carried out in the zero order.

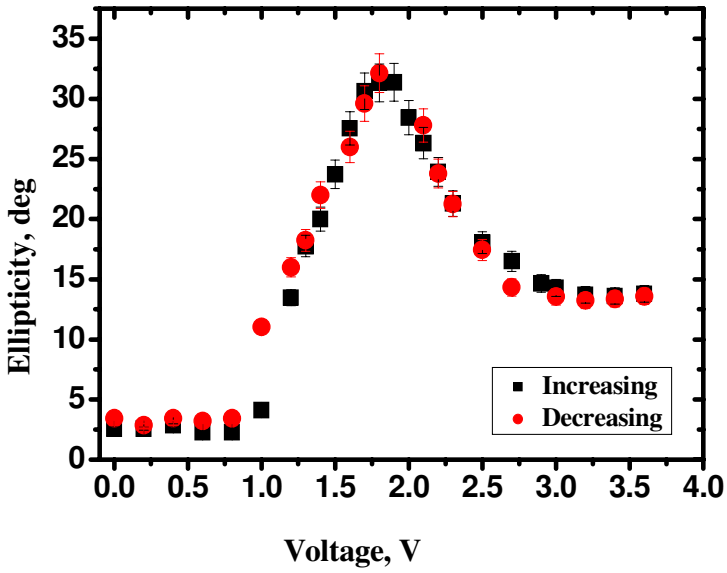

Figure 5.13 Ellipticity verses applied voltage.

From the graph it is seen that at zero voltage the polarization state emerging from the cell is close to linear and with increase in the applied electric field ellipticity increases. Further increase in the applied field decreases the ellipticity. And when the voltage was decreased it was observed that the change in the ellipticity was reversible. Such behaviour was repeatedly observed in five devices. The time required to convert from linear to elliptically polarized state was around 5 to 6 sec and for the reverse effect it was around 8 to 9 sec. A similar switching behaviour of the twist angle and the transmitted intensity with applied electric field was observed in diffracted orders.

5.5 Conclusions

The potential of optically recorded surface relief gratings in IEO photopolymer for fabricating TNLC devices has been demonstrated. A novel technique in which

photoinduced surface relief gratings in combination with rubbing technique were used to orient LCs for the successful fabrication of a TNLC device for rotating the plane of polarization of light has been presented. A twist angle of 92° ± 10º was observed in the zero and diffracted orders. The effects of an applied electric field on the transmitted and the first order diffracted light intensities and on the twist angle were studied. The polarization state of the transmitted light in the zero order was analysed by measuring ellipticity. Ellipticity studies show that with application of electric field linearly polarized light is converted to elliptically polarized light. By adjusting the voltage a required degree of ellipticity can be obtained.

Attempts made to fabricate switchable LC devices by filling surface relief gratings in an acrylamide based photopolymer with LCs were successful. However the diffraction efficiency of these switchable LC diffraction gratings was low. To improve the efficiency of the diffraction gratings, a composite with LCs and photopolymer which is known as PDLCs was developed and the fabrication of switchable holographic volume PDLC diffraction gratings is presented in next chapter.

References

1. B. Bahadur, “Liquid crystals: Applications and uses” Vol.1, World Scientific publisher, 1990.
2. K. Takatoh, M. Hasegawa, M. Koden, N. Itoh, R. Hasegawa and M. Sakamoto, “Alignment technologies and applications of liquid crystal devices.” Taylor & Francis (2005).
3. M. J. Bradshaw, “Liquid crystal devices.” Phys.Educ., 18;pp:20-26,1983.
4. R. S. McEwen, “Instrument Science and Technology: Liquid crystals, displays and devices for optical processing.” J. Phys. E: Sci. Instrum. 20, 364-377, 1987.
5. G. W. Gray and S. M. Kelly, “liquid crystals for twisted nematic display devices.” J. Mater. Chem., 9, 2037-2050, 1999.
6. H. Kawamoto, “The history of liquid crystal displays.” Proc. Of the IEEE, 90(4), 460-500, 2002.
7. http://www.arcoptix.com/PolarizationRotatorDescription.pdf 5-2-2007.
8. J. Cognard, “Alignment of nematic liquid crystals and their mixtures.” Gordon and Breach, New York, p 59. 1982.
9. K. Sakamoto, K. Usami, M. Watanabe, R. Arafune and S.Ushioda, “Surface anisotropy of polyimide film irradiated with linearly polarized ultraviolet light.” Appl. Phys. Lett., 72, 15, 1832-1834, 1998.
10. V. V. Lazarev, M. I. Barnik and N. M. Shtykov, “Liquid crystal alignment by photo-processed polymer films.” Mol. Materials, 8, 235-244, 1997.
11. T. Ikeda, “Photomodulation of liquid crystal orientations for photonic applications.” J.Mater.Chem, 13, 2037-2057, 2003.

12. J. Y. Kim, T. H. Kim, T. Kimura, T. Fukuda and H. Matsuda, “Surface relief grating and LC alignment on azo benzene functionalized polymers.” Opt. Mat., 21, 627-631, 2002.
13. S-T. Wu and G. Xu, “Cell gap and twist angle determinations of a reflective liquid crystal displays.” IEEE transcactions on electron devices, 42(12), 2290-2292, 2000.
14. I. S. Song, S. S. Shin, H. Y. Kim, S. H. Song and S. H. Lee, “Electro-optic charcterizatics of 90º twisted nematic liquid crystal display driven by fringe-electric field.” J. Appl. Phys., 95(4), 1625-1629, 2004.
15. J. M. Geary, J. W. Goodby, A. R. Kmetz and J. S. Patel, “The mechanism of polymer alignment of liquid-crystal materials.” J. Appl. Phys. 62(10), 4100-4108, 1987.
16. J. A. Davis, I. Moreno and P. Tsai, “Polarization eigenstates for twisted-nematic liquid crystal displays.” Appl. Opt., 37(5), 937-945, 1998.
17. I. Naydenova, L. Nikolova, T. Todorov, F. Andruzzi, S. Hvilisted and P. S. Ramanujam, “Polarimetric investigation of materials with both linear and circular anisotropy.” J. Mod. Opt., 44(9), 1643-1650, 1997.

6. FABRICATION OF HOLOGRAPHIC POLYMER DISPERSED LIQUID CRYSTALS DIFFRACTION GRATINGS

6.1 Introduction

The composites in which LC droplets are embedded in a polymer matrix are known as polymer dispersed liquid crystals (PDLCs). These PDLCs show the combined properties of photopolymers and LCs. LC dispersions were first studied by Lehman in 1904. However, the development of PDLC materials for practical applications was begun in mid 1980's. They have a great potential for use in the electro optical devices, display devices, switchable windows and light shutter devices [1-7].

The principle of operation of the PDLCs is based on light scattering [1, 2]. The PDLC layers are sandwiched between two substrates which are conducting electrodes. The micro sized LC droplets in the polymer binder show strong scattering of the light and the layer is seen to be opaque. The layer can be switched from the scattering state to an optically clear state by the application of suitable electric field. This behaviour shown by these materials is the basis for display application. In the absence of a field the directors of the droplets within the layer are randomly oriented. As a result, incident light probes a range of refractive index values between n_o and n_e, which are ordinary and extraordinary refractive indices of LCs. Since nematic LCs are optically uniaxial, indices experienced by incident light cannot be all equal to the polymer refractive index n_p and so incoming light is scattered by the micro droplets, giving rise to the opaque state. This state is known as OFF state. When a sufficiently large electric field is

applied, the LC molecules in the droplets are collectively reoriented with their directors parallel to the applied field. Hence, under this condition the refractive index of polymer (n_p) is equal to n_o of LCs resulting in an optically clear state, so light is transmitted with no scattering [1,2, 8-11]. This state is known as ON state.

6.1.1. PDLC preparation methods

PDLC materials are prepared by two different methods, encapsulation and phase separation. The fundamental difference between these two methods is in the initial solution of the prepolymer and LC. In the encapsulation (NCAP) method the solution is inhomogeneous whereas in the phase separation method the solution of the prepolymer and LCs is homogenous. The latter is the commercially used method to manufacture these PDLC materials. There are three different methods for obtaining phase separation. They are polymerization-induced phase separation (PIPS), thermally-induced phase separation (TIPS) and solvent-induced phase separation (SIPS) [1, 2, 8-10]

Encapsulation (NCAP): In this method the PDLC layer is prepared by dispersing LCs into a polymer which cannot dissolve LCs. The most common polymer used is polyvinyl alcohol (PVA) which is water soluble. This prepared emulsion is coated onto a conductive substrate such as ITO coated glass plate and allowed to dry, to form a polymer film with embedded microdroplets. A second conductive substrate is laminated on top to form the PDLC device. Ammonium polyacrylate and gelatin are also used as encapsulating media for LCs. This method is simple and cheap but it is time consuming. Studies of these samples using scanning electron microscopy (SEM) indicate that the droplets can be interconnected and often are not uniform in size. Basically this type of sample preparation has applications in high contrast light shutters.

Polymerization-induced phase separation (PIPS): In this method the PDLC layers are prepared by dispersing LCs into the prepolymer which may be a liquid or solid formulation. The homogenous solution is sandwiched between conductive substrates and the polymerization reaction is initiated by exposing to uniform or non-uniform light. Phase separation of the LCs and the polymer occurs during polymerization and the LC droplets are trapped in solid polymer. Droplet size and morphology have a strong influence on the electro optical properties of the device. The size of the droplets can be controlled by the rate of polymerization, LC content in the homogenous solution, solubility of LC in polymer, viscosity and rate of diffusion.

Thermally-induced phase separation (TIPS): In this method a mixture of LCs and polymer which has a melting temperature below its decomposition temperature is formed. Usually thermoplastics are preferred for this method as they melt below their decomposition temperature. A phase separation between LCs and polymer is induced by cooling the homogeneous solution at a specific rate. The size of the LC droplets is inversely proportional to the rate of cooling of the solution.

Solvent induced phase separation (SIPS): In this method the LCs and polymer are dissolved in a common solvent to form a homogeneous solution. The solvent is then removed by evaporation, resulting in phase separation and polymer solidification. This method is useful with thermoplastics which melt above the decomposition temperature of the thermoplastic or LCs and also in solvent coating techniques. The droplet size is controlled by controlling the rate of solvent removal. Droplet size is inversely proportional to the rate of solvent removal.

In this work preparation of holographic PDLC layer is based on PIPS.

6.1.2. Holographic polymer dispersed liquid crystals materials

The combination of photopolymer holography and PDLCs has resulted in holographic PDLCs (HPDLC). These HPDLCs are used in multiple applications such as switchable transmissive and reflective diffraction gratings, lenses with switchable focus, optical data storage, photonic crystals and fiber-optic couplers [5, 11-34]. HPDLCs are also studied as novel materials for fabrication of optical components such as polarization gratings [35-37]. A comprehensive review of HPDLC is given by Bunning et al. [5]. The fascinating features of HPDLC material are its high refractive index modulation, volume hologram characteristics, anisotropic nature and electro optical behaviour. In this material hologram recording is a simple single step which offers a unique approach to the economical fabrication of electrically switchable devices. Holographic illumination of the PDLC solution results in the periodical phase separation of LC rich planes. Depending upon the orientation of LC rich droplet planes, the recorded holograms are of two types, transmission or reflection [5]. There are a number of research groups working on HPDLC materials [5, 9, 14, 18, 19, 22, 27, 31, 38]. Although there are a number of impressive reports describing the performance parameters such as diffraction efficiency and switching voltage and transition time between on and off states of these switchable holographic materials [5, 11-38] there is still a growing need to produce materials that offer high diffraction efficiencies (DE), low switching fields and fast response. The purpose of this study was to develop a new HPDLC material and to fabricate switchable devices.

Initially LCs were mixed into an acrylamide based photopolymer. LCs couldn't disperse in this photopolymer which is water soluble and hence a new material which consists of

monomers, co-initiator, photo sensitizer, a reactive diluent and LCs was developed in this work. This PDLC material is not water soluble.

For HPDLC formulation two classes of monomers have been used. One is based on free-radical addition polymerization of materials such as acrylate monomers [5, 32] and urethane resins [30]. In some of the formulations, N-Vinyl pyrrolindinone (NVP) has been used as a reactive diluent. The role of NVP in curing of the polymer is not well understood [5]. The second type of HPDLC formulation utilizes a combination of free-radical and step growth mechanism observed in materials such as Norland resins [21]. In this work acrylamide, N, N'- methylenebisacrylamide and n-vinyl-2-pyrrolidinone (NVP) are used. NVP helps to dissolve the different components in the mixture and to form a homogeneous solution. It was previously observed that by increasing the amount of NVP in the solution helps in decrease the droplet size [39]. The monomers used in this work can participate in a free radical added polymerization. Free radical addition polymerization of multifunctional monomers leads to formation of polymer of high molecular weight. In a free radical polymerization process the generation of free radicals when light is incident onto the materials is an important process. This process is also called the photoinitiation process. In this process the light is absorbed by an appropriate dye, which reacts with an electron donor to produce the necessary initiating free radicals. In the work presented here erythrosine B, a xanthene dye is used as a photoinitiator and triethanolamine (TEA) is used as a co-initiator. The electro optical performance and diffraction efficiency of the HPDLCs depend on the choice of the LC. The refractive index of the polymer matches the ordinary refractive index of the LCs. High optical anisotropy (Δn) and dielectric anisotropy ($\Delta \varepsilon$) are also important when choosing LCs as they result in higher diffraction efficiency (DE) and lower switching

fields. Different kinds of nematic LCs which are mixtures of cyanobiphenyls and higher aromatic homologues (E7 & BL series) and mixtures of chloro and fluoro substituted mesogens are used in HPDLC systems [5]. In this work E7 ($\Delta n = 0.225$ & $n_o = 1.521$) and BL037 ($\Delta n = 0.282$ & $n_o = 1.526$) were used.

This chapter presents a novel PDLC used to record transmission HPDLC diffraction gratings. Preliminary results on the fabrication and characterization of gratings are reported. The electro optical switching behaviour was studied by measuring the light intensity in the first order of diffraction. The performance of HPDLC depends on the different parameters in which morphology of the LC/polymer composite, LC droplet size and redistribution of LC droplets play important roles [5, 40-44]. The redistribution of LC droplets after recording diffraction gratings was observed by using phase contrast microscopy and confocal Raman spectroscopy.

6.2 Theory

When a PDLC layer consisting of monomers, photoinitiator, a reactive dilute and LCs is exposed to an optical interference pattern, PIPS results in spatially periodic structures with alternating polymer and LC rich planes in the volume of the layer. A diffraction grating is created as a result of refractive index modulation between polymer and LC rich planes as shown in figure 6.1.

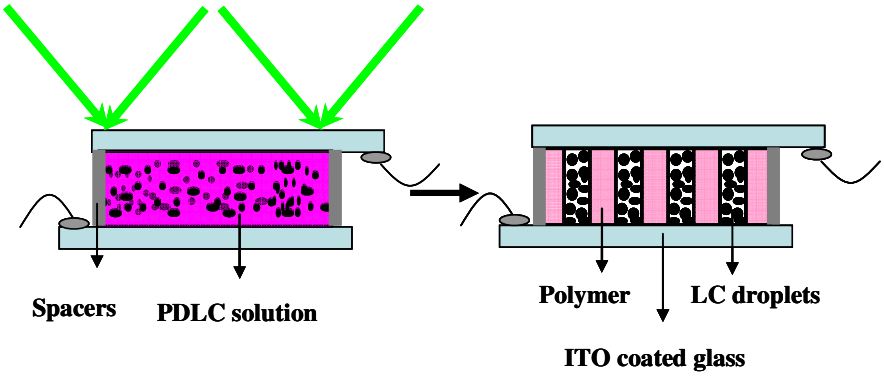

Figure 6.1 Creation of diffraction grating in PDLC layer.

There are different theoretical models explaining the formation of holograms in PDLC material [38, 45-47]. The mechanism of the formation of a diffraction grating in a PDLC layer is a result of counter diffusion of the components of the mixture and their consequent phase separation. The main mechanism of recording in this material could be the formation of polymer chains and diffusion of monomer and LCs. Two different scenarios are possible. The first one is observed where the polymerization process is faster than diffusion. During this the polymer chains grow into the dark fringes in the interference pattern. The second one could be where the polymerization is slow allowing monomer to diffuse from dark to bright regions of the interference pattern. In the first case there is a probability of LC droplets to be trapped in the bright regions whereas in the second case there is a probability of LC droplets to expelled to the dark region [38].

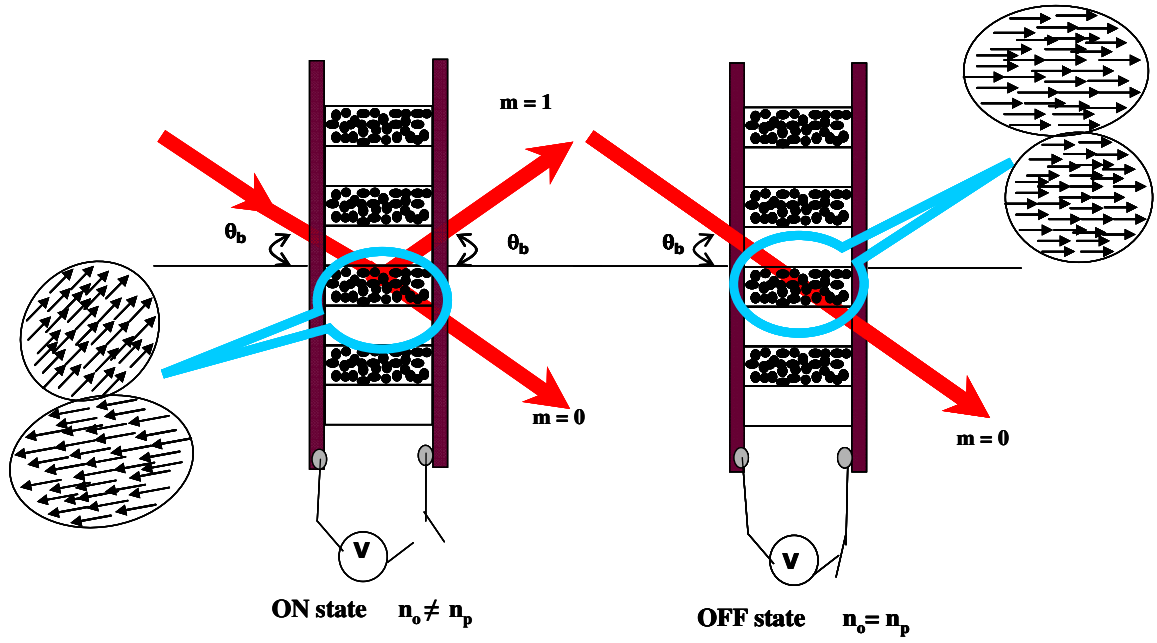

Figure 6.2 Operation of switchable HPDLC diffraction grating.

Linearly polarized light is used to study the electro optical switching behaviour of the gratings. The operation of a HPDLC diffraction grating is shown in figure 6.2. When no field is applied to the grating, the directors of the LC droplets within the layer are randomly oriented. As a result, incident linearly polarized light probes a range of refractive index values between n_o and n_e, which are the ordinary and extraordinary refractive indices of LCs and are different from the refractive index of photopolymer ($n_{p)}$ and hence the diffraction grating is in the ON state. When a sufficiently large electric field is applied, the LC molecules in the droplets are collectively reoriented with their directors parallel to the applied field. Under this condition $n_p = n_o$ resulting in the disappearance of diffraction orders and this is the OFF state [5].

6.3 Experimental

6.3.1. Sample preparation

The components of this material are LCs (E7 or BL), n-vinyl-2-pyrrolidinone (NVP) as reactive diluent, acrylamide and N, N'- methylenebisacrylamide monomers, triethanolamine initiator and Erythrosin B sensitising dye. The LCs and NVP were mixed well by using a magnetic stirrer. The remaining components were added and mixed well with the stirrer. The solution was placed in an ultrasonic bath for 15-30 min and finally the dye was added. The ultrasonic mixing creates uniform PDLCs solution. Cells made from ITO coated glass plates were filled with this solution as shown in figure 6.1. Before fabrication ITO coated glass plates were cleaned as explained in chapter 4. Teflon spacers were placed on one ITO coated glass plate and another ITO coated glass plate was placed on the spacers. Two sides of the assembly were glued, keeping the other two sides open for filling the cell with PDLC material by capillary action. The thickness of the empty cell was measured with WLI. After filling, the open sides of the cell were glued immediately to avoid air gaps. Electrical contacts were made using silver loaded epoxy resin.

6.3.2. Experimental setups

The experimental set up used to record diffraction gratings was shown in figure 3.2. A spatially filtered and collimated laser of wavelength 532 nm was used. The linear s-polarized laser beam was split by a beam splitter into two beams (s-polarized) which were made to interfere at the PDLC layer as shown in figure 6.3. The spatial frequency of the gratings was calculated by using the Bragg equation $2\Lambda\sin\theta = \lambda$, where Λ is the fringe spacing, θ is half the angle between the interfering beams and λ is the wavelength

of the recording beams. The spatial frequency of the interference pattern was adjusted to 200 lines/mm (such spatial frequency was required by the spatial resolution of for Raman spectroscopy studies which will be discussed later), 300 lines/mm, 500 lines/mm (for real time studies) and 1000 lines/mm. The required spatial frequency was obtained by adjusting the angle between the two beams. Figure 6.3 includes the arrangement for real time monitoring of the grating growth using a He-Ne laser of wavelength 633 nm at which the material is not photosensitive.

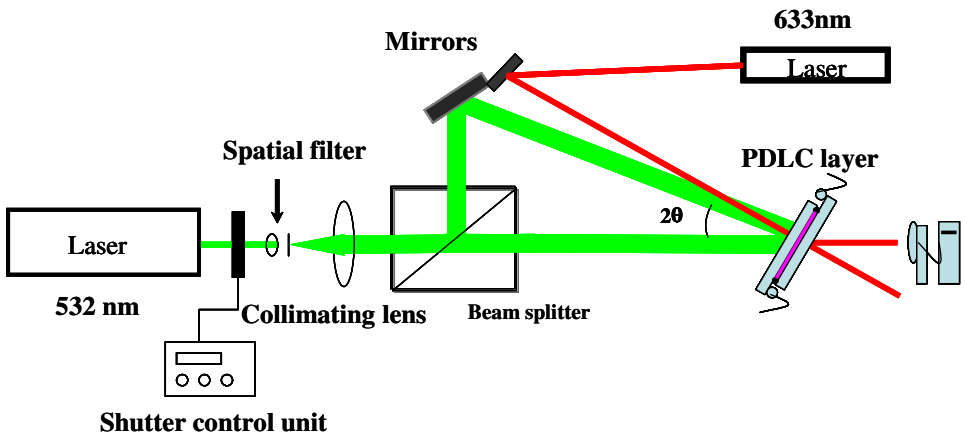

Figure 6.3 Experimental set up for recording and real time monitoring of diffraction gratings.

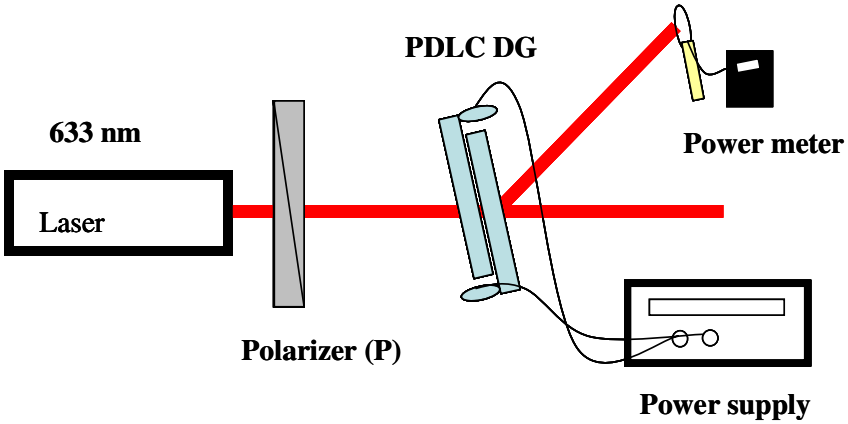

Figure 6.4 Experimental setup to study electro optical properties of PDLC diffraction grating.

The optical setup used to study electro optical switching behaviour of the diffraction grating is shown in figure 6.4. A linearly s-polarized laser beam, wavelength 633 nm, was used to probe the device at the Bragg angle of the diffraction grating. The intensities in the zero and first orders were measured while applying a square wave voltage at 1 KHz. The diffraction efficiency (η) and transmissivity (T), expressed as percentages are given by equations (6.1) & (6.2) respectively.

$$\eta = \frac{I_1}{I_0 + I_1} \times 100 \quad \text{---------- ---------- (6.1)}$$

$$T = \frac{I_0 + I_1}{I_i} \times 100 \quad \text{---------- ---------- (6.2)}$$

Where I_0 is the intensity of the zero order, I_1 is intensity in the first order and I_i is the intensity of the incident beam.

6.4 Results

6.4.1. Switchable HPDLC diffraction gratings with E7 LCs:

6.4.1.1. Real time growth of HPDLC diffraction grating with E7 LCs

Growth of diffraction efficiency of gratings was studied in real time in 10 μm thick PDLC layers with 11 % by weight E7 LCs. Diffraction gratings were recorded at 500 lines/mm at different recording intensities. Figure 6.5 shows dependence of DE on the exposure time. It is seen from the figure that the DE initially raises, and falls and further increase with the increase in the exposure time. This behaviour of the DE with increase in the exposure is usually observed in a system in which the diffusion process is slower

than the polymerization processes. Similar behaviour was observed for different recording intensities. It can also be seen from the figure that the DE is higher at higher recording intensity. It is also seen from graph that the increase in the DE is observed only after 200 sec exposure time.

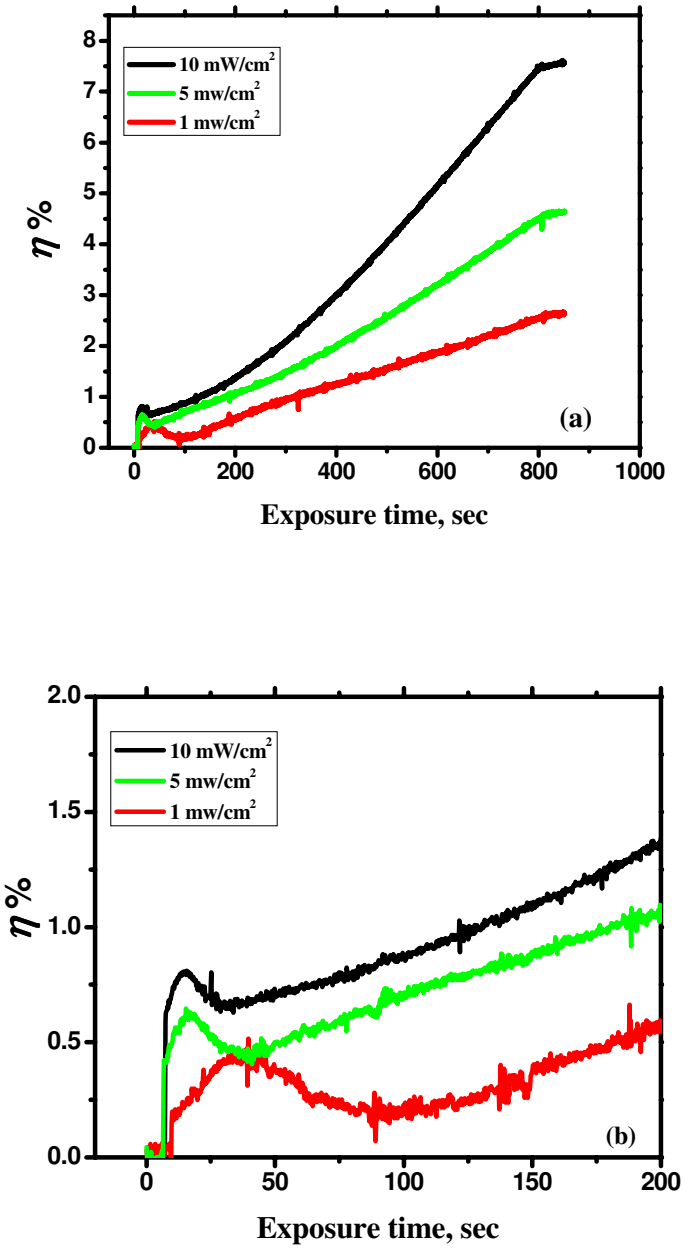

Figure 6.5 Diffraction efficiency growth during recording (a) at longer exposure time (b) at shorter exposure time.

As it is observed from the graph (figure 6.5(a)) the highest DE of the grating corresponds to recording intensity of 10 mW/cm^2. This intensity dependence could be explained as follows. When the layer is exposed to the interference pattern and polymerization is induced in the bright region higher number of short polymer chains will be created at higher intensity and their diffusion from bright to dark regions will assist the LC droplet expel to the dark regions. In addition it has been previously observed [10] that the LC droplet size is inversely dependent on the intensity of the illuminating light. Smaller size droplet will diffuse more easily into dark regions and this is in agreement with the observed kinetics and measured diffraction efficiencies in figure 6.5.

Hence these studies show that using higher intensities and faster polymerization rate is more efficient in diffraction grating formation. However, to understand the mechanism of the formation of diffraction gratings in this material further experiments are needed at different LCs concentrations and at different spatial frequencies.

6.4.1.2. Dependence of switching behaviour of HPDLC diffraction grating on recording intensity:

Experiments were done to study the dependence of the DE of the grating and switching voltage of the device on the recording intensities. The PDLC layers of 6µm thick were exposed to an interference pattern of 1000 lines/mm at 5 and 10 mW/cm^2 for 35 sec and then the recorded gratings were uniformly exposed to UV light for 20 sec.

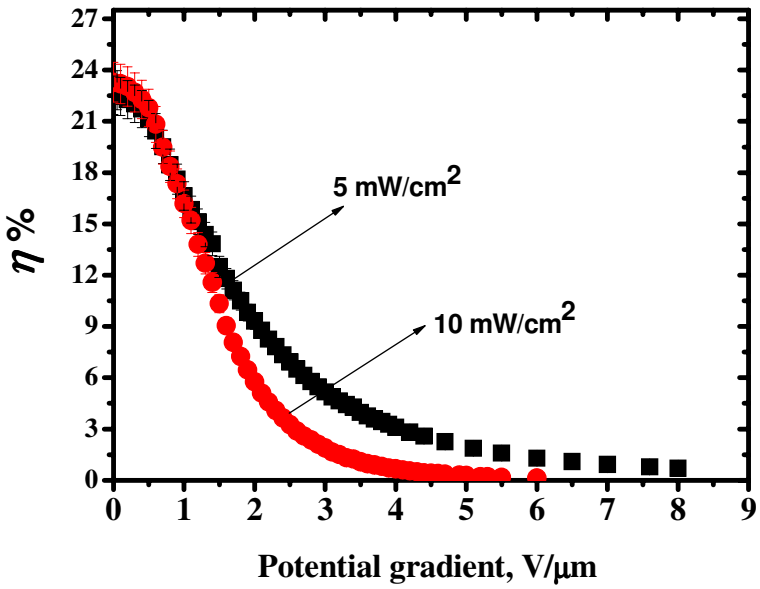

Figure 6.6 DE% Vs potential gradient (V/µm) for gratings recorded at different recording intensities.

The switching behaviour of these devices is shown in figure 6.6. It is observed from the graph there no significant difference between the DE at 10 mW/cm^2 and at 5 mW/cm^2. From the switching behaviour of these devices (figure 6.6) it was observed that the first order diffracted beam disappears at around 3.5 V/µm and 5.5 V/µm for the gratings recorded at 10 mW/cm^2 and 5 mW/cm^2 respectively. This suggests that the LC droplet size is big at higher intensity than at lower intensity. Figure 6.7 shows the normalized transmissivity versus applied electric field at 10 mW/cm^2 and 5 mW/cm^2. At both spatial frequencies transmissivity increases with the field which shows that the scattering losses are high at the beginning and reduce with applied electric field. The slope of the transmissivity curve at 10 mW/cm^2 is greater than that at 5 mW/cm^2. This suggests that scattering is greater at 10 mW/cm^2 than at 5 mW/cm^2. This supports the probability of bigger LC droplets in the device fabricated at 10 mW/cm^2.

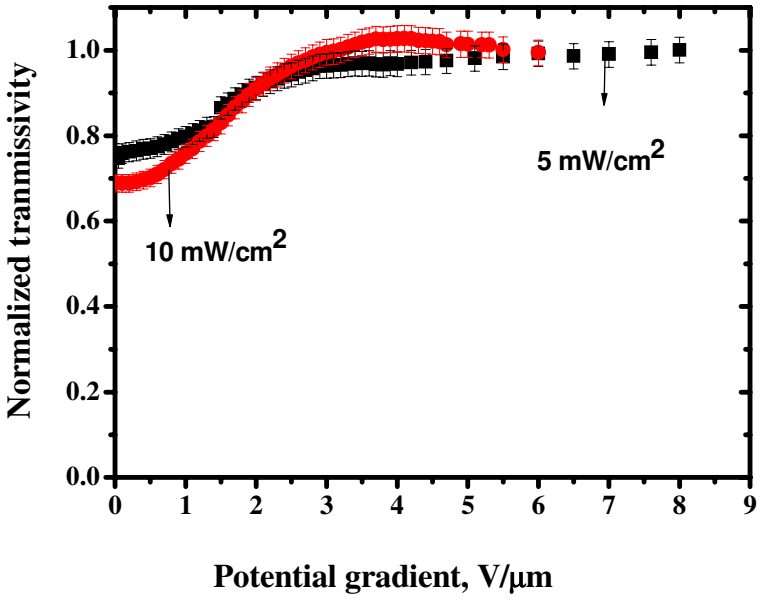

Figure 6.7 Normalized transmissivity Vs potential gradient (V/µm) at 10 mW/cm^2 and at 5 mW/cm^2.

6.4.1.3. Dependence of switching behaviour of HPDLC diffraction grating on spatial frequency:

Switchable diffraction gratings were recorded in PDLC layers with 11 % wt E7 LCs of 10 µm thickness by exposing them to interference patterns of light at 300 lines/mm and 1000 lines/mm with 10 mW/cm^2 recording intensity for 35 sec. After recording the diffraction gratings were uniformly exposed to UV light of intensity 16 W for 20 sec to completely polymerize remaining material.

The diffraction gratings were characterized by measuring the variation of intensities in the first and zero orders of diffraction with applied AC voltage. The value of DE was calculated by using equation 4.1 and is shown in figure 6.8. It was observed that the first order diffracted beam disappears at around 2.5 V/µm in the 300 lines/mm grating and around 4 V/µm for the 1000 lines/mm grating. This disappearance of the diffracted light

is due to the refractive index of the LC droplets (directors aligned parallel to the applied field) matching the refractive index of the polymer. In the HPDLC diffraction grating of 1000 lines/mm in 5 µm thick layer reported by Harbour et al., complete switching was observed at 40 V/µm [32].

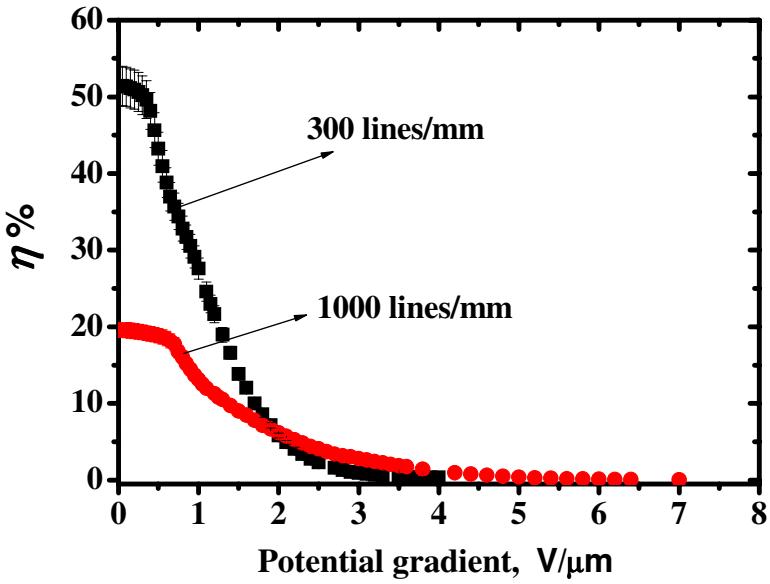

Figure 6.8 DE% Vs potential gradient (V/µm) at 300 lines/mm and at 1000 lines/mm.

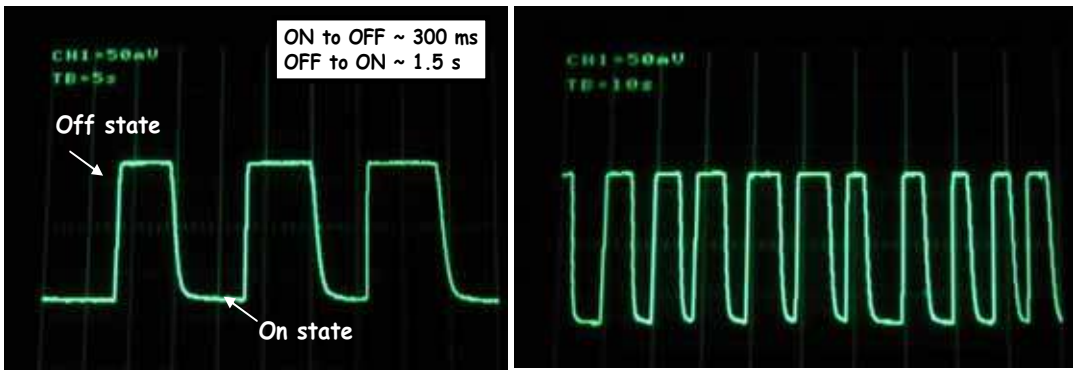

(a) **(b)**

Figure 6.9 The response of the switchable diffraction grating at 1000 lines/mm.

The response time of the switchable diffraction grating at 1000 lines/mm is shown in figure 6.9(a). Repeatability of the switching behaviour is shown in figure 6.9(b). From figure 6.9(a) it is seen that the diffraction grating switches OFF in 300 ms and when voltage is removed the grating switches ON in 1.5 sec. This switching behaviour is slow compared to other reported devices [5, 32, 33] but these are preliminary results and they show promise for the further optimization of the material to obtain low driving voltages and faster switching time. The switching of the diffraction orders at 300 lines/mm is shown in figure 6.10. The redistribution of LC droplets in the grating with spatial frequency of 300 lines/mm was studied using phase contrast microscopy and is shown in figure 6.11. It is observed that the LC droplet size is approximately equal to fringe spacing i.e., around 3 μm. As the droplet size matches the fringe spacing in the 1000 lines/mm grating the LC droplet size would be around 1μm. The faster response of the 300 lines/mm grating also supports the suggestion that the LC droplet size is greater in the gratings with 300 lines/mm.

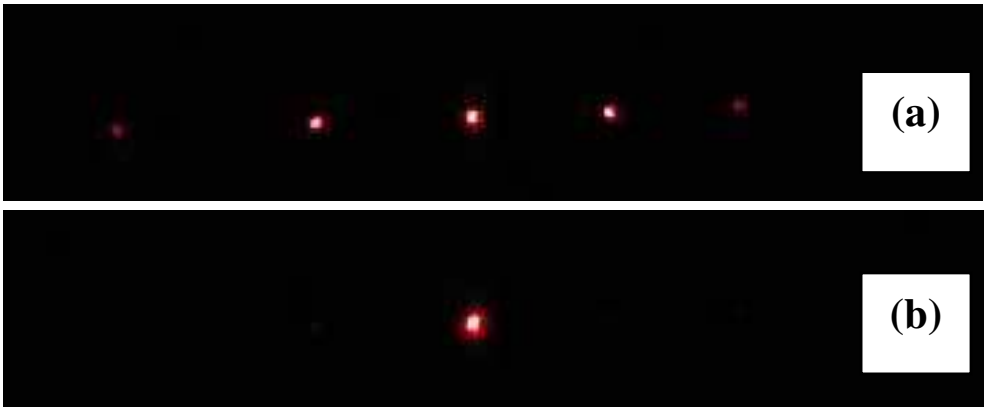

Figure 6.10 Diffraction patterns for 300 lines/mm at V = 0 V/μm (a) and at V =2.5 V/μm (b).

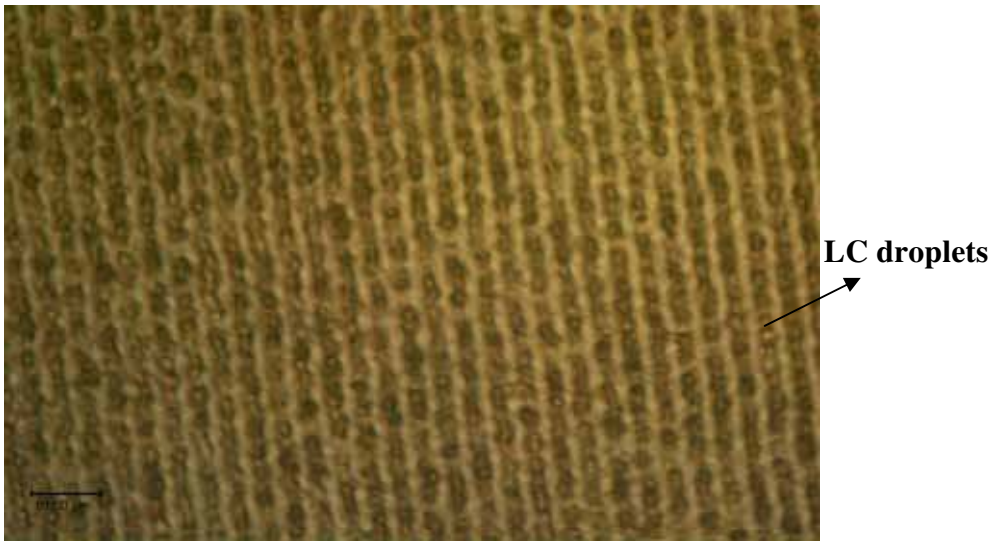

Figure 6.11 Phase contrast microscope image of redistribution of LC droplets at 300 lines/mm.

Figure 6.12 shows the normalized transmissivity versus applied electric field at 300 lines/mm and at 1000 lines/mm. At both spatial frequencies transmissivity increases with the field which shows that the scattering losses are high at the beginning and reduce with applied electric field. The slope of the transmissivity curve at 300 lines/mm is greater than that at 1000 lines/mm. This suggests that scattering is greater at 300 lines/mm than at 1000 lines as expected for larger droplet size at 300 lines/mm. The difference in the LC droplet size is most probably the reason for the higher switching voltage at 1000 lines/mm compared with 300 lines/mm. The switching voltage is expected to be higher when the droplet size is smaller [1, 6]. These results were confirmed by Raman spectroscopy which has several advantages over other spectroscopic techniques such as noninvasiveness and no need for sample preparation.

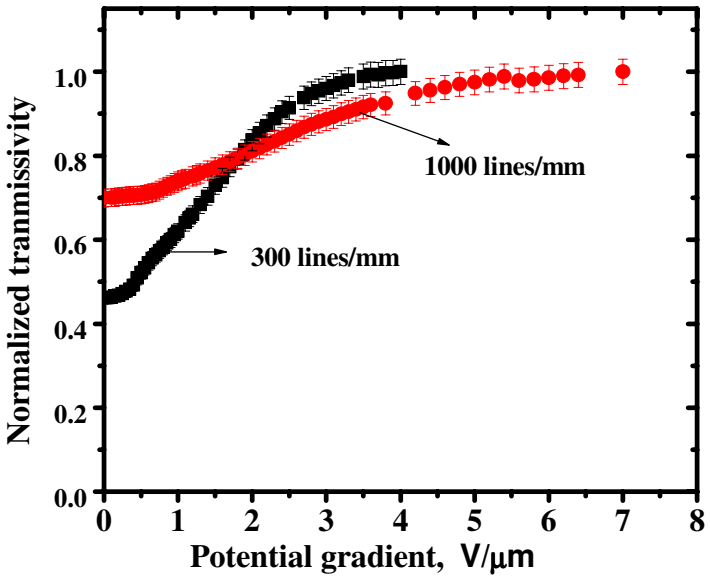

Figure 6.12 Normalized transmissivity Vs potential gradient (V/μm) at 300 lines/mm and at 1000 lines/mm.

6.4.1.4. Raman studies:

Blach et al. studied LC ordering and director field distribution inside individual droplets in PDLC material using confocal micro-Raman spectrometry [23]. To study the orientation of LC droplets in a PDLC diffraction grating the C≡N (carbon–nitrogen triple bond) stretching vibrational band at 2226 cm^{-1} was used [48] and is shown in the figure.6.13.

Samples were recorded at 200 lines/mm, with recording intensity of 5 mW/cm^2 for 140 sec. After recording the sample was uniformly polymerized with UV light intensity of 16 W for 20 min. The probing of the sample was carried out at 514 nm wavelength. The spectra were recorded in the range of 2000-2400 cm^{-1} with a spatial resolution of 1.3 μm. All the spectra were fitted with a Lorentz function and a linear baseline.

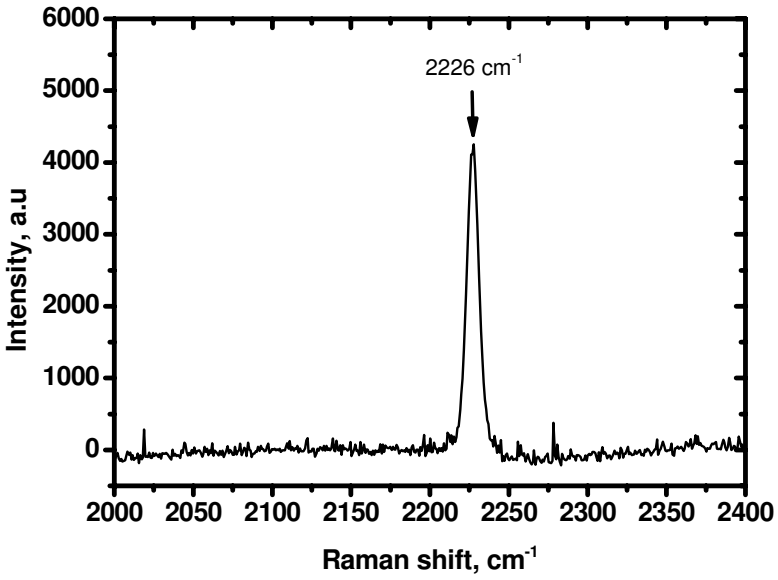

Figure 6.13 Raman Band of the C≡N at 2226cm^{-1}.

Figure 6.14 shows Raman mapping across the PDLC grating at 2226 cm^{-1}. It is observed that the intensity of C≡N is changes periodically with a spatial period of 5 µm which confirms that the LC droplets are aligned regularly and that the size of droplets is equal to the fringe spacing which is 5 µm. Similar behaviour is observed in the PDLC gratings with 20 % E7 LCs as explained below.

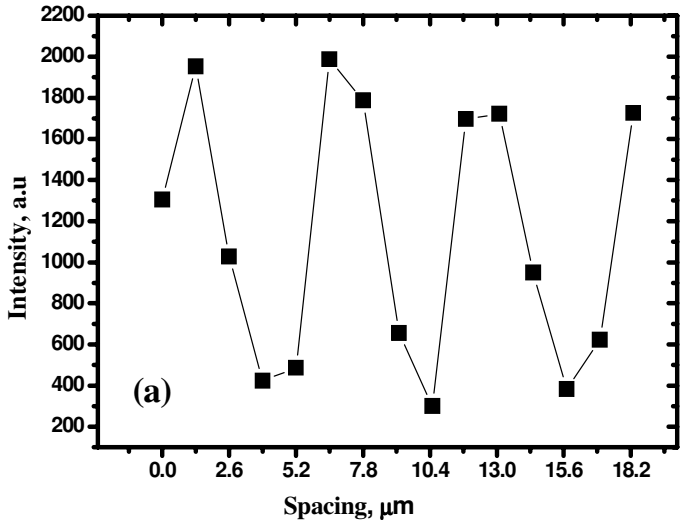

Figure 6.14 Raman mapping of the C≡N band across the PDLC grating with 11 % E7 LCs.

To confirm redistribution of LCs droplets in HPDLC diffraction gratings, two sets of samples were prepared with PDLC material with 20 % E7 LCs. One set of samples were uniformly polymerized with UV light intensity of 16 W and in the other set of samples diffraction gratings were recorded at 200 lines/mm with 10 mW/cm^2 recording intensity for 70 sec exposure time. The spectra were recorded in the range of 2000-2400 cm^{-1} with a spatial resolution of 2 μm.

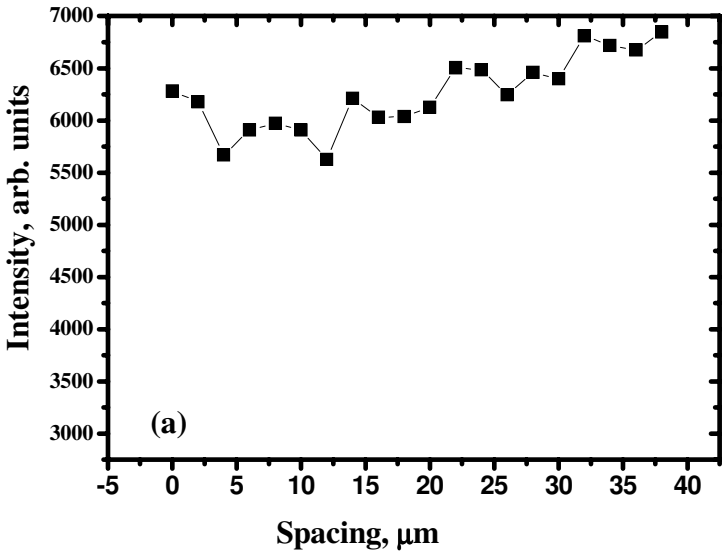

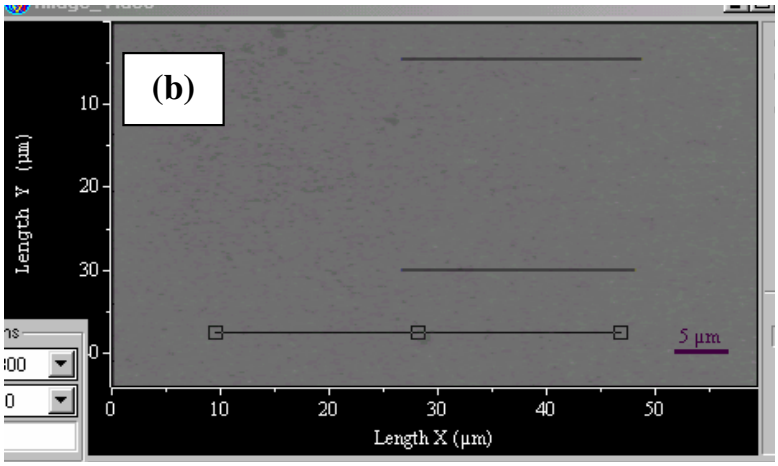

Figure 6.15 Raman mapping of the C≡N band along the uniformly polymerized PDLC layer with 20 % E7 LCs (a) Raman Image of the PDLC grating (b).

Figure 6.15 shows Raman mapping across the PDLC uniform polymerized layer at 2226 cm^{-1} and the Raman image of the layer. It is observed that the intensity of C≡N is fairly constant all over the mapping region which confirms that the LC droplets are not aligned regularly. Figure 6.16 shows Raman mapping across the PDLC grating and the Raman image of the grating. It is observed that the intensity of C≡N is changes

periodically with a spatial period of 5 µm which confirms that the LC droplets are aligned regularly.

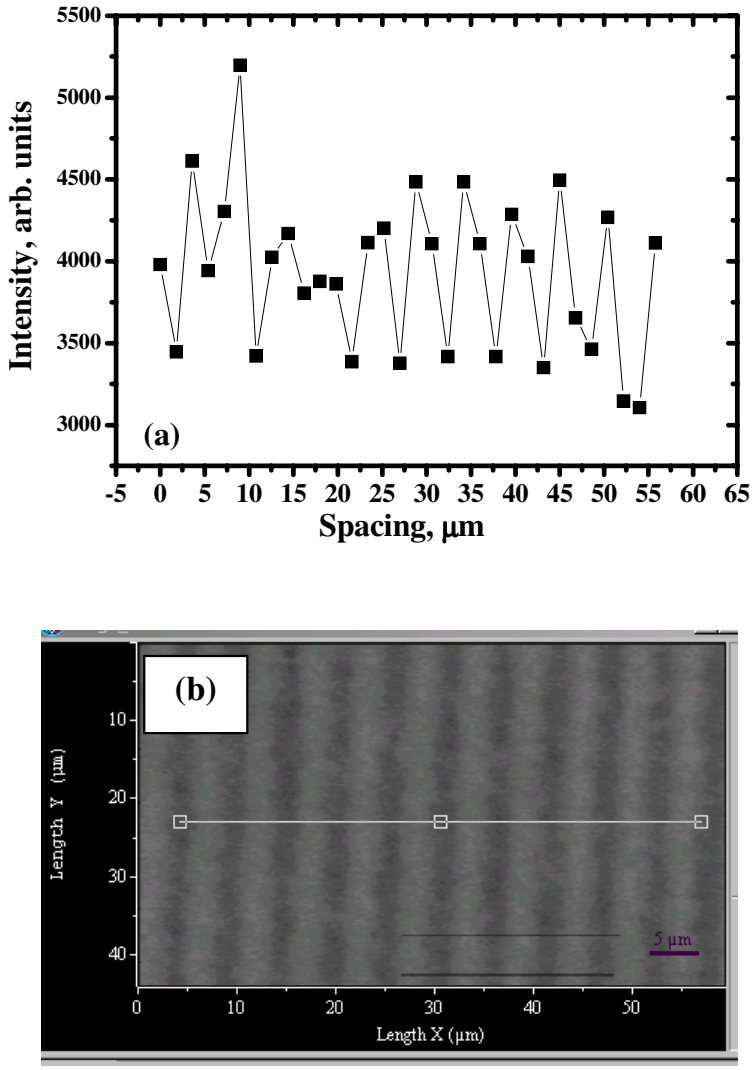

Figure 6.16 Raman mapping of the C≡N band along the PDLC grating with 20 % E7 LCs (a) Raman Image of the PDLC grating (b).

HPDLC diffraction gratings were fabricated with 11 % E7 PDLC material. The electro optical switching of the diffraction grating was studied. When the field was removed the 90 % of the original DE was restored. To study the influence of the LCs on the DE of the gratings, switchable HPDLC diffraction gratings were fabricated with nematic LCs

whose optical anisotropy is more than that of E7 LCs. Here BL037 LCs ($\Delta n = 0.282$ and $n_o = 1.526$) were used.

6.4.2. Switchable HPDLC diffraction gratings with BL037 LCs

Switchable diffraction gratings were recorded in PDLC layers with 11 % wt BL037 LCs, with 6 µm and 3.5 µm thickness spacers by exposing them to interference patterns of 1000 lines/mm with 10 mW/cm^2 recording intensity for 35 sec. After recording the diffraction gratings were uniformly exposed to UV light of intensity 16 W for 20 sec.

Switching behaviour of these devices is shown in figure 6.17. It is observed from the graph that DE is slightly more in layers with 6 µm thick spacers than in a 3.5 µm spacers. It was observed that the first order diffracted beam switched off at around 30 V_{RMS} in 3.5 µm spacer layers and in 6 µm spacer layers at around 50 V_{RMS} that is at the same field strength. Also the slope of the plot of DE versus field during the transition from ON to OFF in the 3.5 µm device is greater than in the thicker one which one would expect. Thus when the thickness is smaller the switching of the device is faster. It is also observed from this graph that the DE of 6 µm layers of BL037 is higher than in the layers of E7 LCs. This could be explained by the fact that the optical anisotropy of BL037 ($\Delta n = 0.282$) is more than the optical anisotropy of E7 LCs ($\Delta n = 0.225$).

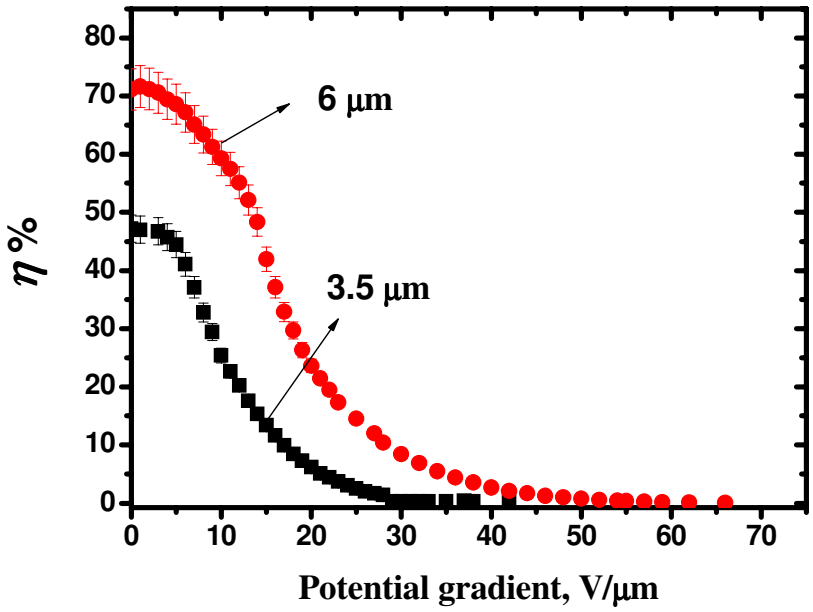

Figure 6.17 DE% Vs potential gradient (V/µm) in layers with 3.5µm and 6µm thick spacers.

Figure 6.18 (a) and (b) shows the response of the switchable diffraction gratings in PDLC layers with 3.5 µm and 6 µm thick spacers respectively. As it is observed that the time taken to switch from ON to OFF state in 3.5 µm is ~ 300 ms which is much faster than for the 6 µm device (10 sec). From OFF state to ON state in the 3.5 µm (spacers) device the time taken is ~ 2 seconds while in the 6 µm (spacers) device it is ~ 20 seconds which shows that the response time is much slower in samples with 6 µm spacers.

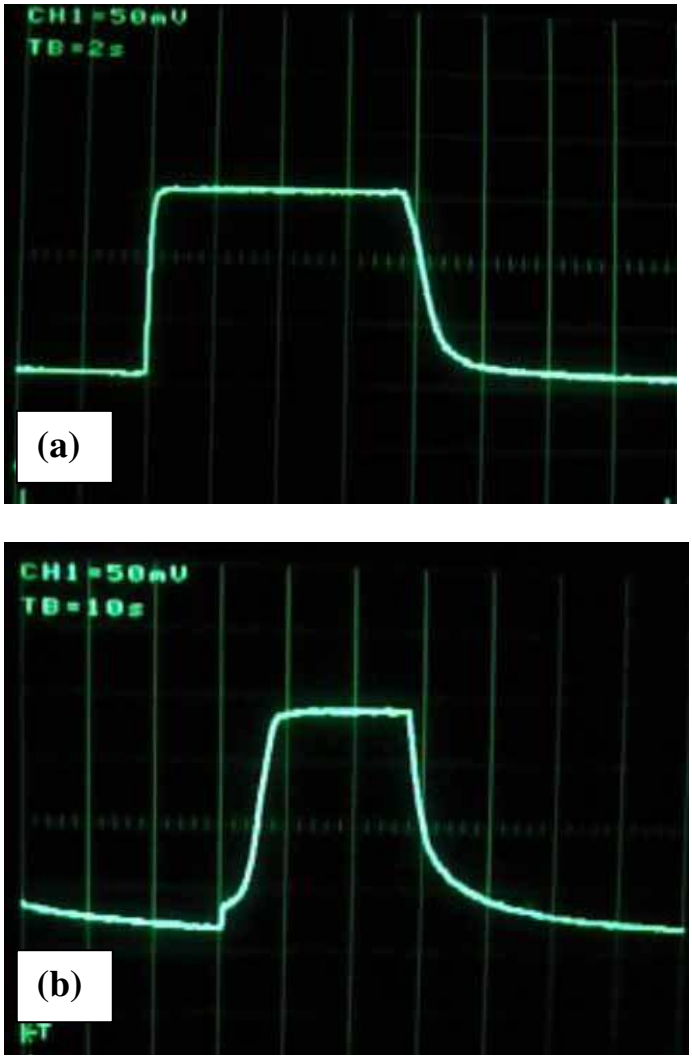

Figure 6.18 The response of the switchable diffraction grating at 1000 lines/mm in 3.5 µm (a) and 6 µm (b)

When the time response is compared with the samples with E7 LCs (figure 6.9), the response of BL037 LCs samples (figure 6.17 (b)) is much slower although the DE is much larger.

Normalized transmissivity versus applied electric field for different thicknesses of the cell are shown in figure 6.19. At both spatial frequencies transmissivity increases with

the field which shows that the scattering losses are high at the beginning and reduce with applied electric field. The slope of the transmissivity curve in thicker layer is greater than that in thin layer. The switching at 1000 lines/mm in the layers with 6µm spacers is shown in figure 6.20.

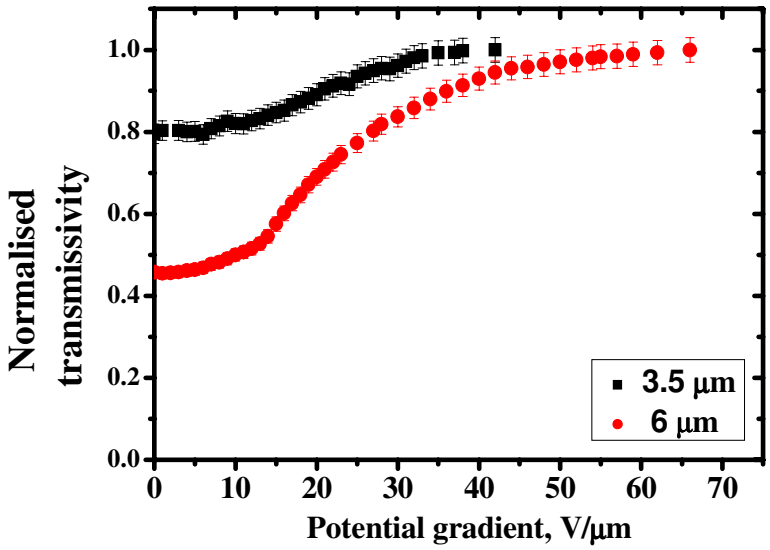

Figure 6.19 Normalized transmissivity Vs potential gradient (V/µm) at different thicknesses of the dveice

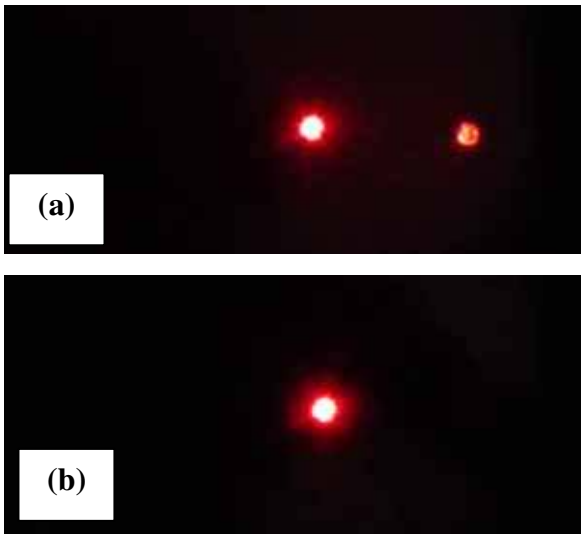

Figure 6.20 Diffraction patterns for 1000 lines/mm in 10µm thick layer at V= 0 V/µm (a) and at V= 6 V/µm (b).

The DE was also observed at different azimuths of the probe beam and seen that the DE changes with azimuth of the probe beam. This suggests that the recorded diffraction gratings are anisotropic in nature. These observations were carried out in both kinds of device with E7 and BL037 LCs.

6.5 Conclusions

Holographic PDLC diffraction gratings were fabricated using a novel PDLC composition. The LCs used to prepare PDLC solutions were E7 and BL037 LCs. The dependence of DE on the recording intensity showed that during recording of diffraction grating the polymerization rate is faster than the diffusion rates in this material. The diffraction gratings prepared with BL037 LCs show higher DE due to high optical anisotropy. The electro-optical switching of these diffraction gratings was demonstrated. The response time of the diffraction gratings fabricated with BL037 LC was slow when compared to E7 LCs. The redistribution of the LC droplets was studied using phase contrast microscopy and confocal Raman spectroscopy. The above studies show the potential of this new PDLC material for the fabrication of electrically switchable LC devices.

To improve the performance of the devices and to understand the mechanism of recording in this material further experiments on recording conditions, composition and thickness of the material are needed.

References

1. J. W. Doane, “Polymer Dispersed Liquid Crystal Displays.” in Liquid crystal: Applications and Uses, B. Bahadur, World Scientific, 362-394, 1990.
2. K. Takatoh, M. Hasegawa, M. Koden, N. Itoh, R. Hasegawa and M. Sakamoto, “Alignment technologies and applications of liquid crystal devices.” Taylor & Francis, 2005.
3. P. J. Collings, “Liquid crystals: Nature’s delicate phase of matter.” Princeton University press, 2002
4. M. Mucha, “Polymer as an important component of blends and composites with liquid crystals.” Prog. Polym. Sci., 28(5), 837-873, 2003.
5. T. J. Bunning, L. V. Natarajan, V. P. Tondiglia and R.L Sutherland “Holographic Polymer-Dispersed Liquid Crystals (H_PDLCs)”, Annu. Rev. Mater. Sci, 30, 83-115, 2000.
6. S. J. Klosowicz, “Polymer-dispersed liquid crystals as prespective media for display and optical elements”, Proceeding of the symposium on photonics technologies for 7th framework program, 238-241, 12-14 Oct 2006.
7. H. Ren and S. T. Wu, “Inhomogeneous nanosacle polymer-dispersed liquid crystals with gradient refractive index.” Appl. Phys. Lett., 81(19), 3537-3539, 2002.
8. R. Karapinar, “Electro-optic response of a polymer dispersed liquid crystal Film.” Tr. J. of Physics, 22, 227-235, 1995.
9. A. Y. G. Fuh, K. L. Huang, C. H Lin, I-I C. Lin and I. M. Jiang, “Studies of the dependence of the electra-optical characteristics of polymer dispersed liquid crystal films on curing temperature.” Chinese J. of. Phy., 28(6), 551-557, 1990.

10. S. J. Klosowicz and M. Aleksander, “Effect of polymer-dispersed liquid crystal morphology on its optical performance”, Opto Electronics review, 12(3), 305-312, 2004.
11. C. Y Huang, MS. Tsai, CH Lin and A. Y. G. Fuh, “Scattering light interference from liquid crystal polymer dispersion films” J. Appl. Phys., 41, 1436-1440, 2002.
12. M. S. Malcuit, M. E. Holmes and M. A. Rodriguez,” Characterization of PDLC Holographic Gratings.” Lasers and Electro-Optics, 395-396, 2002**.**
13. L. V. Natarajan, D. P. Brown, J. M. Wofford, V. P. Tondiglia, R. L. Sutherland, P. F. Lioyd and T. J. Bunning, “Holographic polymer dispersed liquid crystal reflection gratings formed by visible light initiated thiol-ene photopolymeristion.” Polymer, 47(12), 4411-4420, 2006.
14. J. Qi and G. P. Crawford “Holographically formed polymer dispersed liquid crystal displays.” Displays, 25, 177-186, 2004.
15. L. McKenna, L. S. Miller and I. R. Peterson, “Polymer dispersed liquid crystal films for modulating infra-red radiation.” Polymer, 45, 6977-6984, 2005.
16. A. Y. G. Fuh, M. S. Tsai, T. C. Liu and L. J. Huang, “Optically switchable gratings based on polymer-dispersed liquid crystal films doped with a guest-host dye.” ASID, 207-210, 1999.
17. T. J. Bunning, S. M. Kirkpatrick, L. V. Natarajan, V. P. Tondiglia and D. W. Tomlin, “Electrically switchable gratings formed using ultrafast holographic two-photon-induced photopolymerization.” Amer. Chem. Soc., 2000.
18. M. Jazbinsek, I. D. Olenik, M. Zgonik, A. K. Fontecchio and G. P. Crawford, “Characterization of holographic polymer dispersed liquid crystal transmission Gratings.” J. Appl. Phys., 90(8), 3831-3837, 2001.

19. D. E. Lucchetta, L. Criante and F. Simoni, “Optical characterization of polymer dispersed liquid crystals for holographic recording.” J.Appl.Phy, 93(12), 9669-9674, 2003.
20. D. E. Lucchetta, R. Karapinar, A. Manni and F. Simoni, “Phase-only modulation by nanosized polymer-dispersed liquid crystals.” J.Appl.Phys, 91, 9, 2002.
21. Y. J. Liu, X. W. Sun, J. H. Liu, H. T. Dai and K.S. Xu, “ A polarization insensitive 2x2 optical switch fabricated by liquid crystal-polymer composite.” Appl. Phys. Lett., 86, 2005.
22. S. Harbour, T. Galstian, R. S. Akopyan and A. V. Galstyan, “Angular selectivity asymmetry of holograms recorded in near infrared sensitive liquid crystal photopolymerizsable materials.” Opt. Commu., 238, 261-267, 2004.
23. L. V. Natarajan, R. L. Sutherland, V. P. Tondiglia, and T. J. Bunning, “Electro-optical switching of volume holographic gratings recorded in polymer dispersed liquid crsyatls.” IEEE, 744-749, 1996.
24. K. Beev, L. Criante, D. E. Lucchetta, F. Simoni and S. Sainov, “Recording of evanescent waves in holographic polymer dispersed liquid crystals.” J. Opt. A:Pure Appl. Opt., 8, 205-207, 2006.
25. C. C. Bowley, P. A. Kossyrev, G. P. Crawford and S. Faris, “Variable-wavelength switchable Bragg gratings formed in polymer-dispersed liquid crystals.” Appl. Phys. Lett., 79(1), 9-11, 2001.
26. R. L. Sutherland, L. V. Natarajan, V. P. Tondiglia, and T. J. Bunning, “ Bragg Gratings in an acrylate polymer consisting of periodic polymer-dispersed liquid crystal planes.” Chem. Matter. , 5, 1533-1538, 1993.

27. R. A. Ramsey and S. C. Sharma, “Switchable holographic gratings formed in polymer-dispersed liquid crystal cells by use of a He-Ne laser.” Opt. Lett., 30(6), 592-594, 2005.
28. K. Beev, S. Sainov, T. Angelov and A. G. Petrov, “Investigation of Bragg gratings recorded liquid crystals.” J. of optoelectronic and advanced materials, 6(3), 799-803, 2004.
29. V. K. S. Hsiao, T. C. Lin, G. S. He, A. N. Cartwright, P. N. Prasad, L. V. Natarajan, V. P. Tondiglia and T. J. Bunning, “Optical microfabrication of highly reflective volume Bragg gratings”, Appl. Phys. Lett., 86, 131113(1-3), 2005.
30. C. C. Bowley, A. K. Fontecchio, G. P. Crawford, J. J. Lin, L. Li, and S. Faris, “Multiple gratings simultaneously formed in holographic polymer-dispersed liquid-crystal displays.” Appl. Phys. Lett., 76(5), 523-525, 2000.
31. G. Zharkova, I. Samsonova, S. Streltsov, V. Khachaturyan, A. Petrov and N. Rudina, “Electro-optical characterization of switchable Bragg gratings based on nematic liquid crystal-photopolymer composites with spatially ordered structure.” Microelectronic Engineering**,** 81**,** 281-287, 2005.
32. S. Harbour, L. Simonyan and T. Galastian, “Electro-optical study of acrylate based holographic polymer dispersed liquid crystals with broad band photosensitivity” Opt. Commun., 277, 225-227, 2007.
33. J. Zhou, D. M. Collard and M. Srinivasarao, “Switchable gratings by spatially periodic alignment of liquid crystals via patterned photopolymerization” Opt. Lett., 31 (50), 652-654, 2006.
34. L.Criante, F. Vita, R. Castagna, D. E. Lucchetta and F. Simoni, “Characterization of blue sensitive holographic polymer dispersed liquid crystal for micro holographic data storage”, Mol. Cryst. Liq. Cryst., 465, 203-215, 2007.

35. G. Cipparrone, A. Mazzulla and G. Russo, “Diffraction gratings in polymer-dispersed liquid crystals recorded by means of polymerisation holographic technique.” Appl. Phy. Lett., 78(9), 1186-1188, 2001.
36. A. Y. G. Fuh, C. R. lee and T. S. Mo, “Polarization holographic grating based on azo-dye-doped polymer-ball-type polymer-dispersed liquid crystals.” J. Opt. Soc. Am. B, 19(11), 2590-2594, 2002.
37. Y-q. Lu, F. Du and S-T. Wu, “Polarization switch using thick holographic polymer-dispersed liquid crystal grating.” J. App. Phy., 95(3), 810-815, 2004.
38. R. Caputo, A. V. Sukhov, N. V. Tabirian, C. Umeton and R. F. Ushakov, “Mass transfer processes induced by inhomogeneous photo-polymerisation in a Multicomponent medium.” Chem. Phys., 271, 323-335, 2001.32
39. T. J. White, W. B. Liechty, L. V. Natarajan, V. P. Tondiglia, T. J. Bunning and C. A. Guymon, “The influence of N-vinyl-2-pyrrolidinone in polymerization of holographic polymer dispersed liquid crystals (HPDLCs).” Polymer, 47, 2289-2298, 2006.
40. R. M. Henry, S. C. Sharma, R. A. Ramsey, M. L. Cramer and J. B.Atman, “Effects of formulation variables on liquid crystal droplet size distributions in ultraviolet-cured polymer dispersed liquid crystal cells.” J. of Polymer Science: Part B: Polymer physics, 43, 1842-1848, 2005.
41. T. Kyu and H. W. Chiu, “Morphology development during polymerisation-induced phase separation in polymer dispersed liquid crystal.” Polymer 42, 9173-9185, 2001.
42. P. Malik and K. K. Raina, “Droplet orientation and optical properties of polymer dispersed liquid crystal composite films.” Opt. Materials, 27, 613-617, 2004.

43. Y. J. Liu, X. W. Sun, H. T. Dai, J. H. Liu and K.S. Xu, "Effect of surfactant on the electro-optical properties of holographic polymer dispersed liquid crystal Bragg gratings." Opt. Material, 27, 1451-1455, 2005.

44. M. Wang, W. Li, Y. Zou and C. Pan, "A study on the effects of the UV curing process on phase separation and electro-optical properties of a polymer-network-dispersed liquid crystals." J. Phys. D: Appl. Phys., 30, 1815-1819, 1997.

45. S. Massenot, J. Luc Kaiser, R. Chevallier and Y. Renotte, "Study of the dynamic formation of transmission gratings recorded in photopolymers and holographic polymer-dispersed liquid crystals." Appl. Opt., 43(29), 5489-5497, 2004.

46. A. Veltri, R. Caputo, C. Umeton and A. V. Sukhov, "Model for the photoinduced formation of diffraction gratings in liquid crystalline composite materials." Appl. Phys. Lett., 84(18), 3492-3494, 2004.

47. A. V. Galstyan, R. S. Hakobyan, S. Harbour and T. Galstian, "Study of the inhibition period prior to the holographic grating formation in liquid crystal photopolymerizable materials." electronic-Liquid Crystal Communications, May 07, 2004.
http://www.e-lc.org/Documents/Tigran_V_Galstian_2004_05_05_11_13_17.pdf
10-3-2006.

48. J. F. Blach, A. Daoudi, J. M. Buisine and D. Bormann, "Raman mapping of polymer dispersed liquid crystal." Vibrational spectroscopy, 39, 31-36, 2005.

7. CONCLUSIONS

Fabrication of LC optoelectronic devices by exploiting a) the holographic surface relief effect in the photopolymer and b) a novel holographic PDLC material is reported in this thesis. An acrylamide based photopolymer developed in the Centre for Industrial and Engineering Optics was used as an alignment layer for the fabrication of LC devices. The outstanding advantage of this material is the absence of any chemical post recording treatment. Photoinduced surface relief gratings were recorded in an acrylamide based photopolymer and the dependence of surface relief grating amplitude modulation on recording parameters, physical and chemical characteristic properties were studied. The experimental observations reveal that the diffusion of monomer from dark to bright regions is the main mechanism involved in the formation of surface relief grating in this photopolymer.

It was observed that with the increase in the spatial frequency of recorded grating the amplitude of the surface modulation decreases. The dependence of surface relief amplitude modulation on the recording intensity and exposure imply that the optimum intensity and exposure time to record surface relief gratings with higher surface relief amplitude modulation for the fabrication of LCs devices were 10 mW/cm^2 and 35 sec respectively. Post-exposure of the recorded gratings to uniform UV light leads to a 30% increase in the surface relief amplitude.

As the TEA concentration is increased the surface relief amplitude modulation decreases.

The influence of thermal treatment on the surface relief amplitude modulation was studied and it was found that when the surface relief gratings were heated above a given temperature the surface relief amplitude modulation decreases.

The thickness of the alignment layer is very important for the fabrication of LC devices in order to minimize the potential drop required across the device. The dependence of surface relief amplitude modulation on the physical thickness of the layer was studied and from the result it is observed that the most appropriate thickness was 10 μm because for the fabrication of LC devices the thickness of the alignment layer should be small so as to minimize the potential drop required across cell. At low spatial frequencies profiles with doubled spatial frequency were observed and these profiles depend on the thickness of the layer and the time of exposure. This could be due to shrinkage which depends on the thickness of the layer and exposure time, which shows that shrinkage is also responsible for the formation of surface relief gratings. Preliminary results from work on crossed gratings show that there is an optimum exposure time to obtain a crossed grating. These gratings show promise for the fabrication of variable focus lens arrays with LCs.

Surface relief gratings were filled with LCs to fabricate switchable diffraction gratings and a polarization rotator. Switchable diffraction gratings were successfully fabricated by filling surface relief gratings with E7 and E49 LCs. The electro-optical switching of these switchable diffraction gratings was demonstrated. The variation of DE with applied voltage was studied. The diffraction gratings prepared with higher n_e LCs show higher DE because refractive index modulation between polymer and n_e is larger.

A novel technique where photoinduced surface relief gratings in combination with rubbing technique was used to orient LCs for the successful fabrication of a twisted nematic LC device for rotating the plane of polarization of light. A twist angle of 92° ± 10º was observed in the zero and first orders. The presence of the limited number of diffraction orders is the significant advantage of this device compared to commercially available devices because it acts as a polarization rotator and as a beam splitter. The influence of applied electric field on the transmitted and the first order diffracted light intensities was studied by placing the device between crossed polarizers. It was observed that the intensities in the zero and the first order decrease with the applied electric field. The effect of applied electric field on the twist angle was also studied and it was observed that the twist angle decreases with the applied electric field. These results show the successful fabrication of a twisted nematic LC device. The state of polarization of the transmitted light in the zero order as a function of applied electric field was analysed by measuring the ellipticity. Ellipticity studies show that linearly polarized light can be converted to elliptically polarized light with the application of electric field. By adjusting the applied voltage a required degree of ellipticity can be achieved.

These studies show the potential of photoinduced surface relief gratings in an acrylamide based photopolymer for the fabrication of electrically switchable LC optical components. However the drawbacks of this fabrication technique are slow time response and low DE.

To improve diffraction efficiency of the switchable LC diffraction gratings, a new PDLC material for recording holographic volume gratings was developed as a part of

this work. Holographic PDLC diffraction gratings were fabricated by using this novel PDLC composition. The LCs used to prepare PDLC solutions were E7 and BL037 LCs. The dependence of DE on the recording intensity and spatial frequency show both diffusion and shrinkage could be responsible for the growth of diffraction gratings in this material. The diffraction gratings prepared with BL037 LCs show higher DE. The electro-optical switching of these diffraction gratings was demonstrated. The response time of the diffraction gratings fabricated with BL037 LC was slow when compared to E7 LCs.

The redistribution of the LC droplets was studied using phase contrast microscopy and confocal Raman spectroscopy. These studies show the potential of this new PDLC material for the fabrication of electrically switchable LC devices.

The significant contribution of this thesis to the scientific community is the fabrication of LC devices by exploiting photoinduced surface relief gratings in an acrylamide based photopolymer, a system in which there is no photochemical generation of surface anisotropy. A novel fabrication technique for the fabrication of TNLC devices which has advantages over the commercial fabrication method is reported.

A novel PDLC material for holographic recording has also been developed. The successful fabrication of the switchable diffraction gratings shows the potential of this new PDLC material for the fabrication of electrically switchable devices.

PUBLICATIONS AND PRESENTATIONS

Journal publications and proceedings

1. **K. Pavani,** I. Naydenova, S. Martin, R. G. Howard, V. Toal, "Fabrication of switchable liquid crystal devices using surface relief gratings in photopolymer." **J Mater Sci: Mater Electron,** 20, S198-S201, 2009 DOI 10.1007/s10854-007-9537-5, 2008.
2. **K. Pavani,** I. Naydenova, S. Martin, R. Jallapuram, R. G. Howard, V. Toal, "Electro-optical switching of liquid crystal diffraction gratings by using surface relief effect in the photopolymer." **Optics Commun**, 273, 367-369, 2007.
3. **K. Pavani,** I Naydenova, S Martin and V Toal, "Photoinduced surface relief studies in an acrylamide-based photopolymer" **J. Opt. A: Pure Appl. Opt**. 9, 43-48, 2007.
4. **K. Pavani,** I. Naydenova, S. Martin, V. Toal, "Characterization of an acrylamide based photopolymer for fabrication of liquid crystal devices." **Proceeding of International conference on Materials Energy and Design**, DIT, Bolton street, Ireland, 14 – 17th March 2006.
5. I. Naydenova, **K. Pavani,** E. Mihaylova, K. Loudmer, S. Martin, V. Toal, "Holographic recording of patterns in thin film acryl amide-based photopolymer.**" SPIE proceedings of Opto Ireland Conference**, 5827-17, 163-172, 4 – 6th April, 2005.
6. **K. Pavani**, I. Naydenova, J. Raghavendra, S. Martin, V. Toal, "Electro-optical switching of holographic polymer dispersed liquid crystal diffraction gratings." **J. Opt. A: Pure Appl. Opt.,** 11, 024023, 2009.

Poster presentations

1. **K. Pavani,** I. Naydenova, S. Martin, J. Raghavendra, R. G. Howard, V. Toal, "Characterization of holographic polymer dispersed liquid crystal diffraction gratings.", **IOP Spring meeting,** Carrickmacross, Co. Monaghan, Ireland, 7-9 March 2008.
2. **K. Pavani,** I. Naydenova, S. Martin, R. Howard and V. Toal, "Characterizing a twisted nematic liquid crystal device fabricated in an acrylamide based photopolymer.", **Photonics Ireland 2007**, Galway, 24-26 Sept, 2007.
3. **K. Pavani,** I. Naydenova, A. Scarff, R. Howard, S. Martin, V. Toal, "Fabrication of liquid crystal devices using an acrylamide based photopolymer." **IOP Spring Weekend Meeting,** Birr, Co. Offaly, 30th March -1st April, 2007.
4. **K. Pavani,** I. Naydenova, S. Martin, V. Toal, "Electrically switchable liquid crystal diffraction grating using surface relief effect in acrylamide based photopolymer.", **IOP Spring Weekend Meeting,** Bundoran, Co. Donegal, 31st March -2nd April, 2006. In best poster competition **third prize winner**.

Oral presentations

1. **K.Pavani,** I. Naydenova, S. Martin, R. G. Howard, V. Toal, "Fabrication of swit chable liquid crystal devices using surface relief gratings in photopolymer." at **International Conference on Optical, Optoelectronic and Photonic Material s and Applications (ICOOPMA),** Queen Mary, University of London, London, U.K. 30 July - 3 August, 2007.
2. **K. Pavani,** I. Naydenova, S. Martin, V. Toal, "Characterization of an acrylamide based photopolymer for fabrication of liquid crystal devices." at **International conference on Materials Energy and Design**, DIT, Bolton street, Ireland, 14 – 17th March 2006**.**
3. **K. Pavani,** I. Naydenova, S. Martin, V. Toal**, "**Photoinduced surface relief studies in acrylamide based photopolymer." at **Microscopical Society of Ireland, 29th Annual Symposium,** Focas Institute, DIT, Ireland, 7 – 9th September 2005**.**

FUTURE WORK

From the results of this thesis, there is a great deal of scope for further studies for the fabrication of the holographic switchable LC devices using surface relief effect and PDLCs.

The main objectives in future will be

1. Optimizing the recording conditions and physical parameters such as thickness and composition to obtain optimum diffraction efficiency gratings in PDLC composite.
2. To understand and propose a mechanism of formation of gratings in this PDLC.
3. To fabricate and test optoelectronic devices.

   Fabrication of polarization rotators by adjusting the thickness of the cell and using different LCs to improve the performance of the device.

   Adjustable focus lenses based on surface relief gratings.

   Fabrication of switchable diffraction grating (also polarization gratings) and adjustable focus lenses using PDLC.